Experimental Studies of Interfacial Electrochemistry

Thesis by

Bruce Alan Parkinson

In Partial Fulfillment of the Requirements

for the Degree of

Doctor of Philosophy

California Institute of Technology

Pasadena, California

1978

(Submitted December 12, 1977)

TO MY PARENTS

ACKNOWLEDGEMENTS

The names of all the people who have contributed to making my tenure at Caltech enjoyable are to be found in a microdot which makes up the dot of an "i" somewhere within the body of this thesis.

Some people do deserve mention for their macro-contribution, however, Fred Anson for his expert guidance and understanding my desire to obtain an education as well as a degree. Many present and former members of the Anson group, Gray group and Bercaw group are also acknowledged as is Beth Cooper for her skillful typing.

ABSTRACT

Experimental Studies of Interfacial Electrochemistry

Part I. Eu^{+2}, V^{+2} and $Co(NH_3)_6^{3+}$ as Electrode Kinetic Probes of the Structure of the Diffuse Layer in Dilute Electrolytes

The structure of the diffuse double layer at positive electrode charges in dilute perchlorate, fluoride, chloride and bromide electrolytes is inferred from the kinetics of oxidation of the Eu^{+2}, V^{+2} and $Co(NH_3)_6^{3+}$ cations. Diffuse layer potentials calculated from the measured kinetics of the V^{+2} and Eu^{+2} probes disagree, both in magnitude and (in some cases) in sign with potentials calculated from electrocapillary data and Gouy-Chapman-Stern theory. A different kinetic response is observed for $Co(NH_3)_6^{3+}$ and is attributed to the formation of an ion pair with an adsorbed anion. The possible origin of these effects and their consequences in attempts to apply Frumkin double layer corrections or to detect discreteness-of-charge effects is discussed.

Part II. The Formation of Polymeric Surface Phases on Mercury Electrodes from Solutions Containing Thioethercarboxylates and White Metal Cations

The adsorption of thioethercarboxylate ligands and complexes formed by these ligands with white metals (Pb^{+2} in particular) on a mercury surface is investigated. Two distinct phases are apparent in many systems one at positive potentials and the other on more negative electrodes. The large adsorption of metal cations measured in both potential regions is attributed to the formation of a monolayer of polymeric surface phase which has a structure not unlike those observed in the molecular crystals of analogous compounds.

TABLE OF CONTENTS

TABLE OF CONTENTS (Cont.)

PART I

Eu^{+2}, V^{+2} and $Co(NH_3)_6^{3+}$ as Electrode Kinetic Probes of the Structure of the Diffuse Layer in Dilute Electrolytes

PART I

CHAPTER I

INTRODUCTION

The understanding of the rates and mechanisms of electrode reactions is desirable for a number of reasons including solar energy conversion and electrosynthesis. The full potential of these applications cannot be realized without a fundamental knowledge of interfacial electron transfer reactions. These electron transfers are very susceptible to effects brought about by the inhomogeneity of the interfacial region in which the reactions occur. By far the most common method invoked to compensate for the double layer's influence which was introduced by Frumkin[1] relies on thermodynamic measurements of interfacial properties and subsequent application of model-dependent Gouy-Chapman-Stern (GCS) theory to calculate the actual concentration and the driving force experienced by the reactant species at the electrode surface.

Our inclination was to approach the problem of double layer effects on electrode reactions from a kinetic rather than thermodynamic viewpoint. The rates of simple one-electron reactants which carry a high charge are very sensitive probes of the environment in which they react,

particularly in dilute electrolyte systems where double layer effects have been known to be very prominent.

Perbromate and tetrathionate anions have been used as kinetic probes of double layer structure in a variety of supporting electrolytes.[2-7] Damaskin[8] has discussed the effects of adsorbed cations on the kinetics of reduction of several anions as well as the proton. However, electrode processes in which chemical bonds are broken or made are less attractive as probe reactions for surmising double layer structures.

In a recent "reassessment" of the use of electrode kinetic measurements for establishing double layer properties Gierst and co-workers[9] described a number of anionic reactants. However most of the reactants discussed are reduced at rather negative potentials where adsorption of anions from the supporting electrolyte is unimportant.

A recent series of papers by Weaver and Anson[10,11] have evaluated the effectiveness of using the Frumkin approach to correct the rates of electrochemical reactions for the double layers influence in concentrated electrolytes in the presence and absence of adsorbed ions.

The first part of this thesis will offer a comparison and discussion of thermodynamic measurements and kinetic probes as indicators of double layer properties in dilute electrolytes on positively charged electrodes.

ELECTRODE KINETIC PROBES OF DIFFUSE LAYER STRUCTURE

EXPERIMENTAL

Charge densities were measured as a function of potential by integrating the currents flowing into growing mercury drop electrodes using the technique and apparatus described in Appendix II. The electrode potential, drop detachment and data acquisition and analysis were all under computer control which facilitated the collection of a large number of charge density measurements at each potential. The accuracy of the values obtained was assessed by comparison with accepted values of 0.1 M sodium fluoride.[12] The root-mean-square difference was 0.2 $\mu C\ cm^{-2}$ for data covering potentials from +100 to -900 mV with the largest differences never exceeding 0.5 $\mu C\ cm^{-2}$. (Comparison of our experimental data for 1 mM NaF with those in reference 4 showed somewhat larger average differences (ca. $\pm 0.5\ \mu C\ cm^{-2}$)). Polarograms were obtained by means of a PAR 174 (Princeton Applied Research) instrument and an auxilliary X-Y recorder according to conventional procedures. Reactant concentrations were kept as small as possible (usually 0.2 mM) to minimize ohmic potential drops and polarographic maxima as well as contributions to the total ionic strength from the reactants. All potentials are quoted with respect to a standard S.C.E.

Reagent grade chemicals were used without further purification. Solutions of europium(III) were prepared by dissolving high purity Eu_2O_3 (Research Inorganic Chemical Co.) in the appropriate acid. Solutions of Eu^{2+} were prepared by controlled potential reduction of Eu^{3+} at a stirred mercury pool in the same cell subsequently utilized for the polarographic measurements. Solutions of V^{3+} and V^{2+} were prepared similarly by electrolytic reduction of solutions of V(IV) obtained by dissolving NH_4VO_3 in concentrated perchloric acid, adding a slight excess of hydrogen peroxide to reduce the V(V), heating to decompose the excess peroxide and diluting to the final desired concentration. The peroxide procedure was not needed when hydrochloric acid solutions were prepared.

Commercially available $K_3Cr(CN)_6$ (Alfa Inorganics) was recrystallized three times from water before use.

Polarograms were corrected for mass transfer by means of the formula of Oldham and Parry[13] using the current values at the end of drop life. Back-reaction corrections were applied according to the procedure described in the Appendix of reference 10. The diffusion coefficient ratio (D_R/D_{ox}) was measured to be 1.25 for Eu^{2+}/Eu^{3+} and 1.19 for V^{2+}/V^{3+}. The corresponding standard potentials were measured by constructing a Nernst plot and were found to be -620 and -474 mV vs. S.C.E., respectively.

RESULTS

Charge Potential Behavior

A number of studies have reported that in electrolytes composed of anions which specifically adsorb on positively charged mercury electrodes the anion adsorption approached the electrode charge rather than tend towards zero as the activity of the salt decreased.[14-18] This behavior has been observed for a number of anions including chloride,[18] bromide,[15] iodide,[14] and azide.[17] The matching of charges in these electrolytes would lead to the elimination of the diffuse layer along with the potential drop so that rate corrections at potentials positive of the point of zero charge (p.z.c.) would be unnecessary. The ironic result would be that the best way for electrode kineticists to avoid having to apply Frumkin double layer corrections* would be to use very low ($<10^{-2}$ M) concentrations of supporting electrolytes instead of the high values (1 M) customarily employed to avoid (not often successfully) double layer effects. Figure I-1 shows data for potassium chloride solutions taken from reference 19 and demonstrates the asymptotic behavior of the adsorbed charge to the electrode charge for this anion.

---

* See Appendix I for derivations and discussion.

FIGURE I-1

Amount of chloride specifically adsorbed on mercury in potassium chloride at 25° C as a function of the logarithm of activity of KCl. Different charges on the electrode in $\mu C/cm^2$. (Data from Grahame and Parsons, reference 19.)

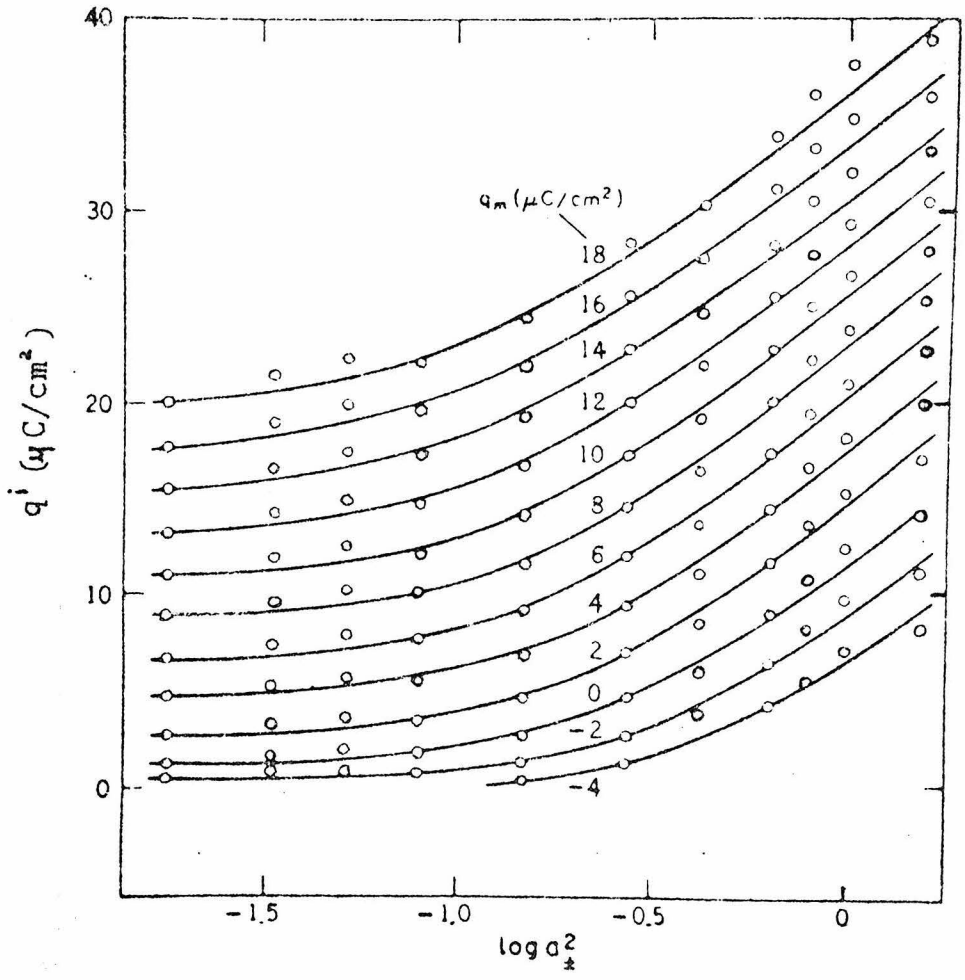
40
30
20
10
0
q^i (μC/cm^2)
q_m (μC/cm^2)
18
16
14
12
10
8
6
4
2
0
−2
−4
−1.5
−1.0
−0.5
0
log $a_\pm^2$

Earlier workers have reported the measurement of surface charge densities on dropping mercury electrodes by electronic integration of the total current passed during drop growth, with extrapolation of the resulting values of charge to separate the faradaic and non-faradaic components yielded quite reliable values of charge densities.[14,20,21] The technique is especially reliable in dilute electrolytes because the current due to faradaic background is low. A detailed discussion of the technique is given in Appendix II. The technique had also been applied to the determination of the accuracy of the diffuse layer equation for evaluating the potential drop across the diffuse layer (ϕ_2) in electrolytes containing ions of mixed valences in the absence of specific adsorption.[21] The use of charge potential curves obtained by this technique to determine the sign and magnitude of the diffuse layer potential in a number of dilute systems has been described by Sears and Anson.[14] The method which they employed was to measure at constant charge the change in potential (if any) produced by the addition of small amounts of multiply charged ions to univalent salt solutions of the anion being investigated. They found an apparent lack of a diffuse layer in several dilute electrolytes and speculated as to the kinetic usefulness of these systems. The same approach was used to compare the properties of the diffuse layers

present in dilute fluoride and perchlorate electrolytes. Figures I-2 and I-3 compare the charge-potential curves for dilute solutions of NaF and $HClO_4$ in the absence and presence of the tri-negative anion, $Cr(CN)_6^{3-}$. This anion is electrochemically unreactive within the potential range of interest and doesn't specifically adsorb on mercury at the concentrations used, but its high negative charge makes it more responsive to attraction into anionic diffuse layers than is the di-negative sulfate anion which was utilized in the previous study.[14] With the NaF electrolyte the changes in the electrode charge, q^m, which the addition of $Cr(CN)_6^{3-}$ produces are in reasonably good accord with those calculated from diffuse layer theory (Figure I-2) and clearly demonstrate the presence of an anionic diffuse layer in this electrolyte. By contrast, the very small changes in the charge-potential curve that result when $Cr(CN)_6^{3-}$ is added to the dilute $HClO_4$ electrolyte (Figure I-3) show that if a diffuse layer is present in this electrolyte the potential difference existing across it is much smaller than in the fluoride electrode. The addition of La^{+3} to a dilute $HClO_4$ electrolyte also produced no measureable shift and thus eliminates the possibility of a substantial negative diffuse layer potential due to superequivalent adsorption of perchlorate anions.

FIGURE I-2

Effect of $Cr(CN)_6^{3-}$ on the charge density vs. potential curves for dilute fluoride electrolytes. (●) Experimental points for 1 mM NaF; (■) Experimental points for 1 mM NaF + 50 μM $K_3Cr(CN)_6$; (△) Points calculated for 1 mM NaF + 50 μM $K_3Cr(CN)_6$ using diffuse-layer theory.[19]

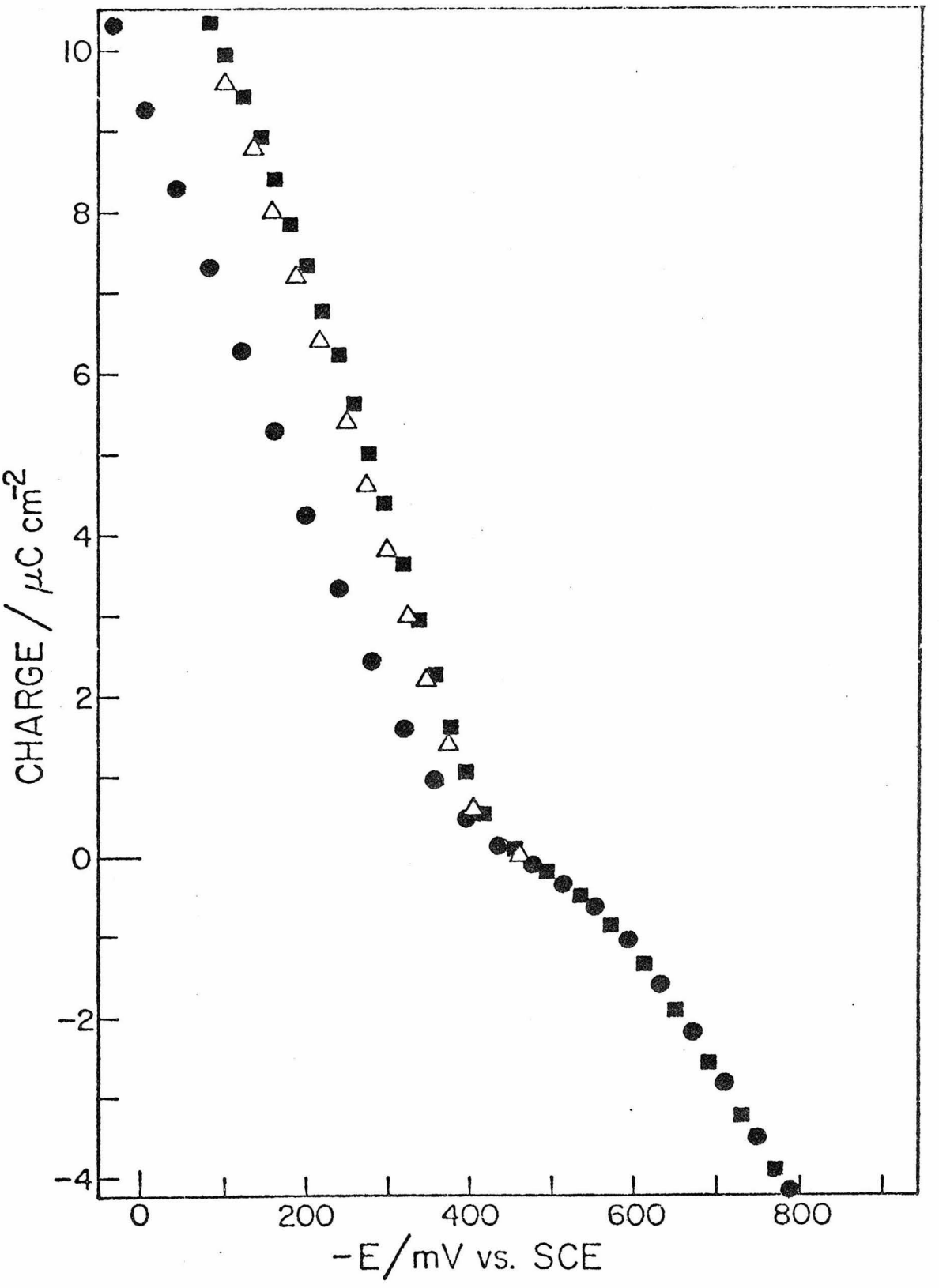
10
8
6
4
2
0
-2
-4
CHARGE / μC cm⁻²
0
200
400
600
800
-E/mV vs. SCE

FIGURE I-3

Effect of $Cr(CN)_6^{3-}$ on the charge density vs. potential curves for dilute perchlorate electrolytes. (●) 0.95 mM $HClO_4$; (□) 0.95 mM $HClO_4$ + 50 μM $K_3Cr(CN)_6$.

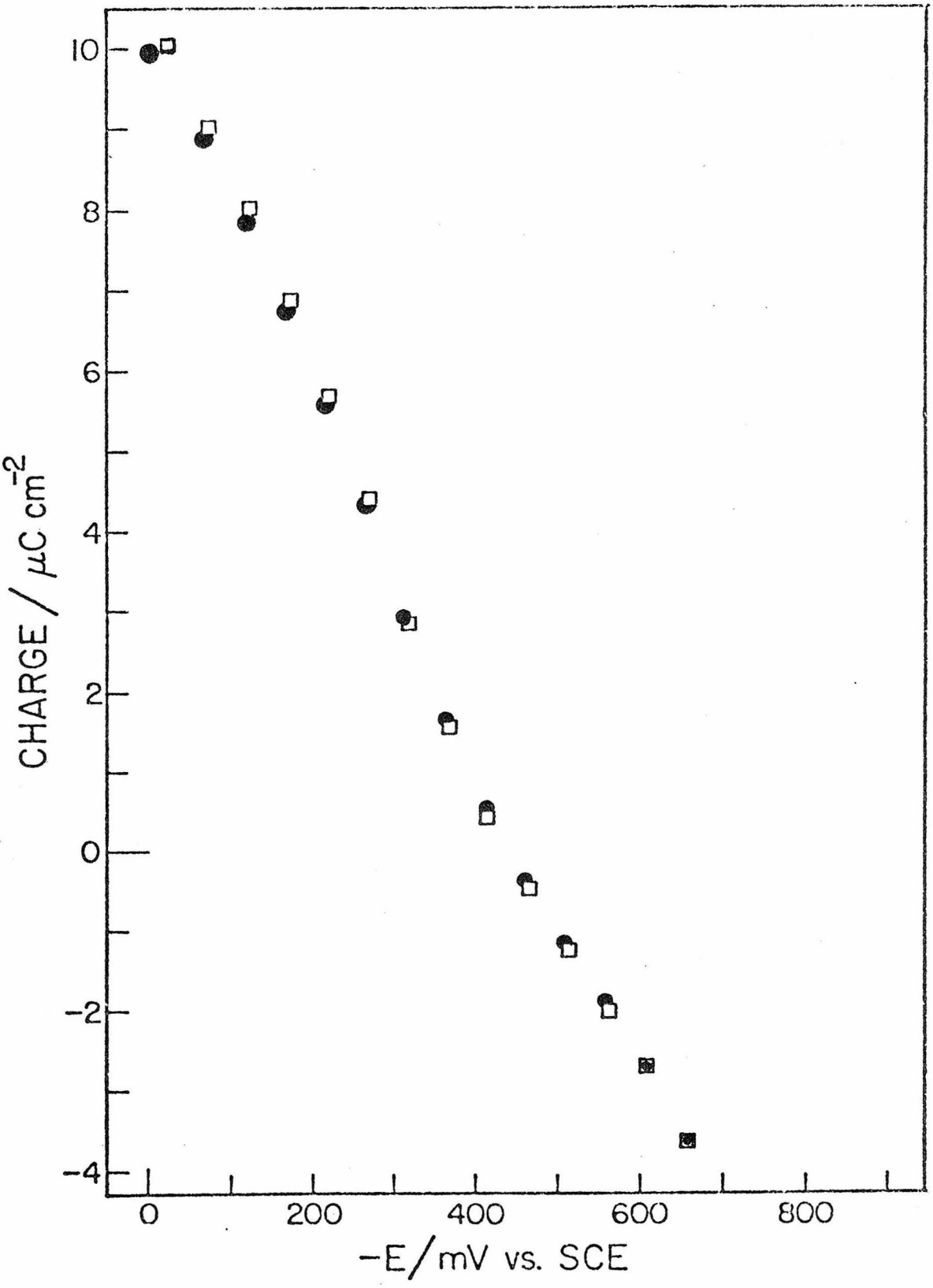
10
8
6
4
2
0
-2
-4
CHARGE / μC cm⁻²
0
200
400
600
800
-E/mV vs. SCE

The experimental precision with which charge-potential curves such as those in Figures I-2 and I-3 can be measured is not high enough to distinguish between the complete absence of a diffuse layer and the presence of a diffuse layer containing a few tenths $\mu C\ cm^{-2}$ of ionic charge. In dilute electrolytes even charges this small are ample to generate quite significant potential drops across the diffuse layer. (For example, with a 1 mM fluoride solution 0.4 $\mu C\ cm^{-2}$ of charge density results in a diffuse layer across which the potential difference is 48.2 mV, a value that would require almost 13 $\mu C\ cm^{-2}$ of charge density in a 1 M fluoride solution).

Simple Outer Sphere Reactants as Diffuse Layer Probes

The rates of suitable electrode reactions can be more responsive to changes in diffuse layer structure than the overall electrode capacitance which determines the magnitude of the changes in charge-potential curves such as Figures I-2 and I-3.

In general a suitable electrode reaction must satisfy several criteria: it should be a one electron process, it should not have any bond breaking or formation (no chemical steps) involved with the electron transfer, the reactant or product should not be specifically adsorbed on the electrode surface, the solution chemistry of both product

and reactant should be compatible with the solvent and electrolytes used (no strong ion pair formation, etc.) and the electrochemical rate constant must be within the limits accessible to modern electrochemical techniques (less than ~1 cm/sec.). Highly charged reactants are also advantageous because of their high sensitivity to diffuse layer effects.

Eu^{+2} Oxidation. The electro-oxidation of Eu^{+2} satisfies the criteria for a probe system very well and has served this purpose previously.[3,22,23] We therefore examined the kinetics of this reaction in several dilute supporting electrolytes to determine the nature of the diffuse layers present (if any). In order to calculate diffuse layer potentials (ϕ_2) from the rate data it is necessary to construct a hypothetical rate-potential line that would be observed if the oxidation of Eu^{+2} could be carried out in the absence of a diffuse layer so that ϕ_2 would be equal to zero at all potentials. Such a line was constructed using the procedure detailed in reference 22 and is outlined below: The experimental rate-potential plot for the reduction of Eu^{+3} in 1 M $NaClO_4$ was extrapolated lineally from potentials beyond -800 mV where the specific adsorption of perchlorate is negligible[25] to -434 mV the potential of zero charge in

a 1 M KF[13] solution, (and, presumably, in all hypothetical electrolytes composed of a non-adsorbing anion) and, therefore, a point through which the Tafel line corresponding to $\phi_2 = 0$ should pass irrespective of the shortcomings of conventional diffuse layer theory. A straight line passing through the same point with a slope corresponding to $\alpha = .5$ is the cathodic rate potential plot corresponding to $\phi_2 = 0$. At the point where this line intersects the formal potential of the Eu^{+3}/Eu^{+2} couple in 1 M $NaClO_4$ (-620 mV)[22] an anodic rate-potential line was constructed with a slope corresponding to $(1 - \alpha) = .5$ which represents the desired, hypothetical rate potential line for the oxidation of Eu^{+2} that would be observed in the absence of a diffuse layer at all potentials. The resulting standard rate constant, 1.2×10^{-4} cm s^{-1}, should be relatively free of uncertainties associated with the inadequacies of GCS theory.[10,22]

This procedure for obtaining the anodic (and cathodic) rate-potential plots for $\phi_2 = 0$ requires that cathodic rate data be obtained at potentials sufficiently negative to eliminate anion adsorption in supporting electrolytes concentrated enough to produce essentially constant values of the coefficient $\left(\frac{\partial \phi_2}{\partial E}\right)_\mu$ because the slope of the cathodic rate-potential plot is given by eqn. (1)

$$\frac{-2.3\ RT}{F}\left(\frac{\partial \log\ k_{app}}{\partial E}\right)_{\mu} = \alpha-(\alpha-z)\quad\frac{\partial \phi_2}{\partial E} \qquad (1)$$

z is the charge on the reactant being reduced (+3 in the case of Eu^{3+}), a one-electron reaction is assumed, and the intrinsic transfer coefficient, α, is regarded as independent of potential (on the basis of empirical observations.[26,27]) Fortunately, $\left(\frac{\partial \phi_2}{\partial E}\right)_{\mu}$ is approximately constant over the relevant range of potentials on either side of the p.z.c. in 1 M fluoride electrolytes as estimated from capacitance data[28] coupled with the GCS model and the same will be true in other 1 M electrolytes within the negative potential ranges where anion adsorption is eliminated.

Note that it is also necessary to know the standard potential and intrinsic transfer coefficient of the reaction being studied. If the latter is not known it may be obtained from eqn. (1) and measured values of $\left(\frac{\partial \phi_2}{\partial E}\right)_{\mu}$.[2] However, absolute values of ϕ_2 and standard rate constant are not required in order to construct the Tafel lines corresponding to $\phi_2 = 0$. This is the most attractive feature of the procedure just described.

In the case of the Eu^{3+}/Eu^{2+} reaction, α was previously determined to be 0.49 ± 0.02[10] which was the

justification for using $\alpha = (1 - \alpha) = 0.5$ in constructing the $\phi_2 = 0$ line.

Figure I-4 shows a set of logarithmic rate-potential plots for the Eu^{+2} electrode reaction that were measured in electrolytes having total ionic strengths near 1 mM. Also shown is the $\phi_2 = 0$ line constructed as discussed above. The large differences between the experimental curves and the calculated line at potentials positive of ca. -480 mV implies that Eu^{+2} cations are being repelled from the diffuse layer. Any uncertainties in the procedure used to construct the $\phi_2 = 0$ line are not likely to be large enough to alter this qualitative conclusion.

A quantitative idea of the magnitude of the potential experienced by the Eu^{+2} cation at its reaction site (ϕ_r) can be obtained by combining the rate differences at constant potential from Figure I-4 with the Frumkin formula.[1] If the reaction site is assumed to be the outer Helmholtz plane ϕ_r can be equated with ϕ_2 and calculated according to eqns. (2) and (3):

$$\Delta \ln k_{app} = \frac{(\alpha + z)F\phi_2}{RT} \qquad (2)$$

For Eu^{+2}, $z = 2$ and $\alpha = .5$ so at 25° C

$$\phi_2(mV) = 23.6 \, \Delta \log k_{app} \qquad (3)$$

FIGURE I-4

Rate-potential plots for the oxidation of Eu^{2+} in dilute supporting electrolytes. (●) 1.55 mM $HClO_4$; (■) 0.8 mM HCl; (▲) 0.48 mM HBr. Concentrations of Eu(II) (as perchlorate, chloride or bromide, respectively) was 0.2 mM in each case. (----) Hypothetical rate-potential plot for $\phi_2 = 0$ in all electrolytes at all potentials (see text).

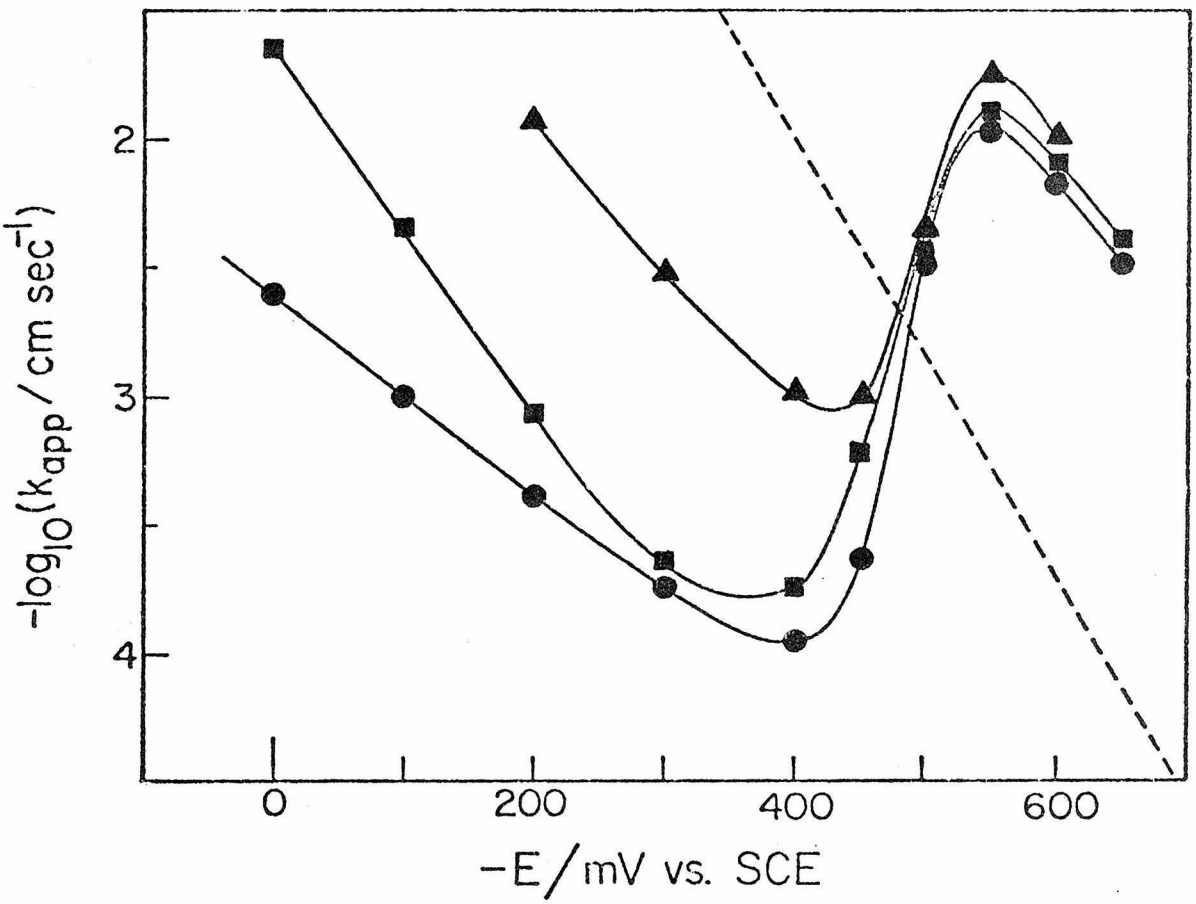
$-\log_{10}(k_{app}$ / cm sec^{-1})
2
3
4
0
200
400
600
$-E$/mV vs. SCE

Values of ϕ_2 calculated in this way are plotted in Figure I-5 along with values given in Russell's Tables for 1 mM NaF.[12] It is evident that the specific adsorption of the anions from the perchlorate, chloride and bromide electrolytes causes ϕ_r to be substantially smaller than is ϕ_2 in a 1 mM non-adsorbing electrolyte. Russell's calculation of the NaF ϕ_2 values used data from Grahame[28] and assumed no fluoride adsorption and the validity of GCS theory.[12]

V^{+2} Oxidation. In order to ascertain that the Eu^{+2} oxidation reaction was not anomalous in its kinetic behavior the kinetics of the oxidation of V^{+2} in several of the same supporting electrolytes were also investigated. The D.C. polarographic response for the oxidation of V^{+2} in a series of perchloric acid solutions is shown in Figure I-6. The figure reveals that, despite its larger standard rate constant,[29] minima appear in the current-potential curves for the V^{+2}/V^{+3} couple at low ionic strengths that are just as prominent as those exhibited by the Eu^{+2}/Eu^{+3} couple.[3] Rate depressions of this type are observed in only two situations: oxidation of a cationic reactant with an $E_{1/2}$ potential more negative than the p.z.c. and reduction of anions with an $E_{1/2}$ potential more positive than the p.z.c. This is the first time such a phenomenon has been observed

FIGURE I-5

Comparison of diffuse layer potentials evaluated from the kinetics of oxidation of 0.2 mM Eu^{2+} with those for dilute NaF. (○) 1 mM NaF (from ref. 15). Supporting electrolytes (●) 1.55 mM $HClO_4$; (■) 0.8 mM HCl; (▲) 0.48 mM HBr.

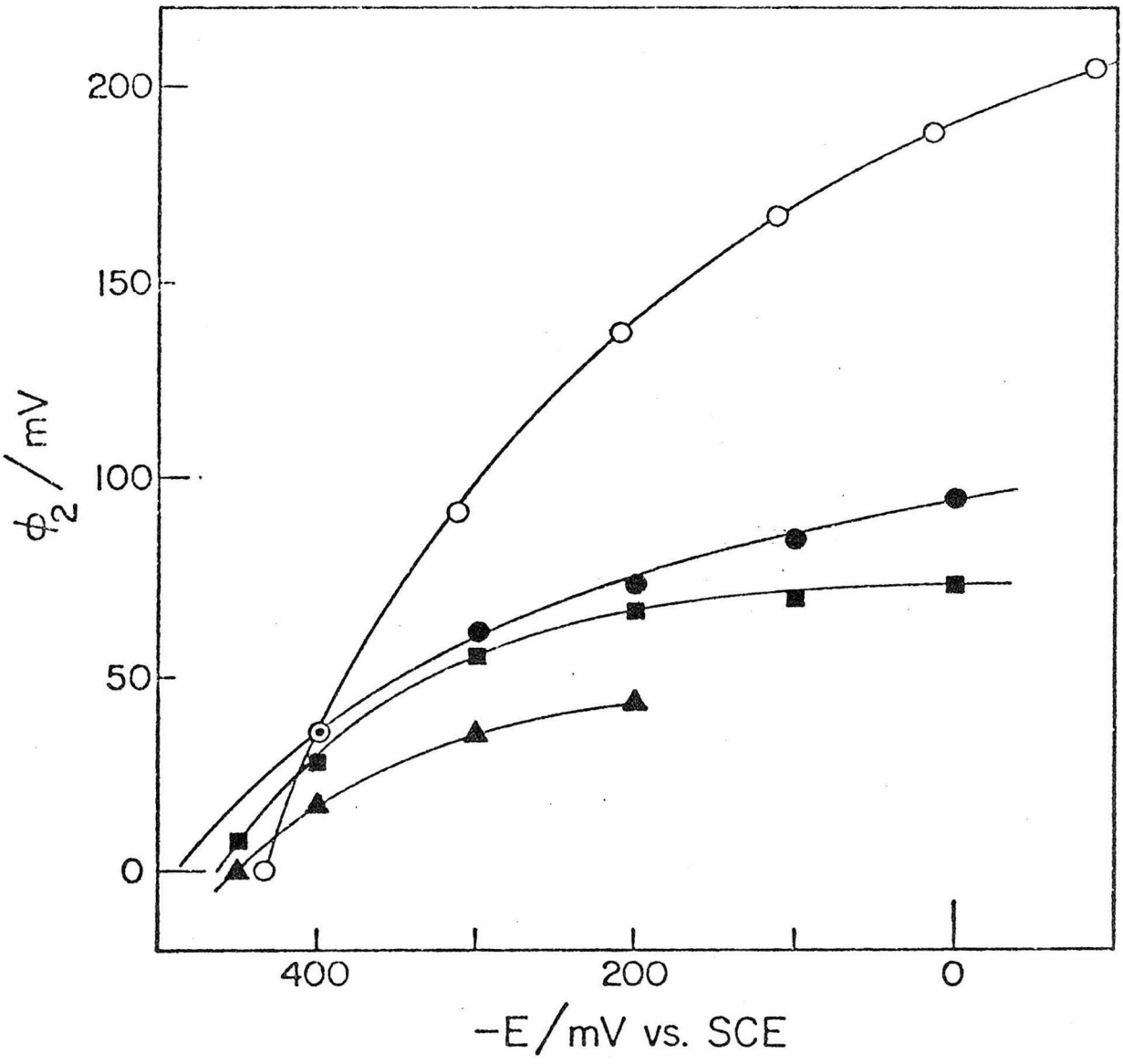
200
150
100
50
0
ϕ_2 / mV
400
200
0
−E / mV vs. SCE

FIGURE I-6

Polarograms for the oxidation of V^{2+} in perchloric acid. Currents flowing at the end of drop life are shown. Concentrations of $HClO_4$, mM: (1) 0.8 (break in curve denotes potential region where polarographic maxima were evident); (2) 1.8; (3) 4.8; (4) 9.8; (5) 19.8; (6) 99.8. Concentration of $V(ClO_4)_2$ = 0.2 mM in each case. DME characteristics: drop time 4.5 s; mercury flow rate 1.25 mg s^{-1}.

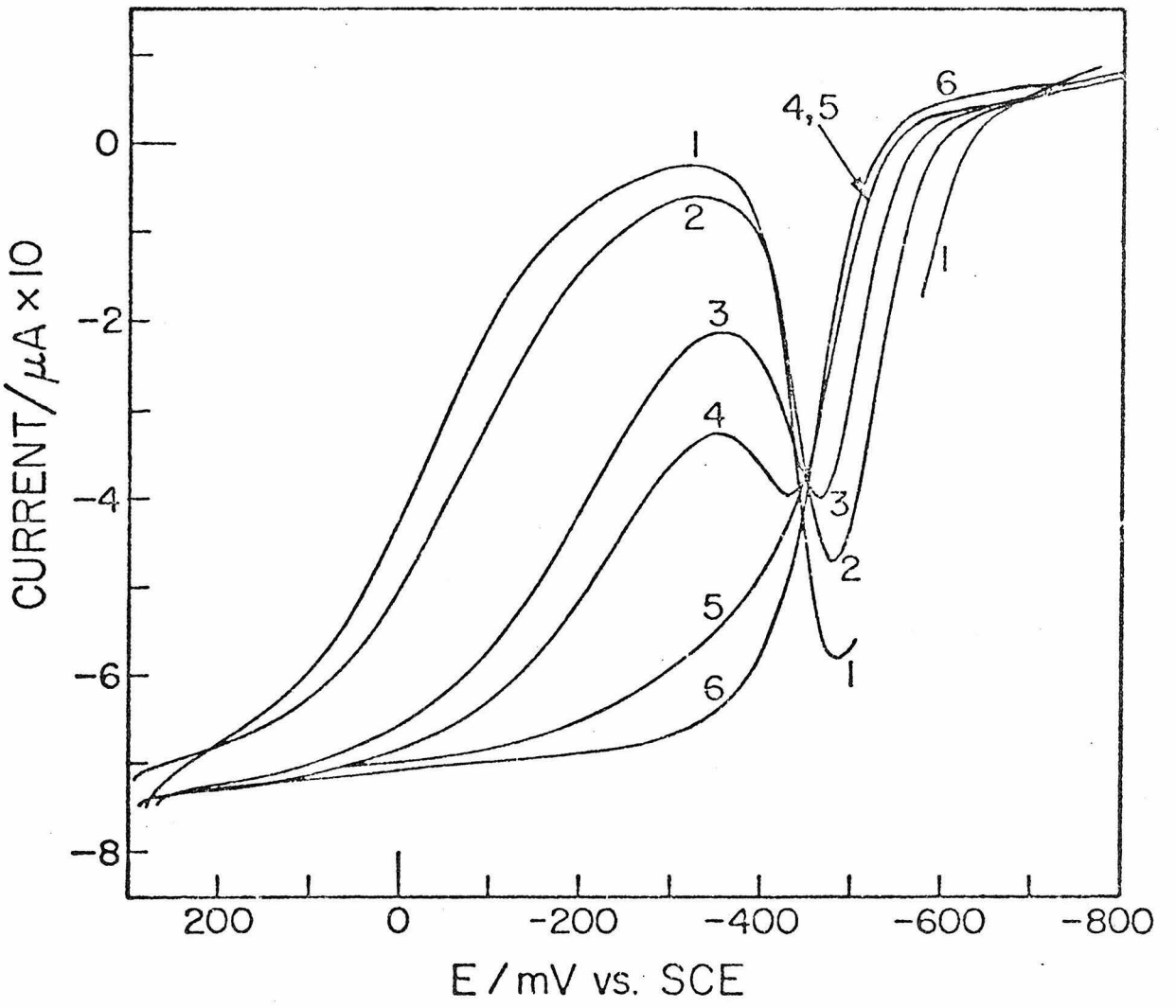
CURRENT/μA × 10
0
-2
-4
-6
-8
200
0
-200
-400
-600
-800
E / mV vs. SCE
1
2
3
4
4,5
6
5

for V^{+2} oxidation. This behavior is also observed in hydrochloric acid solutions as shown in Figure I-7. To obtain values of the potential experienced by the V^{+2} ion at its reaction site the polarograms in Figures I-6 and I-7 were analyzed in the same manner as described for Eu^{+2} with the exception of the construction of a $\phi_2 = 0$ line. The higher standard rate constant for the vanadium couple[29] made it impossible to measure the reduction rate of the +3 state at a potential negative enough to eliminate the adsorption of perchlorate anions. At these potentials (<-800 mV) the reduction rate is beyond the practical limit of chronocoulometric kinetic measurements ($k_{app} > 0.1$ cm s^{-1}). The alternate procedure used to determine the $\phi_2 = 0$ Tafel line necessitated the use of standard rate constant and potential for the V^{+2}/ V^{+3} couple. The standard rate constant was estimated from the values given by Randles[29] using double layer data from reference 25. The formal potential was measured in 0.1 M $HClO_4$. The formal potential of the V(II) - V(III) couple is pH dependant at pH values much above 1 because of the high acidity of the $V(OH_2)_6^{3+}$ cation.[30] Thus, in order to examine ionic strengths much below 0.1 the extent of hydrolysis of V(III) had to be calculated and appropriate adjustments made in the formal potential employed when oxidation currents were measured at

FIGURE I-7

Polarograms for the oxidation of V^{+2} in hydrochloric acid currents flowing at the end of drop life are shown. Concentrations of HCl mM: (1) .8 (break in curve denotes potential region where polarographic maxima were evident.); (2) 4.8; (3) 19.8; (4) 99.8.

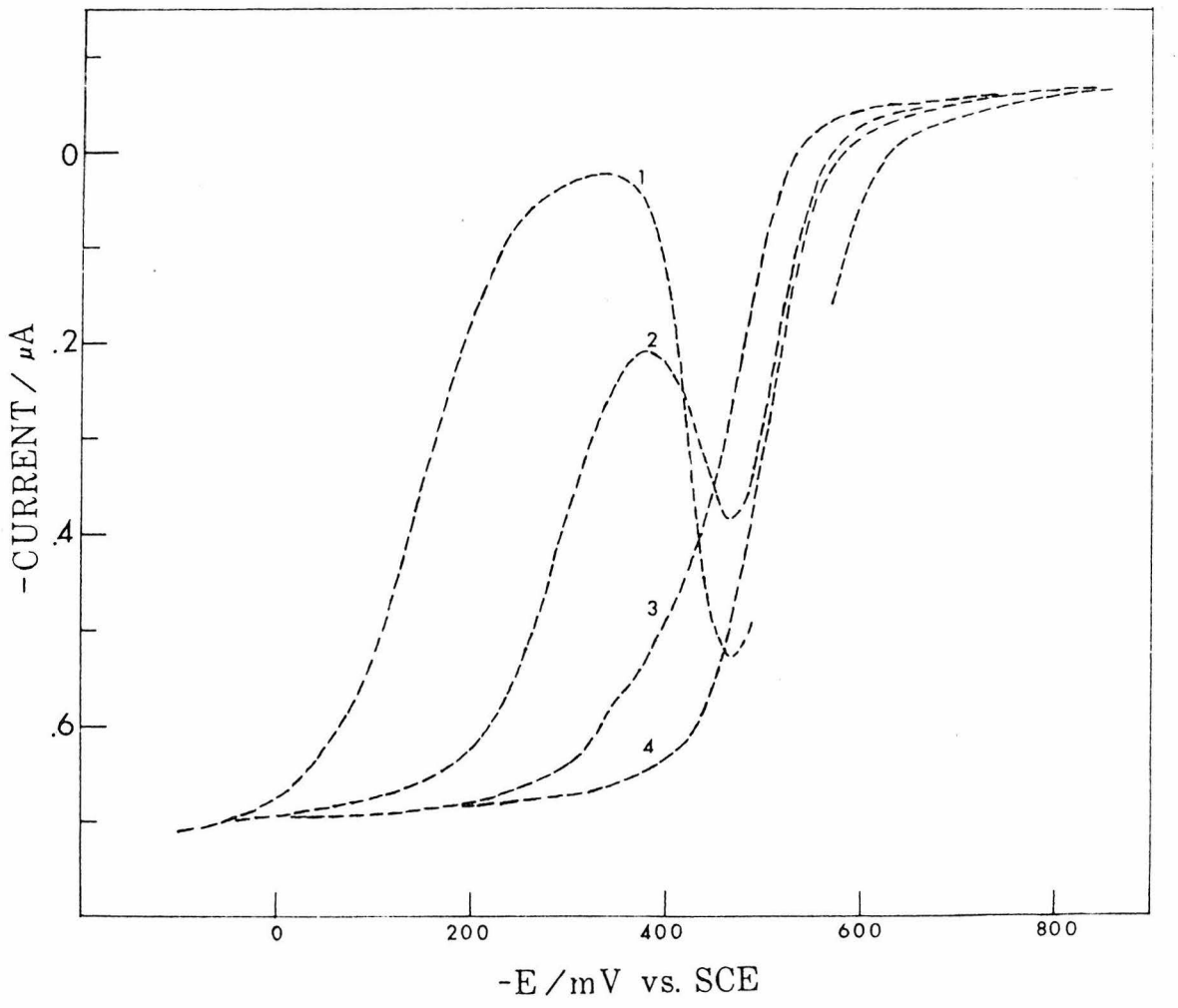
0
.2
.4
.6
-CURRENT / μA
1
2
3
4
0
200
400
600
800
-E / mV vs. SCE

potentials where back-reaction corrections were required. These complications could introduce greater uncertainties in the ϕ_r values obtained from the V^{2+} data when compared with those from Eu^{2+} data. Figure I-8 shows a comparison of the ϕ_2 values yielded by the two kinetic probes in perchlorate electrolytes. Reasonable qualitative agreement between the probes leaves little doubt regarding the existence of a diffuse layer in the dilute electrolytes examined. The fact that the ratios of the ϕ_r potentials shown in Figure I-8 for the two probes in the same electrolytes are constant suggests the possibility of electron transfer occurring at different sites for the two probes (errors in calculation of the vanadium $\phi_2 = 0$ line would result in constant differences). Weaver[31] has suggested that the reaction site for strongly hydrated outer sphere reactants is a distance from the electrode equal to the hydrated radius of the reactant plus the dimension of an additional adsorbed water molecule which can be considered the hydration sheath of the electrode.[32] Vanadium ions with their smaller hydrated radii would have to overcome a slightly larger repulsive potential than the larger europium ions[33] to attain a reaction site. Simple double layer theory assumes a static reaction site (the outer Helmholtz plane) and does not account for variations in the size of the reactant.[1]

FIGURE I-8

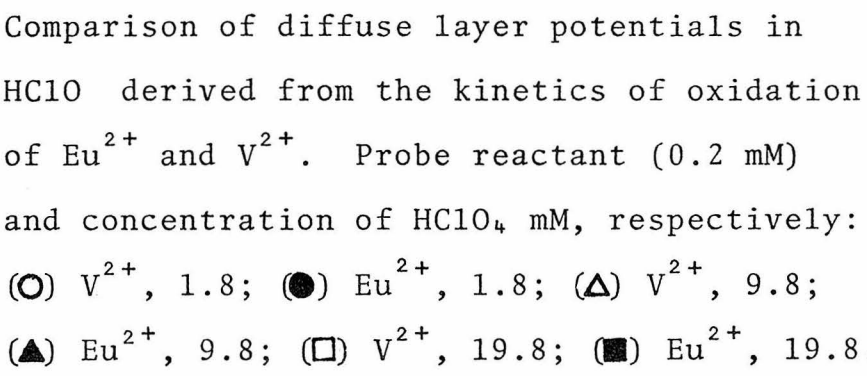
Comparison of diffuse layer potentials in
HClO derived from the kinetics of oxidation
of Eu^{2+} and V^{2+}. Probe reactant (0.2 mM)
and concentration of $HClO_4$ mM, respectively:
(○) V^{2+}, 1.8; (●) Eu^{2+}, 1.8; (△) V^{2+}, 9.8;
(▲) Eu^{2+}, 9.8; (□) V^{2+}, 19.8; (■) Eu^{2+}, 19.8.

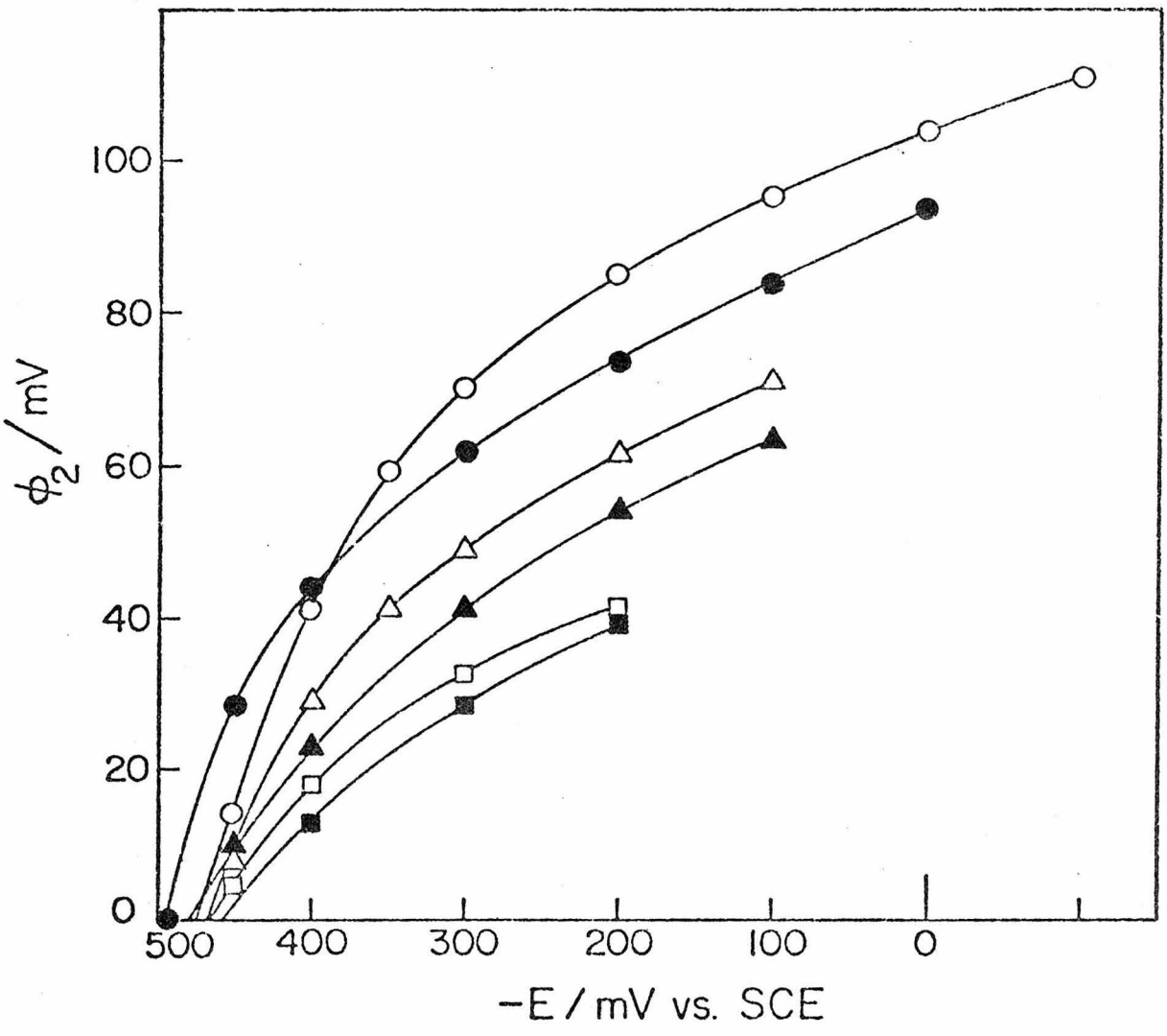
100
80
60
40
20
0
ϕ_2 / mV
500
400
300
200
100
0
-E / mV vs. SCE

Effect of Multiply-Charged Anions

At potentials where the kinetics of oxidation of both Eu^{2+} and V^{2+} indicate positive values of ϕ_2 the diffuse layer should be populated chiefly by the anions of the particular supporting electrolyte employed. If a multiply-charged anion such as $Cr(CN)_6^{3-}$ is made a component of the supporting electrolyte, less positive ϕ_2 values should result at potentials where the diffuse layer is composed of anions because of the preferential incorporation of multiply-charged ions into diffuse layers.[34] The rate of oxidation of a cation such as Eu^{2+} is therefore expected to be enhanced by the addition of $Cr(CN)_6^{3-}$ at potentials on the positive side of the p.z.c. Figure I-9 shows how the addition of $Cr(CN)_6^{3-}$ anions affects the kinetics of oxidation of Eu^{2+} in a dilute perchlorate electrolyte. As expected, the $Cr(CN)_6^{3-}$ produces no effect at potentials more negative than the p.z.c. and the increases in reaction rate at potentials positive of the p.z.c. are in reasonable agreement with those calculated from diffuse layer theory[34] if the values of ϕ_2 used in the calculations are those for the pure perchlorate electrolyte obtained from the kinetic data of Figure I-4. Similar comparisons based on ϕ_2 values obtained from differential capacitance data[25] produce gross disagreements as would be expected if the kinetic response of the Eu^{2+}

FIGURE I-9

Effect of $Cr(CN)_6^{3-}$ on the kinetics of oxidation of Eu^{2+} in dilute perchloric acid. (1) 1.5 mM $HClO_4$; (2) 1.55 mM $HClO_4$ + 70 μM K $Cr(CN)_6$; (3) Calculated response using curve 1, ϕ_2 potentials in Figure 4, diffuse layer theory[19] and the Frumkin formula[14]. (4) Hypothetical rate-potential plot of $\phi_2 = 0$ at all potentials (see text).

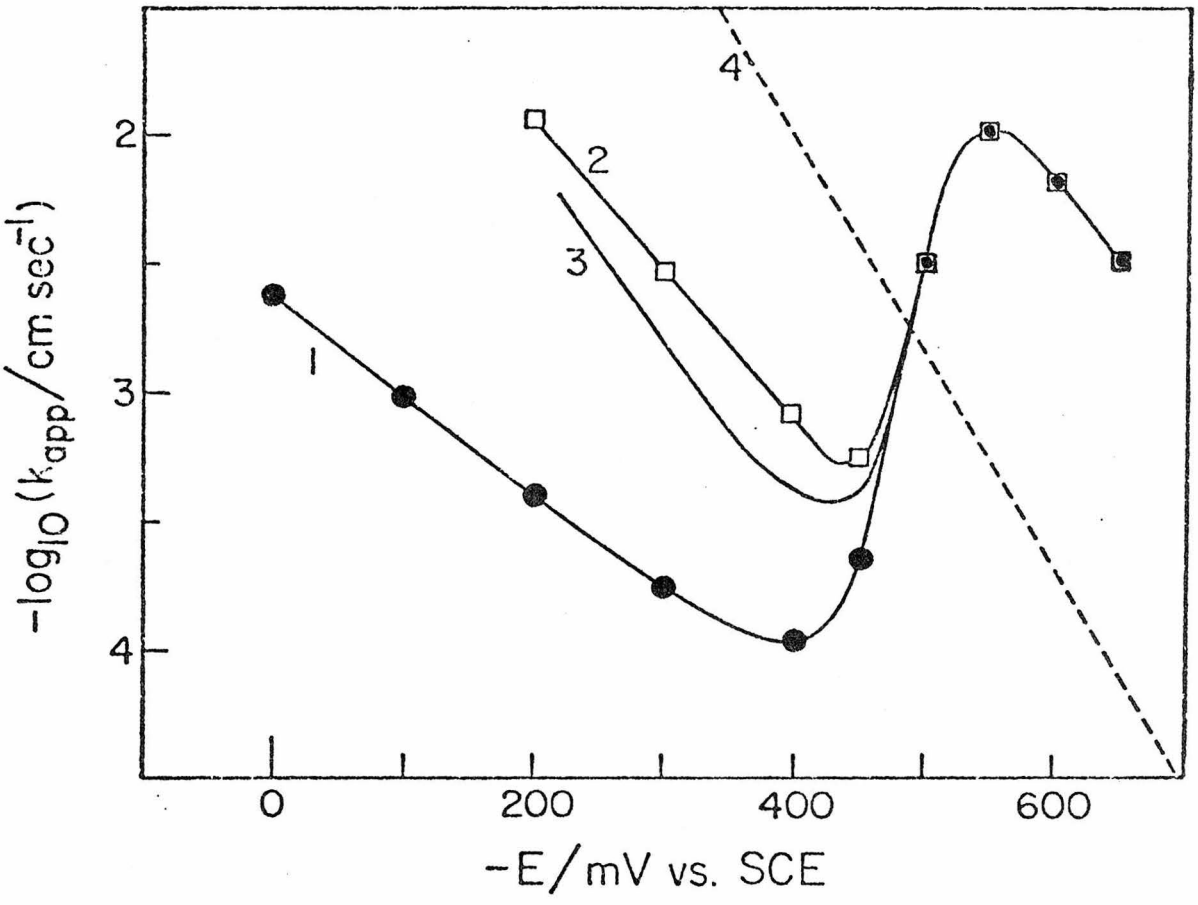
4
2
3
1
2
3
4
0
200
400
600
-E/mV vs. SCE
$-\log_{10}(k_{app}/cm\ sec^{-1})$

oxidation reaction is regarded as the more reliable indicator of the potential it experiences at its reaction site. This experiment is a quantitative demonstration of the exceptional sensitivity of the kinetic probe. Large kinetic responses are observed under the same conditions where the previous charge measurements detected no difference in the diffuse layer structure (Figure I-3).

DISCUSSION

The previous speculation[14] that it might be possible to eliminate the diffuse layer by utilizing sufficiently dilute solutions of specifically adsorbed anions seems clearly to be ruled out on the basis of both the present experiments and the related results of de Levie and Neves.[2] However, the diffuse layers which are formed in dilute supporting electrolytes affect the rates of electrode reactions in ways which differ substantially from those predicted on the basis of diffuse layer structures deduced from conventional interpretations of electrocapillary data.[35] The results described in the present work only add to the body of previous data which contains evidence of the same discrepancies (e.g., reference 8) although they have not previously been pointed out explicitly for reactions as intrinsically simple as the one-electron

oxidation of V^{2+} and Eu^{2+}. For example, in the original, seminal paper of Gierst and Cornelisson[3] considerable emphasis was laid on the observation that the polarograms for the oxidation of Eu^{2+} in perchlorate electrolytes of varying ionic strength all intersect at a single potential which was identified with the point of zero charge. However, the measurements of Parsons and Payne[25] show that the point of zero charge shifts from -445 mV to -515 mV (vs. S.C.E.) on changing from 0.01 M to 1 M $HClO_4$, respectively. Moreover, if the data of Parsons and Payne are used to determine the potentials where the electronic and adsorbed anionic charges match, so that $\phi_2 = 0$, i.e., the condition assumed to prevail in the interpretation of the common intersection point of the polarograms in reference 3, potentials result which are very dependent on ionic strength (Table I) and which fall nowhere near the common intersection potential (ca - 450 mV) reported by Gierst and Cornelisson for Eu^{2+} oxidation[3] and also observed in the present study for the oxidation of V^{2+} (Figure I-6) in perchloric acid. No common intersection is observed for V^{+2} oxidation in hydrochloric acid (Figure I-7).

Discrepancies between values of ϕ_2 obtained from kinetic and electrocapillary measurements are not confined to the point of zero charge or to dilute supporting electrolytes.[22] It is particularly striking that even the

TABLE 1

Potentials at which the negative charge density, q^i resulting from the adsorption of perchlorate anions from perchloric acid solutions matches the positive electronic charge density, q^m, on mercury electrodes. Data from reference 17.

Conc. of HClO , M	$-E(q^m = q^i)$, mV vs. SCE
0.01085	132 & -394
0.02713	none[a]
0.05426	none[a]
0.1085	261
0.2170	193
0.5426	146
0.9307	131

[a] $q^i > q^m$ at all potentials where $q^m > 0$.

signs of the two sets of ϕ_2 values disagree at potentials where anion adsorption is significant. Thus, the rate of oxidation of Eu^{2+} is retarded (i.e., $\phi_r > 0$) in electrolytes and potential ranges where the electrocapillary data lead to negative values of ϕ_2. Similar discrepancies are also observed in chloride and bromide supporting electrolytes[22] although the difference in the sign of ϕ_r and ϕ_2 is not present at concentrations above about 0.2 M*.

In all cases the discrepancies observed are in the direction that would be expected if the concentrations of specifically adsorbed anions were smaller than those determined from the electrocapillary data, so that an assessment of the reliability of the determination of the quantity of adsorbed anions is in order. The most commonly used procedure for obtaining concentrations of specifically adsorbed anions from electrocapillary data is that introduced by Grahame.[36] It depends upon the use of the Gouy-Chapman-Stern theory to go from the measured ionic

---

* A recent kinetic study of the $V^{2+/3+}$ and $Eu^{2+/3+}$ couples in various 1 M supporting electrolytes claimed that coincident corrected Tafel plots result when the Frumkin correction was applied using ϕ_2 values obtained from conventional diffuse layer theory.[23] Reasons for doubting this claim were given in reference 22.

superficial excesses to the concentration of adsorbed anions and includes the assumption that cations are not specifically adsorbed. This part of the Grahame procedure is recognized to be a source of some uncertainty[33] and is a likely target in the search for an explanation for the discrepancies between the ϕ_2 values resulting from the static (electrocapillary) and dynamic (kinetic) measurements. For this reason ϕ_2 values obtained by the constant ionic strength procedure of Hurwitz[37] and Parsons[38] were also inspected because this procedure allows the concentration of adsorbed anions to be evaluated without resort to diffuse layer theory.

Payne[39] analyzed his data for mixed NH_4ClO_4 - NH_4F electrolytes having a constant ionic strength of 1 M according to the Hurwitz-Parsons procedure and obtained charge densities of specifically adsorbed perchlorate anions that exceed the positive electronic charge densities on the electrode at perchlorate concentrations of 0.05 M and above. However, positive values of ϕ_r are deduced from kinetic data in fluoride-free perchlorate solutions at the same concentrations.[22] Since the addition of non-absorbing salt to solutions from which the specific adsorption of anions exceeds the positive electronic charge density on the electrode is known to produce increases in the adsorption of anions,[40] the

discrepancies between the ϕ_2 and ϕ_r values resulting from static and dynamic measurements, respectively, with pure salt solutions are not eliminated if the measurements are conducted at constant ionic strength*. Thus, the use of the diffuse layer theory in the Grahame[36] procedure for analyzing electrocapillary data does not appear to be responsible for the observed discrepancies.

The discrepancy between the signs of the values of ϕ_2 and ϕ_r resulting from electrocapillary and kinetic measurements presents serious interpretive difficulties. So long as the specific adsorption of cations is assumed to be negligible at electrodes bearing positive electronic charge densities, the Grahame procedure[36] will always lead to negative values of ϕ_2 when the electrocapillary data indicate positive superficial excesses of cations, Γ_+. Since Γ_+ is directly accessible from experimental measurements of interfacial tensions, γ, as a function of μ, the chemical potential of the absorbing salt,[48]

$$-\Gamma_+ = \left(\frac{\partial \gamma}{\partial \mu}\right)_{E_-} \qquad (4)$$

---

*It was not possible to make kinetic measurements in the fluoride-perchlorate electrolytes both because acidic media were required to avoid hydrolysis of Eu^{3+} and V^{3+} and because of the insolubility of europium(III) fluoride.

it follows that negative values of ϕ_2 correspond to the sign of the coefficient $\left(\frac{\partial\gamma}{\partial\mu}\right)_{E_-}$ being opposite to that observed when positive values of ϕ_2 are derived. Thus, to attribute the discrepancies between the signs of ϕ_r and ϕ_2 derived from kinetic and electrocapillary data to possible experimental uncertainties in the latter would imply that increases in interfacial tension had been measured as decreases (or vice versa). The good agreement between interfacial tension values that have been measured for numerous electrolytes in many different laboratories makes this interpretation seem highly unlikely.

One is left with a clear dilemma in the form of electrocapillary data that show cations to be attracted into the interfacial region in electrolytes where electrode kinetic data imply that the reactant cation is repelled from the diffuse layer. This disagreement between the results of the two kinds of experiments seems too fundamental to yield to explanations based on proposed differences in planes of closest approach of reactant and supporting electrolyte ions or to the types of discreteness-of-charge effects that have been invoked to explain less glaring kinetic anomalies.[6,19,49,50] The source of the discrepancy seems most likely to lie with the kinetic results. The observed behavior indicates

that, although there is a net attraction of cations into the diffuse layer when anion adsorption exceeds the positive electronic charge on the electrode, no corresponding enhancement in the rate of reaction of cationic reactants ensues. One might infer, therefore, that the site to which the cationic reactants must gain access before they can react retains a net positive potential even when the sum of the electronic and anionic charge on the electrode surface is negative. At sufficiently high concentrations of adsorbing anions cationic reaction rates are accelerated rather than retarded,[22] but this may simply reflect the fact that when the adsorption of anions becomes sufficiently extensive, the positive electronic charge density on the electrode is finally neutralized and the potential at the reaction site becomes negative. In addition, if the reaction site lay far enough from the electrode surface to be partially screened from the charges on the electrode by the ionic atmosphere of the diffuse layer, one might expect an ionic strength dependence of the effective potential at the reaction site for that reason as well. The kinetic data seem to show clearly that (at low to intermediate ionic strengths) specifically adsorbed anions do not effectively compensate for an equivalent quantity of positive electronic charge density on the electrode

surface as viewed by cationic reactants at their reaction sites. Under these conditions the reactant appears to be able to differentiate between electronic and ionic charge on the electrode surface and to respond differently to each.

PART I

CHAPTER II

KINETICS OF THE ELECTROREDUCTION OF $Co(NH_3)_6^{3+}$

Hexaamminecobalt(III) was also utilized as a diffuse layer probe reactant. The electroreduction of this cation has been rather extensively investigated as an example of a totally irreversible electrode reaction.[51-57] Laitinen and Kivalo[55] have proposed a mechanism for the electroreduction of the cobalt(III) to the labile cobalt(II) species.

$$[Co^{III}(NH_3)_6]^{3+} \xrightarrow{e^-} [Co^{II}(NH_3)_6]^{+2}_{labile}$$

$$\downarrow \text{fast}$$

$$[Co^{II}OH(NH_3)_4]OH_{ppt} + 2NH_4^+$$

$$\downarrow$$

$$[Co^{II}(H_2O)_6]^{2+}$$

The instability of the reduced product makes standard potential (and thus standard rate constant) determinations very unreliable. The release of ammine ligands by the labile cobalt(II) species raises the pH near the electrode surface and causes precipitation of intermediate cobalt(II) hydroxy-ammine complexes[51-53] in neutral or basic electrolytes.

Despite these drawbacks $Co(NH_3)_6^{3+}$ offers several appealing advantages for kinetically probing the diffuse layer. It carries a large symmetrical positive charge and reduces on positively charged mercury electrodes without chemical interaction with the electrode. The most attractive feature of this probe is its compatability with fluoride electrolytes which allows the investigation of electrode kinetics on a positively charged electrode under conditions where there is little or no specific adsorption of anions.[58] At the point of zero charge in fluoride (-434 mV) there is almost certainly no diffuse layer or diffuse layer potential present. Fortunately the rate of reduction of the complex is measurable at this potential (Figure I-10) which, in turn, yields a point on the $\phi_2 = 0$ line. This point coupled with an assumption that the intrinsic electrochemical transfer coefficient (α) is equal to 0.5 and independent of potential (see page 17) allows the construction of a $\phi_2 = 0$ line for the reduction of cobalt(III) hexaammine.

EXPERIMENTAL

Polarograms were measured with a Princeton Applied Research Model 174 Polarographic Analyzer and a Hewlett-

Packard X-Y Recorder. Cobalt(III) hexaammine trichloride was found on the shelf and recrystallized twice as the perchlorate salt. Stock solutions of cobalt hexaammine were made fresh the day of the particular experiment. All water was triply distilled and all electrolyte chemicals were reagent grade and used without purification. Polarograms were corrected for mass transfer by means of the formula of Oldham and Parry[13] using the current values at the end of drop life.

RESULTS AND DISCUSSION

Figure I-10 shows a set of polarograms for the reduction of $Co(NH_3)_6^{3+}$ in 1 M potassium fluoride buffered with a small amount of hydrofluoric acid to which small amounts of various adsorbable anions have been added. Large anodic shifts in the polarographic wave, corresponding to rate enhancements, are exhibited when even small amounts (as little as 40 μM iodide shifts the half wave ~100 millivolts) of anions are present in the bulk of the solution. The rate enhancements correlated with the strength of the specific adsorption of the anion.[36]

$$I^- > SCN^- > Br^- > Cl^- > ClO_4^-$$

The Tafel line for the reduction of $Co(NH_3)_6^{3+}$ in 1M potassium fluoride is shown in the right side of Figure I-11A and illustrates the construction of the $\phi_2 = 0$ line

FIGURE I-10

Polarograms from current at the end of drop life for the reduction of .2 mM $Co(NH_3)_6^{3+}$ in 1 M KF+1.2 mM HF with the addition of various adsorable anions; (1) no addition; (2) 1 mM KBr; (3) 1 mM KSCN; (4) 4 mM KBr; (5) 40 μM KI. (Flow rate = 1.78 mg/sec; drop time = 4.8 sec)

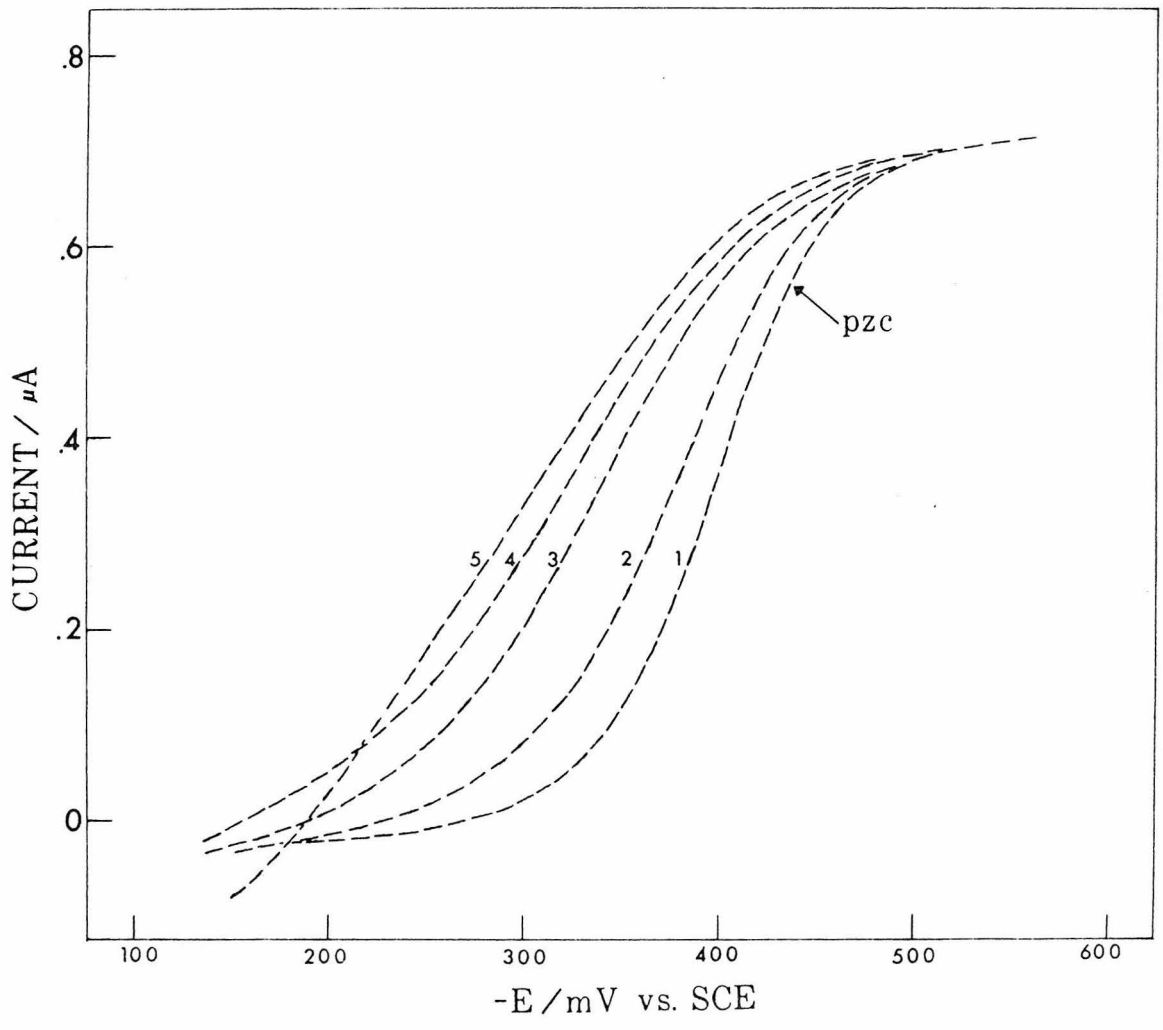
.8
.6
.4
.2
0
CURRENT / μA
pzc
5
4
3
2
1
100
200
300
400
500
600
-E / mV vs. SCE

FIGURE I-11 A and B

A. Tafel lines for the reduction of $Co(NH_3)_6^{3+}$ in the following electrolytes; (○) 1 M KF + 1.2 mM HF, (△) 10 mM $HClO_4$, (□) 10 mM $HClO_4$ + .4 mM KBr, (⬡) 10 mM $HClO_4$ + .8 mM KBr, (◇) 10 mM $HClO_4$ + 2 mM KBr.

B. Tafel lines for the oxidation of Eu^{+2} in the following electrolytes; (○) 10 mM $HClO_4$, (⬡) 10 mM $HClO_4$ + .8 mM KBr, (◇) 10 mM $HClO_4$ + 2 mM KBr.

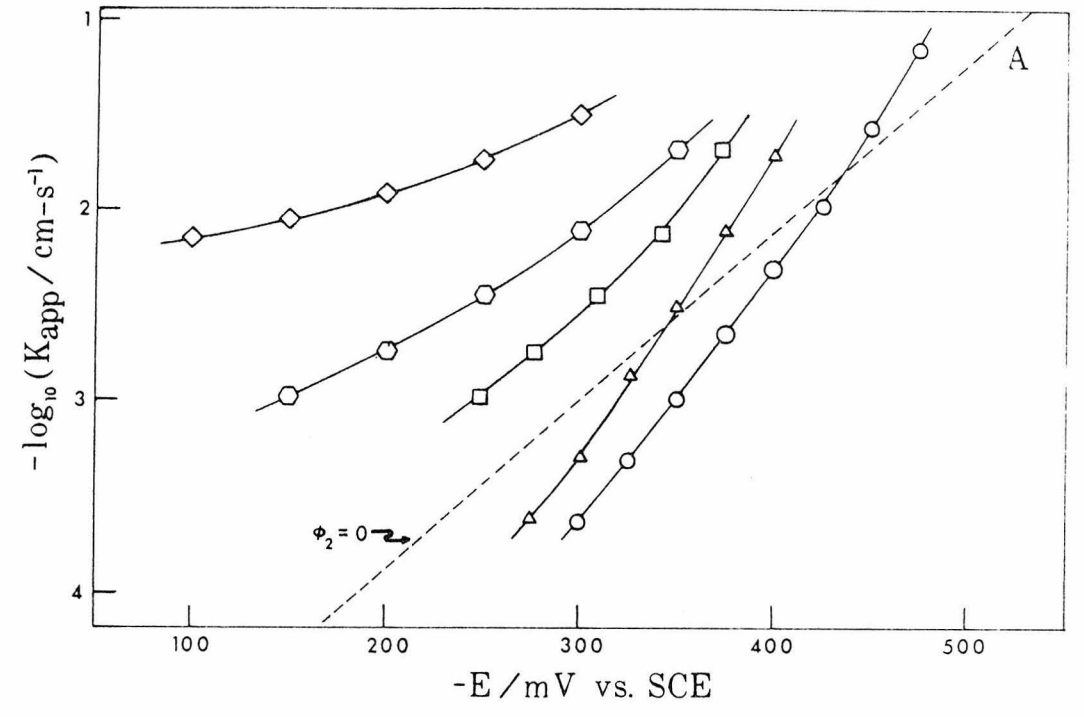
A
$\Phi_2 = 0$
$-\log_{10}(K_{app}/cm\text{-}s^{-1})$
1
2
3
4
100
200
300
400
500
-E/mV vs. SCE

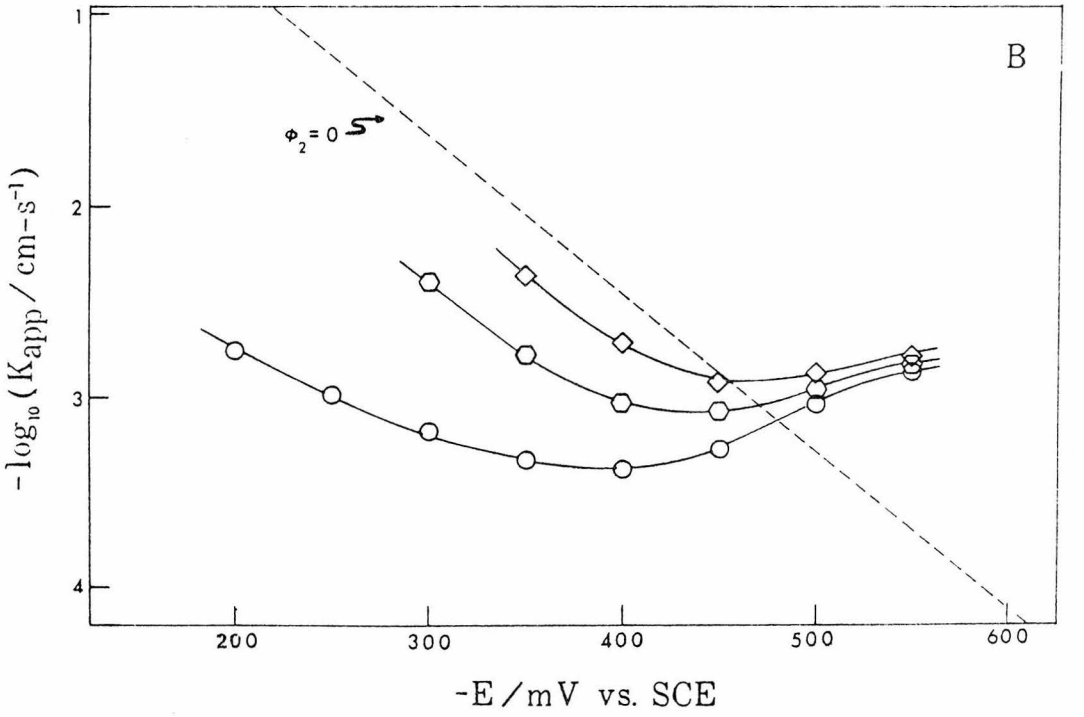
B
$\Phi_2 = 0$
$-\log_{10}(K_{app}/cm\text{-}s^{-1})$
1
2
3
4
200
300
400
500
600
-E/mV vs. SCE

for this system. The reduction rate at the p.z.c. was not a function of the fluoride ion concentration from .01 M to 1 M which is a good justification for the method of constructing the $\phi_2 = 0$ line. Apparently the extent of ion pair formation (if any) of $Co(NH_3)_6^{3+}$ and fluoride does not influence the intrinsic reaction rate.

A comparison of the response of the reduction rate of $Co(NH_3)_6^{3+}$ and the oxidation rate of a bona fide outer sphere reactant, $Eu(H_2O)_x^{2+}$, to the addition of small amounts of bromide to a 10 mM perchloric acid electrolyte (an electrolyte compatible with both reactants) is shown in Figure I-11A and I-11B. The figure reveals not only the greater response of $Co(NH_3)_6^{3+}$ reduction to the anion addition but also that this ion is experiencing an apparently negative potential at its reaction site.* The negative ϕ_r values are in contrast to the positive ϕ_r values rather convincingly established by Eu^{+2} at many of the same potentials in the same electrolytes (Figure I-11B).

Almost parallel behavior has been reported by Weaver and Satterburg[31] and Anson, et.al.,[59] for the

---

* In both Figure I-11A and I-11B Tafel lines below the $\phi_2 = 0$ line indicate positive ϕ_r values while a line lying above indicates negative ϕ_r values.

reduction of a variety of chromium(III) ammine complexes in constant ionic strength electrolytes at mercury electrodes with varying iodide coverages. The rate increases observed by them for $Cr(H_2O)_6^{3+}$ reduction in the same electrolytes were not as great as with the ammine complexes and more in accord with the increases calculated from iodide adsorption data and GCS theory. The larger than expected rate increases for $Cr(NH_3)_6^{3+}$ reduction were explained in reference 31 by the smaller hydrated radii [$Cr(NH_3)_6^{3+}$ = 2.80 Å[61] $Cr(H_2O)_6^{3+}$ = 4.12 Å[61]] for the ammine complex which results in a reaction site much closer to the electrode surface which would make the reactant more susceptible to the discrete nature of the now less screened adsorbed anions. Values of α_{app} were presented in reference 31 as evidence that the reduction of the complex still proceeded by an outer-sphere electron transfer pathway.[62]

Homogeneous electron transfer reactions involving ammine complexes have also shown rate increases upon addition of potentially bridging anions.[63-66] Sutin[66] has studied the reduction of $Co(NH_3)_6^{3+}$ by chromium(II) and vanadium(II) and found large rate enhancements when chloride or thiocyanate were present in the reaction mixture. He proposes an anion assisted outer-sphere

electron transfer mechanism where the anion is bridging the oxidant and reductant in the transition state.*

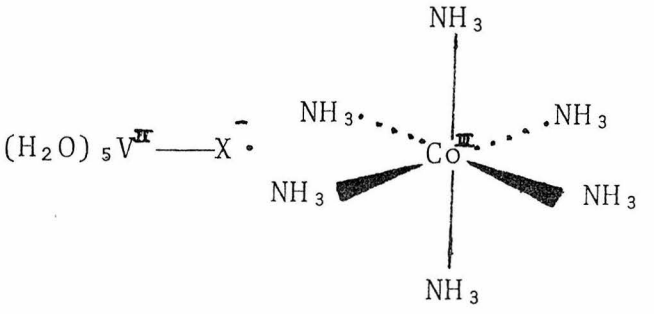

Thiocyanate was found to be a more effective bridge than chloride. Evidence was presented to support the fact that the bridging anion (in the case of thiocyanate) had entered the coordination sphere of the reductant before electron transfer when vanadium(II) was utilized as the reductant.

A similar pathway could be envisioned for the electrode reduction of $Co(NH_3)_6^{3+}$ on a mercury electrode where the anion is now adsorbed on the electrode.

---

* It is unclear whether an anion assisted pathway means that the anion is actually involved in the conduction of the electron or merely acts to help bring the two positively charged reactants together.

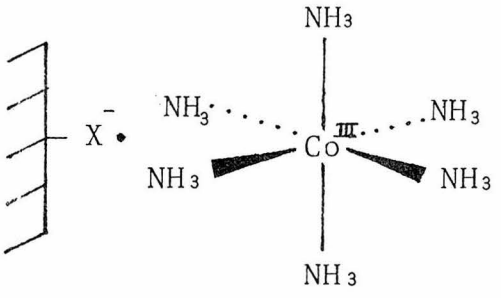

This mechanism would be favored over the direct reduction of a cobalt hexaammine-halide ion pair diffusing to the electrode because of Sutin's observation that the thiocyanate ion had entered the coordination sphere of the reductant in the homogeneous case. Also the catalysis observed at an electrode is not a function of the ion pair concentration in the bulk of the solution.

In both chromium(III) and cobalt(III) ammine complexes a significant barrier exists to electron transfer. In chromium(III) the electron goes into an e_g orbital which will destroy the relative stability of a half filled t_{2g} level.

The cobalt(III) reactants are in low-spin $t_{2g}^6 e_g^0$ states while the ground states of cobalt(II) products are usually high spin $t_{2g}^5 e_g^2$. Reduction reactions of cobalt(III) are thus partially spin forbidden and for this reason could be non-adiabatic. Several mechanisms for cobalt(III) reduction have been proposed:[66] If the

cobalt(III) must rearrange to a $t_{2g}^5 e_g^1$ state before electron transfer occurs the promotional energy required to excite the low spin cobalt(III) complex to the high spin state could cause the reaction to proceed only at very high over-potentials and only (in the absence of adsorbed anions) on negatively charged or slightly positively charged electrodes due to the repulsion between the highly charged reactant and the electrode.

The second mechanism postulates the cobalt(II) product is formed in the $t_{2g}^6 e_g^1$ state, the unfavorable energetics for the production of such an excited cobalt(II) could be responsible for the sluggishness of the reaction.

$[Co(III)(NH_3)_6 \cdot X]^{2+}$ ion pairs have been observed in solution by examination of a charge transfer band in the ultraviolet absorption spectra arising from an electron transfer from the halide (X^-) to the cobalt center.[67,68] This tendency for ion pair formation in the bulk make it attractive to postulate that such ion pairs may be formed with the relative excesses of anions found at the mercury-solution interface. Ion pairing in the inner layer would result in a configuration resembling the transition state depicted on page 54.

An unambiguous differentiation between rate enhancements brought about by adsorbed anions due to purely double layer effects or as a result of an anion-

assisted electron transfer pathway is non-trivial. However, the contrasting behavior shown in Figure I-11 for europium and cobalt hexaammine certainly suggests that different factors are involved in controlling their respective electron transfer rates.

Guildelli and Foresti[69] have introduced a model which contains a linear term for the adsorbed charge density into a rate expression. The model was employed to explain adsorbed anion effects on a variety of inner-sphere anion reduction rates at mercury electrodes.[4-7] It has not been applied to cationic reactants where adsorbed anions attract rather than repel the reacting ion. The model is not invoked in dilute elctrolytes or where the coverage of the electrode by adsorbed anions is low[70] as is the case with the electrolytes in this study.

Coulombic effects on the electrode reaction due to the singly charged adsorbed halide ions would be relatively insensitive to the chemical nature of the anion whereas the anion assisted electron transfer mechanism would be dependent on chemical interactions between the reactant and adsorbed ions. Lack of reliable double layer data for the range of halide electrolytes needed to do rate comparisons at constant adsorbed charge density presents a problem. Also the

different (and perhaps unknown) extent of ion pair formation with $Co(NH_3)_6^{3+}$ by the various anions in the bulk of solution would make the charge on the reactant unknown which in turn would make the o.H.p. concentration of the reactant uncertain.

Haim[71] has explained reactivity pattern in homogeneous inner-sphere electron transfer reactions of $Co(NH_3)_5X^{2+}$ complexes by considering the stability constants for the formation of a bridged transition state. Quantitative evaluation of the transition state stabilities at an electrode surface are not reliable because of the uncertain $Co(NH_3)_6^{3+}$ halide ion pair constants.[66] However the differences between the reported values of the ion pair constants for the various halides are not large[67,68] whereas the strength of the interaction of an iodide ion with a mercury electrode is considerably stronger than the interaction of a chloride or fluoride ion with mercury. This reasoning would predict the reactivity order observed:

$$I^- > Br^- > Cl^- \approx ClO^- >> F^-$$

This model would explain the extreme sensitivity of the $Co(NH_3)_6^{3+}$ reduction reaction to adsorbed iodide (Koltoff[52] observed a significant effect for as little as 1 micromolar iodide). Perchlorate ions which

are adsorbed to about the same extent as chloride ions catalyze the reduction of $Co(NH_3)_6^{3+}$ to about the same extent. The fact that perchlorate would be expected to be a rather poor electron transfer bridge would indicate that the adsorbed anion acts as an agent for bringing a highly positively charged reactant and a positive electrode together into a more stable lower charged transition state.

A possible diagnostic test for the anion assisted electron transfer pathway would involve studying the temperature dependence of the electrode reaction rate at constant potential and electrolyte composition. Decreases in electrode reaction rates have been observed with increasing temperature[72] for the oxidation of chromium(II) in thiocyanate electrolytes. The rate decreases as a result of the desorption of thiocyanate ions at higher temperatures outstripping the intrinsic increase in the ligand bridged inner-sphere reaction rate. A similar effect for the reduction of hexaammine cobalt(III) would be good but not conclusive evidence that the anion was involved in the transition state.

CONCLUSION

To construct an overall model which will encompass the electrode kinetic behavior of both the aquo and ammine

metal ion complexes is not an easy task. One might visualize the situation as follows:* The secondary hydration of the aquo ions (Eu^{+2}, V^{+2}, Cr^{+2}, Eu^{+3}, Cr^{+3}) does not allow them to penetrate the hydration of the electrode and confines them to a position where there is considerable sheilding of the charge on the electrode due to the adsorbed anions. The ammine complexes ($Cr(NH_3)_6^{3+}$, $Co(NH_3)_6^{3+}$) are not as strongly hydrated which allows them to penetrate to the inner layer and thus be more influenced by the adsorbed anions residing there. $Cr(NH_3)_6^{3+}$ is reduced on a negatively charged electrode by parallel anion assisted and outer-sphere pathways whereas $Co(NH_3)_6^{3+}$ reacts of a positively charged electrode and is restricted to reacting by the anion assisted pathway because of the repulsion between the electrode and the $Co(NH_3)_6^{3+}$ cation at these potentials.

---

* That is if one is allowed some speculation in one's thesis.

REFERENCES AND NOTES

(1) A. Frumkin, Z. Phys. Chem., 164A, 121 (1933).

(2) R. de Levie and M. Neves, J. Electroanal. Chem., 58, 123 (1975).

(3) L. Gierst and Cornelisson, Col. Czech. Chem. Com., 25, 3004 (1960).

(4) D. Cozzi, M. Foresti and R. Guidelli, J. Electroanal. Chem., 47, App. 31 (1973).

(5) M. Foresti and R. Guidelli, J. Electroanal. Chem., 53, 219 (1974).

(6) M. Foresti, D. Cozzi and R. Guidelli, J. Electroanal. Chem., 53, 235 (1974).

(7) R. Guidelli and M. Foresti, J. Electroanal. Chem., 67, 231 (1976).

(8) B. Damaskin, J. Electroanal. Chem., 65, 799 (1975).

(9) L. Gierst, E. Nicolas and L. Tytgat-Vandenberghen, Croat. Chem. Acta., 42, 117 (1970).

(10) M. J. Weaver and F. C. Anson, J. Electroanal. Chem., 65, 711 (1975).

(11) M. J. Weaver and F. C. Anson, J. Electroanal. Chem., 65, 737 (1975).

(12) C. D. Russell, J. Electroanal. Chem., 6, 486 (1963).

(13) K. B. Oldham and E. P. Parry, Anal. Chem., 40, 65 (1968).

(14) A. R. Sears and F. C. Anson, J. Electroanal. Chem., 47, 521 (1973).

(15) J. Lawrence, R. Parsons and R. Payne, J. Electroanal. Chem., 16, 193 (1968).

(16) R. de Levie, J. Electrochem. Soc., 118, 185c (1971).

(17) C. V. D'Alkaine, E. R. Gonzalez and R. Parsons, J. Electroanal. Chem., 32, 57 (1971).

(18) R. Parsons and S. Trasatti, Trans. Faraday Soc., 65, 3314 (1969).

(19) D. C. Grahame and R. Parsons, J. Am. Chem. Soc., 83, 1291 (1961).

(20) G. Lauer and R. A. Osteryoung, Anal. Chem., 39, 1866 (1967).

(21) F. C. Anson, R. Martin and C. Yarnitzky, J. Phy. Chem., 73, 1835 (1969).

(22) M. J. Weaver and F. C. Anson, J. Electroanal. Chem., in press.

(23) K. Niki and H. Mizota, J. Electroanal. Chem., 72, 307 (1976).

(24) R. Payne, Trans. Faraday Soc., 64, 1638 (1968).

(25) R. Parsons and R. Payne, Z. Phys. Chem. N.F., 98, 9 (1975).

(26) M. J. Weaver and F. C. Anson, J. Phys. Chem., 80, 1861 (1976).

(27) F. C. Anson, N. Rathjen and R. Frisbee, J. Electrochem. Soc., 117, 477 (1970).

(28) D. C. Grahame, J. Am. Chem. Soc., 76, 4819 (1954).

(29) J. E. B. Randles and D. R. Whitehouse, Trans. Faraday Soc., 64, 1376 (1968).

(30) L. G. Sillen and A. E. Martell, "Stability Constants", Chem. Soc. London, 1964.

(31) M. J. Weaver and T. L. Satterburg, J, Phys. Chem., 81, 1772 (1977).

(32) J. L'M Bockris and A. K. Reddy, "Modern Electrochemistry", Vol. II, 1973

(33) V^{+2} would be expected to be close to the hydrated radii for other 2+ transition metals ~3.4 Å while E^{+2} will be close to analogous rare earth hydrates 23.9 Å.

(34) K. M. Joshi and R. Parsons, Electrochem. Acta., 4, 129 (1961).

(35) R. Payne in Prog. in Surface and Membrane Science, J. T. Danelli, M. D. Rosenberg and D. A. Cadenhead eds., Academic Press, N.Y., 1973, Vol. VI, p. 51.

(36) D. C. Grahame, Chem. Rev., 47, 441 (1947).

(37) H. D. Hurwitz, J. Electroanal. Chem., 10, 35 (1965).

(38) Dutkiewitz and R. Parsons, J. Electroanal. Chem., 11, 1100 (1966).

(39) R. Payne, J. Phys. Chem., 70, 204 (1966).

(40) This asserted behavior is readily verified for several anions by comparing data in the following pairs of

references: chloride (24 and 41) nitrate (42 and 43); bromide (44 and 45) iodide (46 and 47).

(41) D. C. Grahame and R. Parsons, J. Am. Chem. Soc., 83, 1291 (1961).

(42) R. Payne, J. Phys. Chem., 69, 4113 (1965).

(43) R. Payne, J. Electrochem. Soc., 113, 999 (1966).

(44) J. Lawrence, R. Parsons and R. Payne, J. Electroanal. Chem., 16, 193 (1968).

(45) A. R. Sears and P. J. Lyons, J. Electroanal. Chem., 42, 69 (1973).

(46) D. C. Grahame, J. Am. Chem. Soc., 80, 4201 (1958).

(47) W. R. Fawcett and T. A. McCarrick, J. Electrochem. Soc., 127, 1325 (1976).

(48) D. M. Mohilner in Electroanalytical Chemistry, A. J. Bard, ed., M. Dekker Inc., N.Y., 1966, Vol. I

(49) W. R. Fawcett and S. Levine, J. Electroanal. Chem., 43, 175 (1973).

(50) K. Alias, W. R. Fawcett and R. Parsons, J. Chem. Soc. Faraday Trans. I, 70, 1046 (1974).

(51) I. M. Kolthoff and S. E. Khalafalla, Rev. Polarogr. (Japan), 11, 11 (1963).

(52) I. M. Kolthoff and S. E. Khalafalla, Inorg. Chem., 2, 133 (1963).

(53) I. M. Kolthoff and S. E. Khalafalla, J. Am. Chem. Soc., 85, 664 (1963).

(54) H. A. Laitinen, J. C. Bailar, Jr., H. F. Holtzclan, Jr. and J. V. Quagliano, J. Am. Chem. Soc., 70, 2999 (1948).

(55) H. A. Laitinen and P. Kivalo, J. Am. Chem. Soc., 75, 2198 (1953).

(56) H. A. Laitinen, A. J. Frank and P. Kivalo, J. Am. Chem. Soc., 75, 2865 (1945).

(57) L. N. Klatt and W. J. Blaedel, Anal. Chem., 39, 1065 (1967).

(58) D. C. Grahame, J. Am. Chem. Soc., 76, 4821 (1954).

(59) F. C. Anson, A. Yamada and M. G. Finn, Inorg. Chem., 16, 2124 (1977).

(60) T. Takahashi, T. Koiso, Bul. Chem. Soc. Japan, 49, 2784 (1976).

(61) E. R. Nightingale, J. Phys. Chem., 63, 1381 (1959).

(62) M. J. Weaver and F. C. Anson, Inorg. Chem., 15, 1871 (1976).

(63) A. Zwickel and H. Taube, Inorg. Chem., 4, 1029 (1965).

(64) J. F. Endicott and H. Taube, Inorg. Chem., 4, 437, (1965).

(65) P. V. Manning and R. C. Jarnagin, J. Phys. Chem., 67, 2284 (1963).

(66) T. J. Przystas and N. Sutin, J. Am. Chem. Soc., 95, 5545 (1973).

(67) M. G. Evans and G. H. Nancollas, Trans. Faraday Soc., 49, 363 (1953).

(68) E. L. King, J. H. Espenson and R. E. Visco, J. Phys. Chem., 63, 755 (1959).

(69) R. Guidelli and M. L. Foresti, Electrochim. Acta., 18, 201 (1973).

(70) R. Guidelli, J. Electroanal. Chem., 53, 205 (1970).

(71) A. Haim, Inorg. Chem., 7, 1475 (1968).

(72) D. J. Barclay, E. P. Passeron and F. C. Anson, Inorg. Chem., 9, 1024 (1970).

PART II

The Formation of Polymeric Surface Phases on Mercury Electrodes from Solutions Containing Thioethercarboxylates and White Metal Cations

PART II

CHAPTER I

INTRODUCTION

CLASSES OF ADSORPTION AT MERCURY ELECTRODES

Adsorption at electrodes is an important aspect of virtually all areas of electrochemistry. It is of prime importance to the fields of electrocatalysis, electrosynthesis, electrochemical energy conversion and electrode kinetics. The adsorption process has been most extensively studied and perhaps best understood at mercury electrodes because of mercury's readily renewable surface and the accessibility to measurement of qualities thermodynamically related to the interfacial tension of the metal.

In a recent article, Anson[1] has loosely grouped the types of adsorption encountered at the mercury-solution interface into five classes which will be briefly discussed below.

The first class of adsorbates contains the simple inorganic anions and cations. The class was divided into class IA and class IB ions. The adsorption of class IA ions is due to purely electrostatic forces and the hydrophobic nature of the ions in this class which includes ClO_4^-, PF_6^- and NO_3^-.

Class IB ions are distinguished from class IA by the strength of their adsorption which is a result of both covalent and electrostatic interactions between the adsorbate and the electrode. Halide ions are the best known examples of this class.

The potential dependence of class I adsorbates is inverse to the charge carried by the ion. Cations are adsorbed at more negative potentials while the maximum adsorption observed for anions is upon positively charged electrodes.

Neutral organic molecules compose the second class of adsorbates. These molecules are adsorbed due to hydrophobic nature of organic molecules or because of π electrons or lone pair electrons being shared with the metal surface.

The maximum adsorption for organic molecules is usually at or near the point of zero charge of the electrode because the water-electrode interaction is weakest in this potential region which allows the organic molecule to penetrate the solvation sheath of the electrode.

Class III adsorption differs from the first two classes in that it involves the co-adsorption of two materials one of which induces the adsorption of the other. Cations from the groups immediately following the transition metals such as Zn(II), Cd(II), Pb(II), Tl(I) and In(III) can be induced to adsorb from solutions containing class IB anions but show

very little tendency to adsorb from solutions of non-adsorbing anions such as F^- or from solutions of class IA anions. The potential dependence of class III adsorption is a function of the amount of the class IB anion which is co-adsorbed. The adsorption is also dependent upon the strength and speciation of the metal ion complexes with the ligand in the bulk of the solution.

The fourth class of adsorbates consists of transition metal complex ions whose adsorption on mercury is induced by chemical interactions between the ligand ions (usually thiocyanate) and the electrode. This class is distinguished from the anion-induced adsorption of class III by the fact that no anion need be adsorbed to facilitate metal adsorption and class IV adsorbates are much more strongly adsorbed (saturation coverages can be observed for some complexes in submillimolar concentration ranges). Apparently attractive interactions between like charged adsorbed complexes is an intriging aspect of this class of adsorbates. Ligand field stabilization energy gains for some metal d electron configurations when bridged by a ligand to Hg^o have been invoked to explain the strength and attractive interactions associated with this type of adsorption. Chromium (III) (d^3) and ruthenium(III) (d^5) isothiocyanate complexes are the best examples of this class of adsorbates.

The final class of adsorbates is the newest and as yet contains only a few members. The property which characterizes

class V adsorption is the formation of metal-metal bonds between the adsorbing complex and the electrode surface. The rate of adsorption for these compounds is much smaller than adsorption rates for most all adsorbates perhaps due to the sluggishness of forming the metal-metal bonds or to a chemical step preceding the adsorption process. Examples of this class include bisethylenediammine rhodium(I) and pentacyanocobalt(II).

SURFACE PHASE FORMATION AT MERCURY ELECTRODES

The formation of a film or surface phase on a mercury electrode is a process which is closely akin to the adsorption process. Surface phases do not fit neatly into the categories outlined above, however their formation and stability is most likely controlled by some of the same forces. Some of the types of films which have been described are briefly discussed below.

Anodic films are formed from the oxidation of a mercury or analgam surface in the presence of sparingly soluble complex forming species.

Organic films can be formed at or near the p.z.c. from solutions containing reasonably large concentrations of very hydrophobic organic molecules.

Murray and co-workers[2-4] have reported so called "crystalline bilayer" formation on mercury electrodes from solutions slightly less than saturated with respect to three dimensional crystal formation. This behavior is usually seen with solutions from which anion assisted adsorption is observed at lower concentrations.

in particular Pb(II) and Tl(I) solutions containing halide ions. Sharp discontinuities in both the potential dependence and anion concentration dependence of the adsorption indicate that attractive interactions exist between the adsorbed units as in class IV adsorbates. The exact structure and stoichiometry of the adsorbed bilayers remains to be determined but the quantity of metal cation adsorbed beyond the discontinuity is close to monolayer coverage of adsorbed metal halide. For Tl(I) in bromide, two discontinuities are observed and the adsorption increases by almost exactly two-fold on going from the first to the second.

In Part II of this thesis a number of new examples of surface phases on mercury electrodes will be presented. The most striking of these phases and the ones which will be emphasized are made up of Pb(II) and ligands containing both carboxylate and thioether functionality although other metals and ligands may also form similar phases but to a lesser degree.

EXPERIMENTAL

Reagents

All water used was triply distilled with the second distillation from an alkaline permanganate solution. $NaClO_4$ was obtained from reagent grade perchloric acid neutralized with reagent sodium carbonate, filtered and

reacidified to pH ~3. The perchlorate ion concentration was standardized using a perchlorate ion selective electrode from Orion Research Inc.

2,2'-Thiodiacetic acid (TDA) and 3,3'-thiodipropionic (TDP) acid were obtained from Matheson Coleman and Bell. Thiodisuccinic acid (TDS), methylene bisthioacetate (MBTA) and thioacetatosuccinate (TAS) were kindly supplied by Evans Chemetics Co. Ethylthioacetate, diglycollic acid (DCA) and sodium mercaptaacetate were purchased from Aldrich Chemical Co. 2,2'-Thiobis[ethyliminodi(acetate)] (DDSTA) was prepared by Pam Peerce. All ligands were recrystallized as the sodium salts two or three times from water by adding ethanol until the salt precipitated. The recrystallizations were repeated until no odor could be detected from the solid and no time dependent spurious peaks in the potential range +200 to -600 were observed with cyclic voltammetry at a hanging mercury drop electrode equilibrated 30 to 60 seconds in an electrolyte solution containing the ligand. It was found such precautions were necessary to eliminate mercaptan impurities which were likely starting materials in the thioether synthesis.

Lead nitrate, cadmium nitrate, thalium nitrate and zinc nitrate were reagent grade and used without further purification. Solutions were deoxygenated with prepurified argon or nitrogen which had been passed through an acidic

vanadium(II) solution to remove traces of oxygen. Mercury was triply distilled and obtained from Bethlehem Instrument Company. Europium(III) perchlorate was prepared as described in the Experimental Secion of Part I-A of this thesis.

Apparatus

A hanging mercury drop electrode (HMDE) from Brinkman Instruments was used with a drop of an area of .032 cm^2. A saturated sodium calomel electrode was used as a reference electrode and all potentials are reported relative to it. Double potential step chronocoulometry[5,6] was performed on a potentiostat and integrator controlled by a PDP 11/40 mini-computer system with a program written by Don Glover and modified for graphic output and rapid repetitive operation.

Most chronocoulometric data were obtained using a procedure as follows: A drop was extruded into a solution of 1 M $NaClO_4$ with lead and ligand present and shortly thereafter the computer would connect the potentiostat at the initial potential for an equilibration time, usually five seconds. Just before the potential step, the integrator was connected and 50 baseline points were taken after which the potential was stepped to -1000 mV and 100 points were converted from the integrator by the analog to digital converter, then the potential was returned to the initial value and another 100 points were stored. The usual time between points was 200 microseconds. (There was very little difference in the final parameters for data acquisition times from 75 to

2000 microseconds.) When data collection was complete the computer would disconnect the working electrode and integrator and reduce the data with the appropriate least square routines and output forward and reverse slopes and intercepts, double layer charge and nFΓ (the surface excess of reducible species). The entire procedure was usually repeated three times at each potential before the computer would set a new initial potential. After a complete potential dependence was measured an aliquot of the sodium salt of the ligand being studied was added via a microliter syringe to avoid dilution and the complete process was again repeated.

The reproducibility of surface coverages for lead was usually better than two percent at any given potential but larger deviations could be observed in potential regions where there was a large potential dependence of the adsorption or when cadmium was the adsorbing metal. Variation of the equilibration time (the time the electrode was exposed to the solution at the initial potential before the potential step) from 5 seconds to 60 seconds had only a small effect (<10%) on the amount of lead accumulated at the interface at potentials where the potential dependence of the adsorption was not large. The lead thiodipropionate system had a somewhat greater equilibration time dependence as did all of the ligands studied when cadmium was the metal present in the solution.

Capacity and resistance measurements were made with a HMDE by applying an A.C. signal of known frequency and amplitude to the electrochemical cell and measuring the in-phase and out-of-phase components of the cell current by using an Ithaco Model 391-A Lock-in Amplifier and a Fluke Model 2000A Digital Voltmeter. Measurements were made at a frequency of 1000 Hertz with an amplitude of 5 millivolts. A Princeton Applied Research Model 173 Potentiostat was employed for these measurements.

A time dependence of the in- and out-of-phase signals was observed for both solutions from which strong adsorption was observed and the blank of 1 M $NaClO_4$ electrolyte. A slow decrease in the capacitance of the blank required that measurements be made within five seconds of drop extrusion. In the solutions from which strong adsorption had been measured an initial rapid capacity change occurred followed by a slow decrease similar to that observed in the electrolyte alone Measurements were taken immediately after the short time capacity transient which was usually within ten seconds of drop extrusion.

RESULTS AND DISCUSSION

THE ADSORPTION OF LOW VALENT SULFUR CONTAINING CARBOXYLYTE LIGANDS

The original intent of this research was to "functionalize" a mercury electrode in the same manner as graphite,[5] platinum[6] and tin oxide[7,8] electrodes have been modified by

workers in various laboratories. The well characterized and reproducible surface of mercury would be an excellent system to model the more complicated and less well characterized surfaces usually employed for chemical modification.

It was thought that ligands containing a low valent sulfur atom would provide a stable anchor to the electrode surface because of the propensity for strong interaction usually displayed by low valent sulfur atoms and mercury electrodes while other groups on the molecule would complex with other metal ions. (Sulfide ion is one of the strongest simple ionic adsorbates.[9]) Mercaptide ligands proved to be unsuitable as an anchor for two reasons. 1) They are electrochemically reactive at positive potentials forming both disulfides and mercury mercaptide compounds with complicated surface chemical mechansims.[10,11] 2) Mercaptans were found to be extremely efficient catalysts for hydrogen reduction on the mercury surface which is usually relatively inert to this process. Hydrogen evolution appeared at potentials as low as -600 mV in a pH 3 solution of perchloric acid in 1 M $NaClO_4$ with 1 mM mercaptoacetate ion present. The stabilization of hydrogen atoms bonded to the sulfur atom near the surface is perhaps the intermediate in this hydrogen ion reduction reaction.

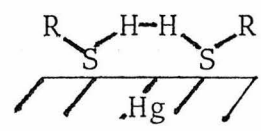

By replacing the hydrogen of the mercaptan with another R group intermediates of this type would be eliminated along with the complex mercaptan-disulfide electrochemistry.

Table I shows the structure of all the thioether compounds which will be discussed and the abreviations for the ligands that will be employed in the rest of this discussion. As expected these ligands do not catalyze hydrogen evolution at potentials positive of -1200 mV in solutions of pH 2 or above. Anodic polarograms of solutions containing thioether carboxylate ligands (with the exception of the strong mercury binder, DDSTA) did not reveal the presence of any mercury dissolution or ligand oxidation at potentials less positive than +250 mV.

The adsorption of carboxylic acids and carboxylate anions has not received much attention in the literature, however, studies of a few systems analogous to the ligands used in this study have been reported. The adsorption of butyric and isobutyric acid has been studied[12] in .1 M KBr. These compounds behaved like typical organic adsorbates with the maximum adsorption accurring near the p.z.c. Pospíšil and Kůta[13] studied the adsorption of maelic and succinic acid from .1 M $NaClO_4$, .05 M $HClO_4$ where the acids are fully protonated and from .1 M acetate buffer where the monovalent anion AH^- of the acid prevails. They found that the acids were typical of organic adsorbates

TABLE II-1

Summary of Ligands

Abrev.	Name	Structure	pK_A	$\log K_f^{Pb^{+2}}$
ETA	Ethylthioacetate	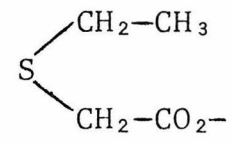	3.61	3.7 2.9
TDA	Thiodiacetate	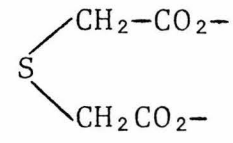	3.15 4.13	3.6
TDP	Thiodipropionate	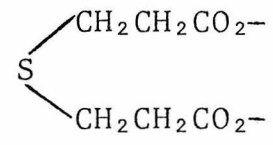	4.9 4.0	2.7
MBTA	Methylene-bisthioacetate	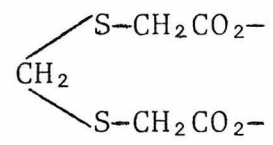	4.2 3.4	3.7
TAS	Thioacetatosuccinate	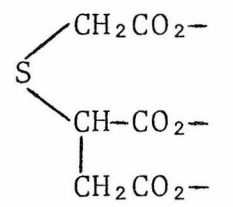	---	---
TDS	Thiodisuccinate	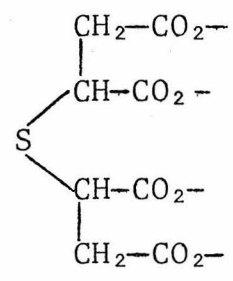	---	---

TABLE II-1 cont.

Abrev.	Name	Structure	pK_A	$\log K_f^{Pb^{+2}}$
DDSTA	2,2'thiobis[ethyliminodi(acetate)]	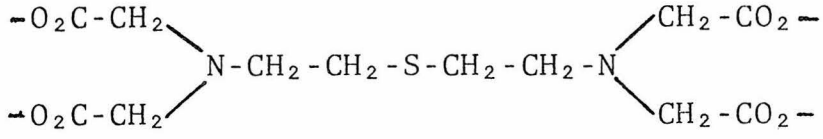	9.4 8.5 2.5 1.8	13.9
DGA	Diglycolate	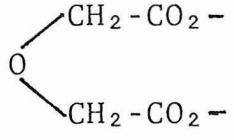	2.77 3.92	4.4

while the anion exhibited behavior not unlike class IA anions by adsorbing only on positive electrode surfaces. No studies of carboxylate dianion or thioether adsorption on mercury electrodes are available.

A study of the adsorption of the TDA dianion from a .3 M sodium fluoride solution was carried out using the technique by which the charge flowing into a growing mercury drop is measured. This technique is detailed in Appendix II.

Small increases (2 - 4 $\mu C/cm^2$) in the electrode charge (q^m) were observed when 50 mM TDA dianion was present in a .3 M NaF solution at potentials from -100 to -800 mV. Larger increases (5 - 15 $\mu C/cm^2$) in q^m were apparent at potentials positive of -100 mV.

Essentially the same behavior was observed for solutions containing anions of several other ligands in both fluoride and perchlorate electrolytes, however the charge changes in perchlorate were smaller due to competitive ClO_4^- adsorption.

It appears from these results that in the potential region from -800 mV to -100 mV the adsorbtion of the anions is similar to that observed for the monovalent anion of maleic acid.[13] At potentials positive of -100 mV the sudden increase in the measured electrode charge suggests that a different interaction has become important in particlar the specific interaction between the mercury surface and the sulfur atom. A structure similar to that depicted below could be visualized.

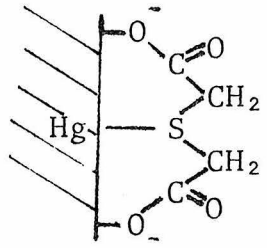

It appears as though the original aim of the research, the functionalization of a mercury surface, is thwarted by the lack of a strong interaction between the thioether sulfur atom and the mercury surface over most of the useful potential range on a mercury electrode. This conclusion follows from the lack of any dramatic change in the electrode charge at most potentials when relatively large concentrations of thioether-carboxylate ligands are present in the bulk of the solution.

Metal complexes of some ligands can be adsorbed much more strongly than the free ligands themselves, as in the case of class IV adsorption.[14] For this reason adsorption studies for a variety of metals from solutions containing thioethercarboxylate ligands were undertaken.

Adsorption of Thioethercarboxylates with Lead(II)

Similarities with Surface Precipitation

Very large adsorption as measured by DPSCC occurs from electrolyte solutions which contain lead(II) and thio-ethercarboxylate anions. The adsorption is characterized by several remarkable properties.

The first thing which is evident upon examining Figures II-1 - II-12 is the large amounts of lead accumulated at the interface with values as large as 8.3×10^{-10} moles per square centimeter for some of the more complex ligands (TAS, TDS).

The potential dependence of the adsorpiton is unusual, at low ligand concentrations all the ligands studied (with the possible exception of TDS) showed a minimum in the lead adsorption in the potential region of -50 to +50 mV and increasing adsorption at more positive or more negative potentials (Figures II-1, II-3, II-5, II-7, II-9, II-11). An isopotential point of the adsorption in the vicinity of +200 mV was observed for most of the ligands. Many systems also extrapolate to convergence at a single point at a negative potential which was beyond the potential where free lead ion is reduced and thus is inaccessible to chronocoulometric measurement when lead is present in the solution.

Another remarkable feature is the rapid increases observed in the adsorption over a narrow range of ligand concentration and the plateau regions which succeed the occasionally discontinuous increases (Figures II-2, II-4, II-6, II-8, II-10).

All of these properties are consistent with the formation of stable surface phases on the mercury surface

FIGURE II-1

Potential dependence of the amount of adsorbed lead as determined by chronocoulometry for solutions containing .5 mM Pb^{+2} in 1 M $NaClO_4$ with the following concentrations of sodium ethylthioacetate (ETA). A - 2 mM; B - .6 mM; C - .8 mM; D - 1.2 mM; E - 1.5 mM; F - 2.0 mM; G - 2.5 mM; H - 3.5 mM; I - 5.5 mM; J 7.5 mM. Each point represents an average of three chronocoulometric experiments.

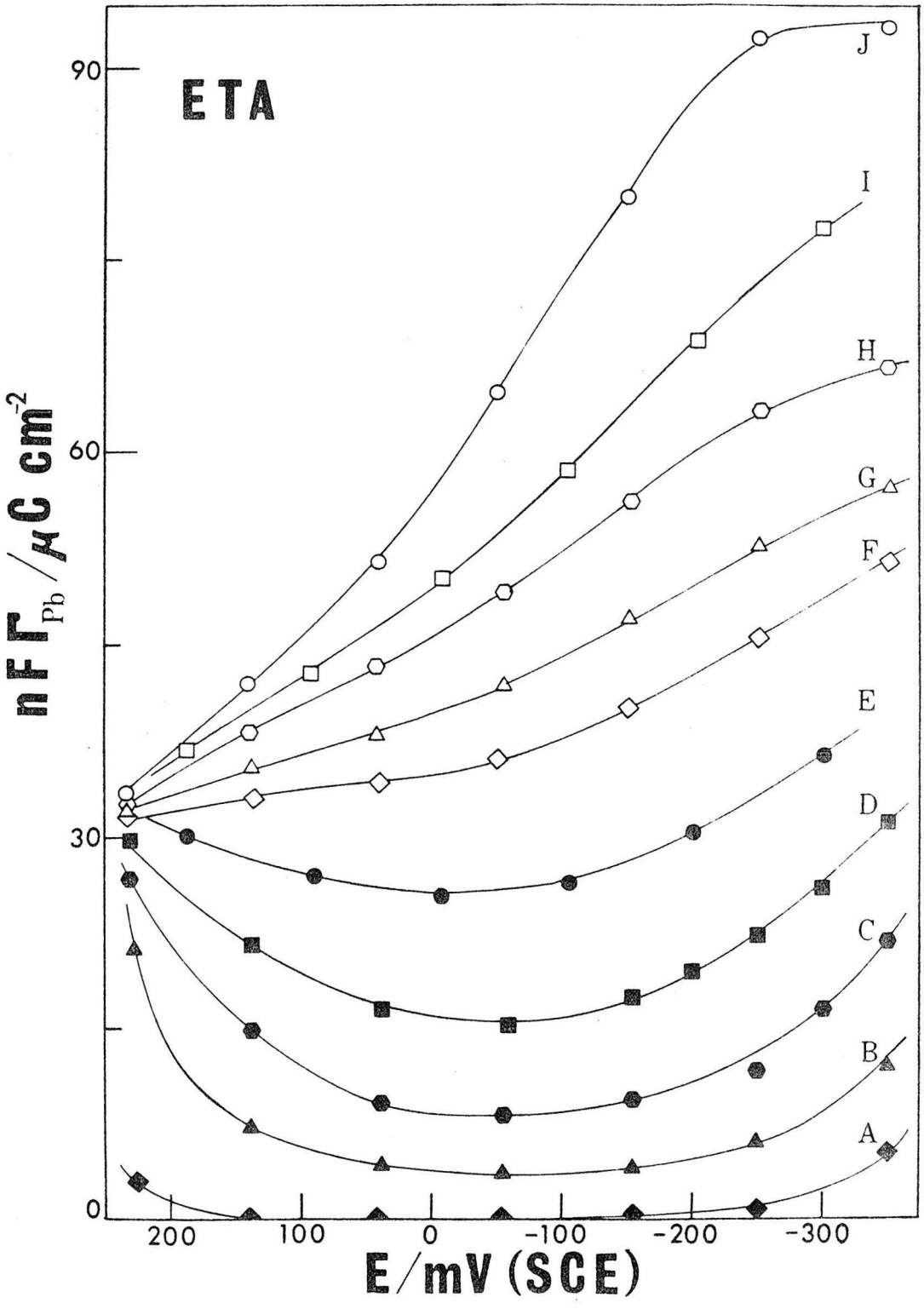
ETA
90
60
30
0
J
I
H
G
F
E
D
C
B
A
200
100
0
-100
-200
-300
E/mV (SCE)
nF Γ Pb /μC cm-2

FIGURE II-2

Amount of lead adsorbed as a function of the logarithm of ethylthioacetate ion concentration for a solution containing .5 mM Pb^{+2} and 1 M $NaClO_4$ at the following potentials: (△) +200 mV; (□) 0.0 mV; (○) -300 mV.

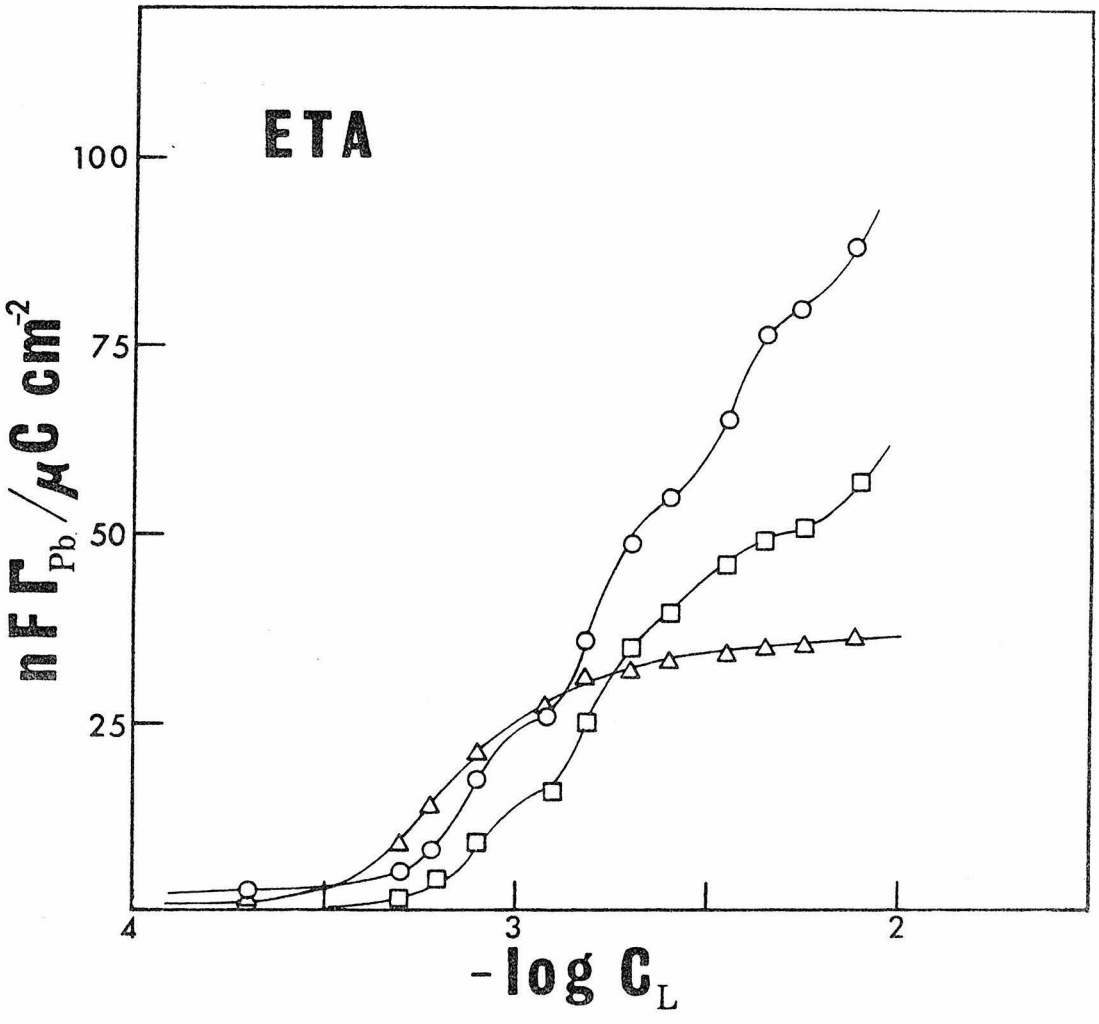
ETA
100
75
50
25
4
3
2
$nF\Gamma_{Pb}/\mu C\ cm^{-2}$
$-\log C_L$

FIGURE II-3

Potential dependence of the amount of adsorbed lead as determined by chronocoulometry for solutions containing .5 mM Pb^{+2} in 1 M $NaClO_4$ with the following concentrations of disodium thiodiacetate (TDA). A - .8 mM; B - 1.4 mM; C - 2.2 mM; D - 3.0 mM; E - 6.0 mM; F - 18.4 mM. Each point represents an average of three chronocoulometric experiments.

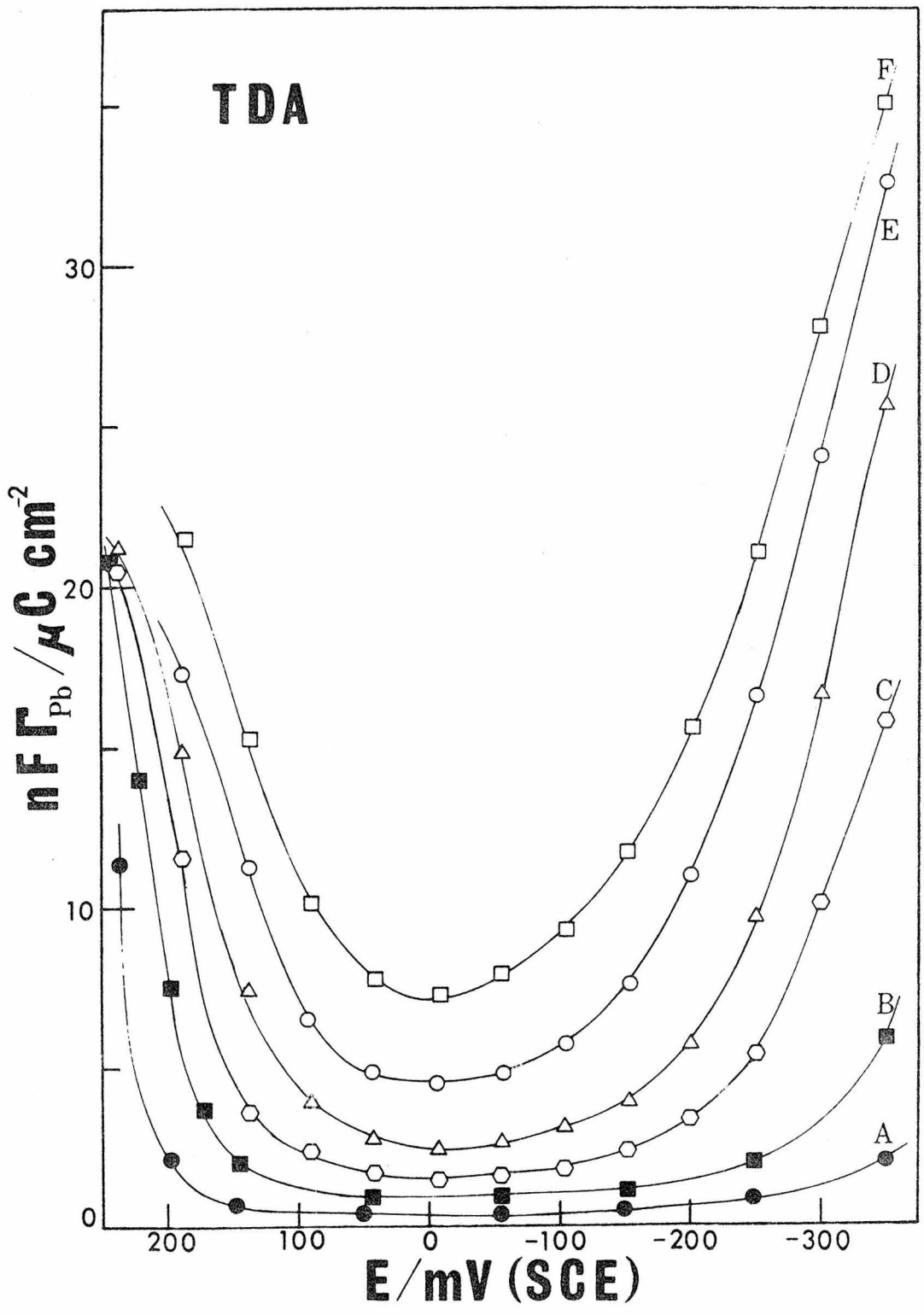
TDA
F
E
D
C
B
A
30
20
10
0
200
100
0
-100
-200
-300
E/mV (SCE)
nF Γ Pb /μC cm-2

FIGURE II-4

Amount of lead adsorbed as a function of the logarithm of thiodiacetate ion concentration in a solution 0.5 mM in Pb^{+2} and the following conditions: 1 M $NaClO_4$ - (■) +200 mV; (●) 0.0 mV; (▲) -300 mV. 0.1 M $NaClO_4$ - (□) +200 mV; (○) 0.0 mV; (△) -300 mV.

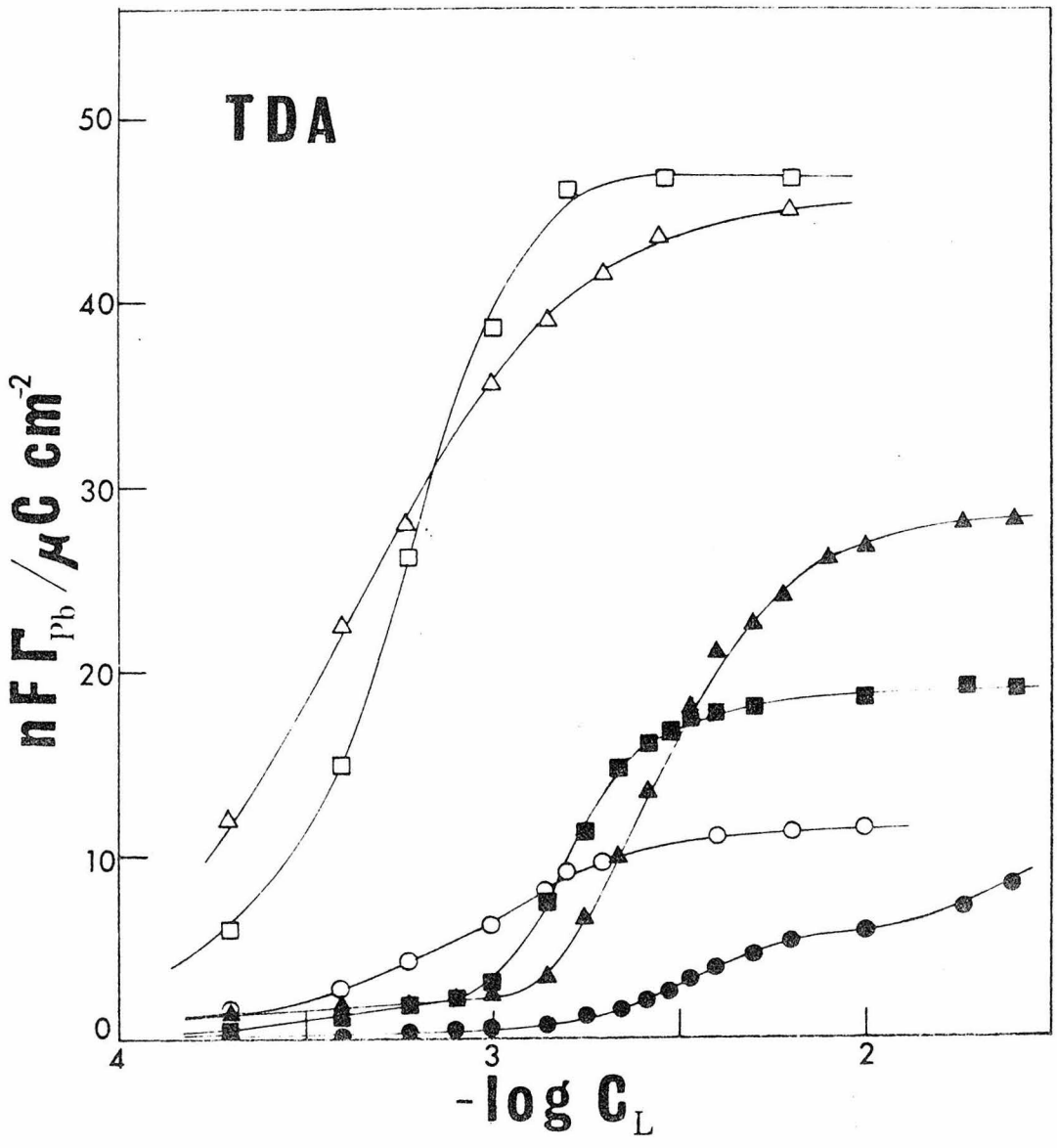
TDA
50
40
30
20
10
0
4
3
2
nF Γ Pb /μC cm-2
-log C L

FIGURE II-5

Potential dependence of the amount of adsorbed lead as determined by chronocoulometry for solutions containing .5 mM Pb^{+2} in 1M $NaClO_4$ with the following concentrations of disodium thiodipropionate (TDP). A - .4 mM; B - .8 mM; C - 1.2 mM; D - 1.6 mM; E - 2.0 mM; F - 2.8 mM; G - 4.0 mM. Each point represents an average of three chronocoulometric experiments.

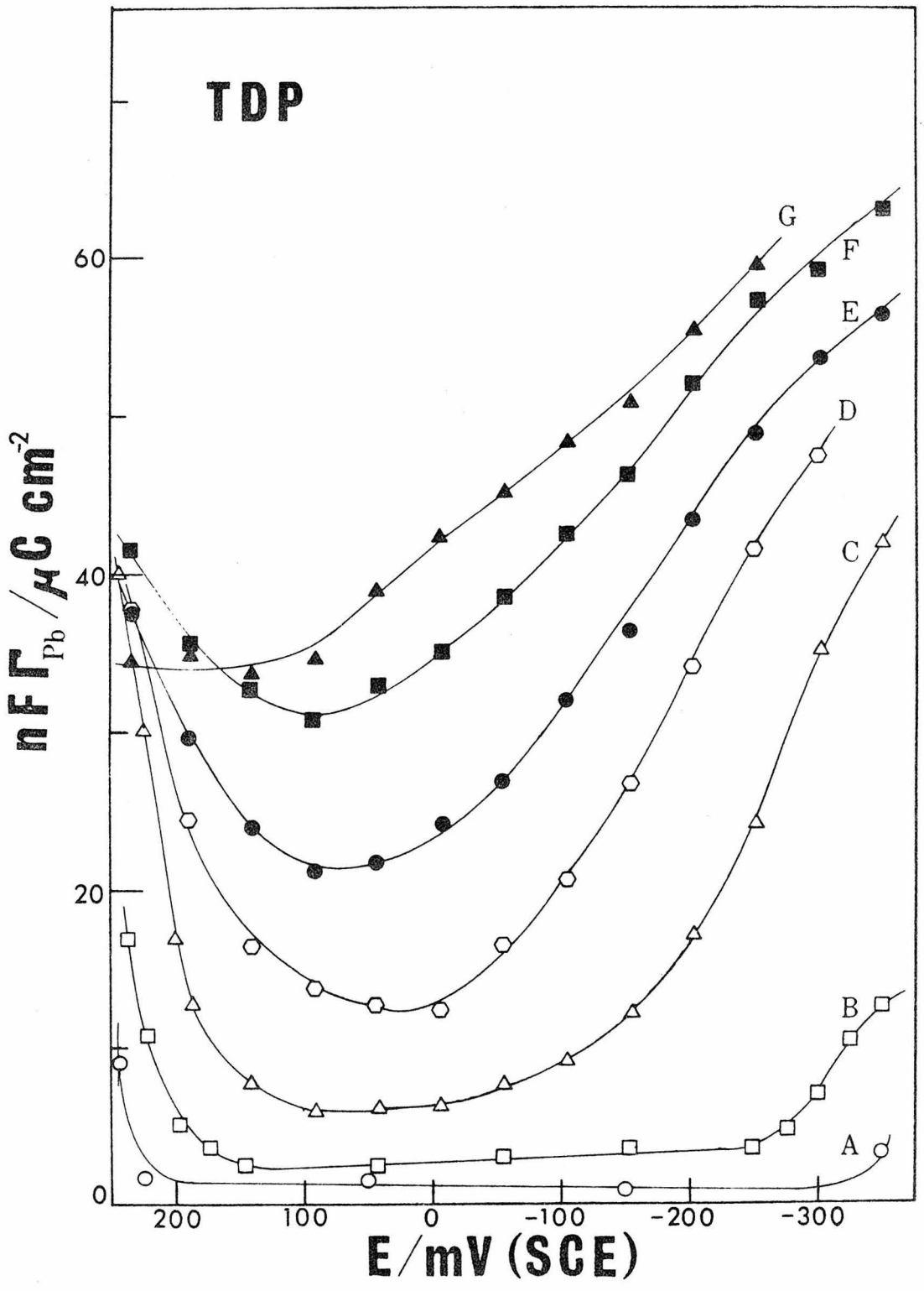
TDP
G
F
E
D
C
B
A
60
40
20
0
200
100
0
-100
-200
-300
E/mV (SCE)
nF Γ Pb /μC cm-2

FIGURE II-6

Amount of lead adsorbed as a function of the logarithm of thiodipropionate ion concentration in a solution of .5 mM Pb^{+2} in 1 M $NaClO_4$ at the following potentials: (□) +200 mV; (○) 0.0 mV; (△) -300 mV.

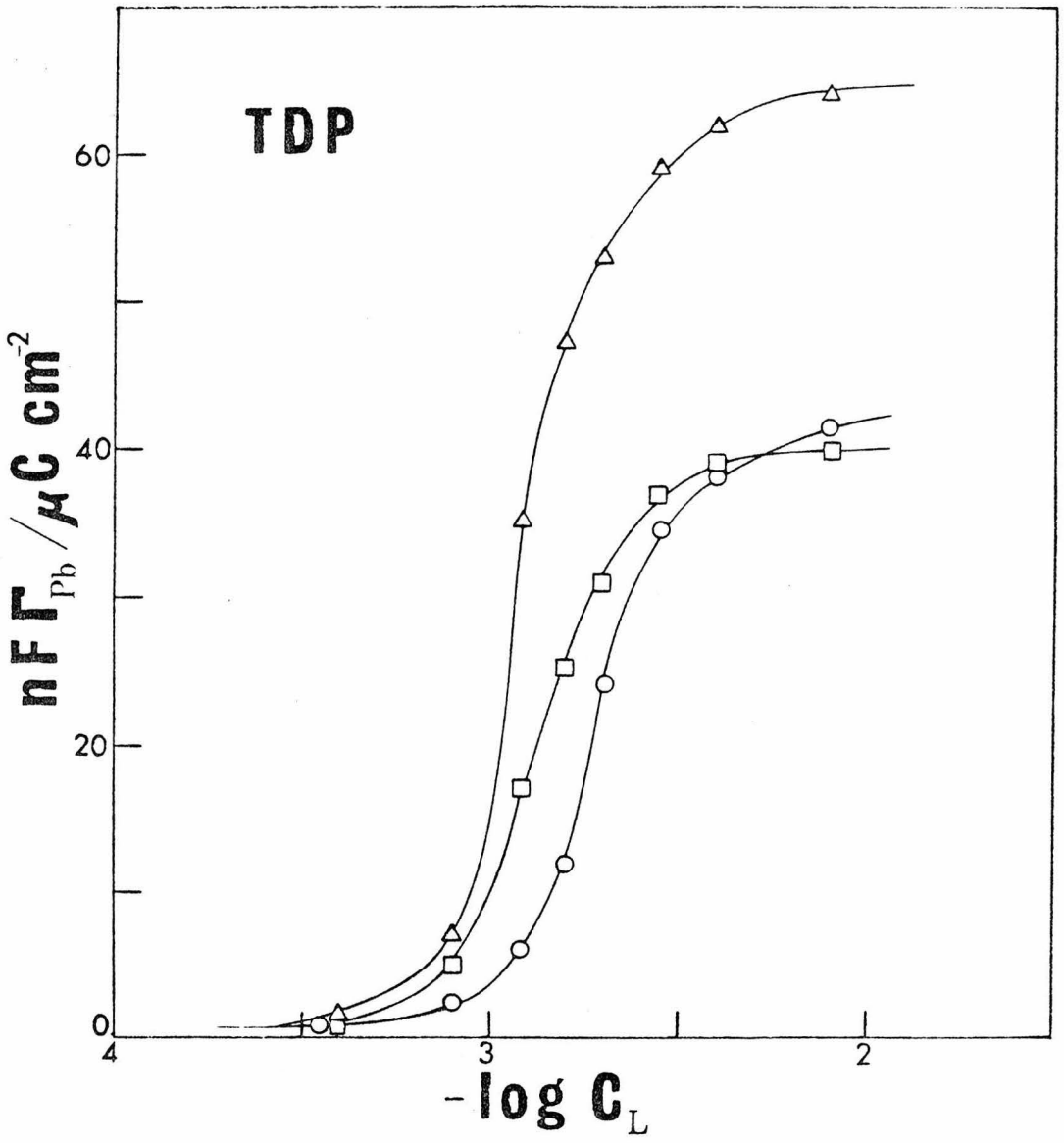
TDP
60
40
20
0
4
3
2
nF Γ Pb /μC cm-2
-log CL

FIGURE II-7

Potential dependence of the amount of adsorbed lead as determined by chronocoulometry for solutions containing .5 mM Pb^{+2} in 1 M $NaClO_4$ with the following concentrations of disodium methylenebis-thioacetate (MBTA). A - .6 mM; B - 1.0 mM; C - 1.4 mM; D - 1.8 mM; E - 2.2 mM; F - 3.2 mM; G - 4.0 mM; H - 7.0 mM. Each point represents an average of three chronocoulometric experiments.

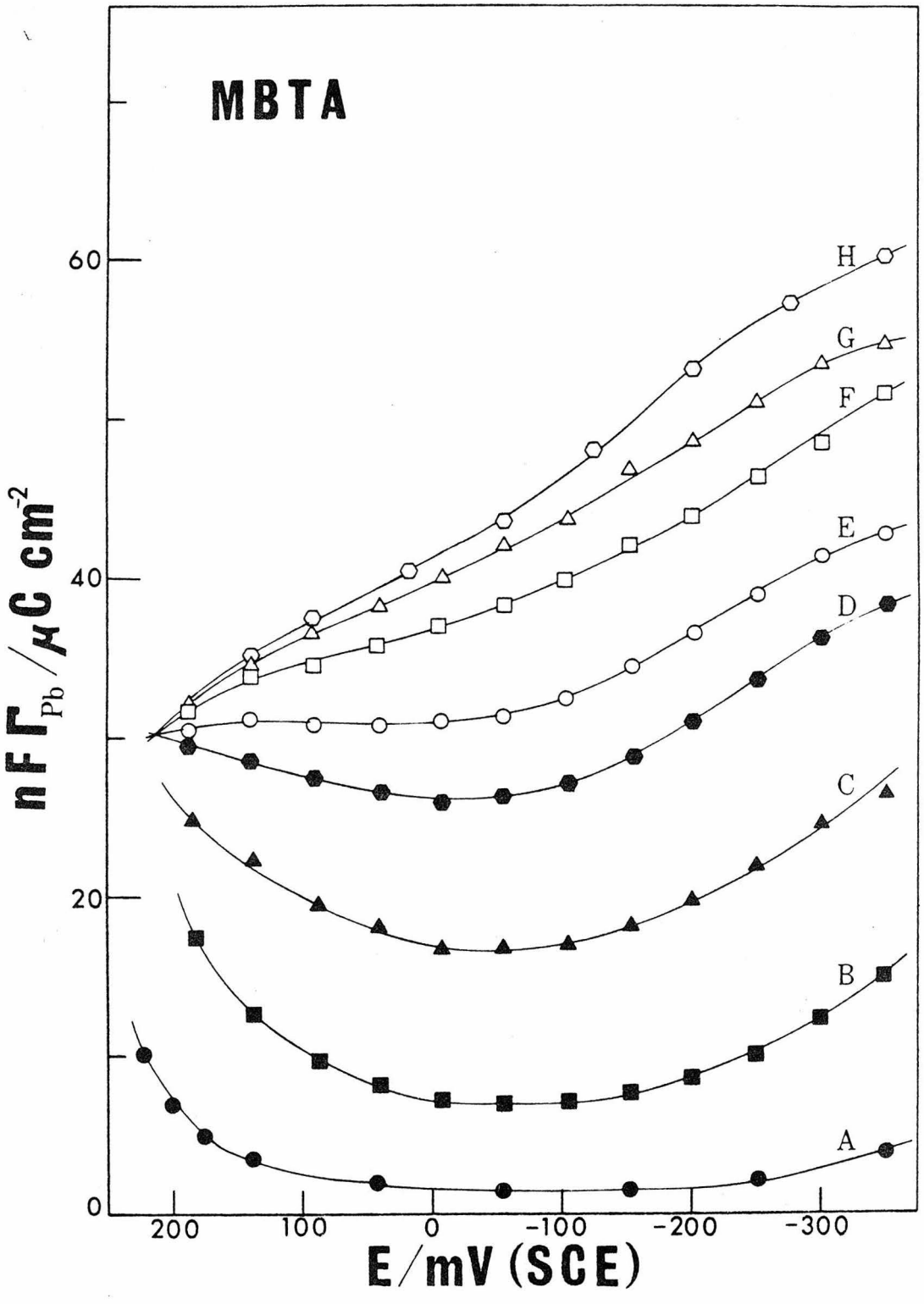
MBTA
60
40
20
0
nF Γ Pb /μC cm-2
H
G
F
E
D
C
B
A
200
100
0
-100
-200
-300
E/mV (SCE)

FIGURE II-8

Amount of adsorbed lead as a function of the logarithm of methylbisthioacetate ion concentration for a solution of .5 mM Pb^{+2} in 1 M $NaClO_4$ at the following potentials: (△) +200 mV; (□) 0.0 mV; (○) -300 mV.

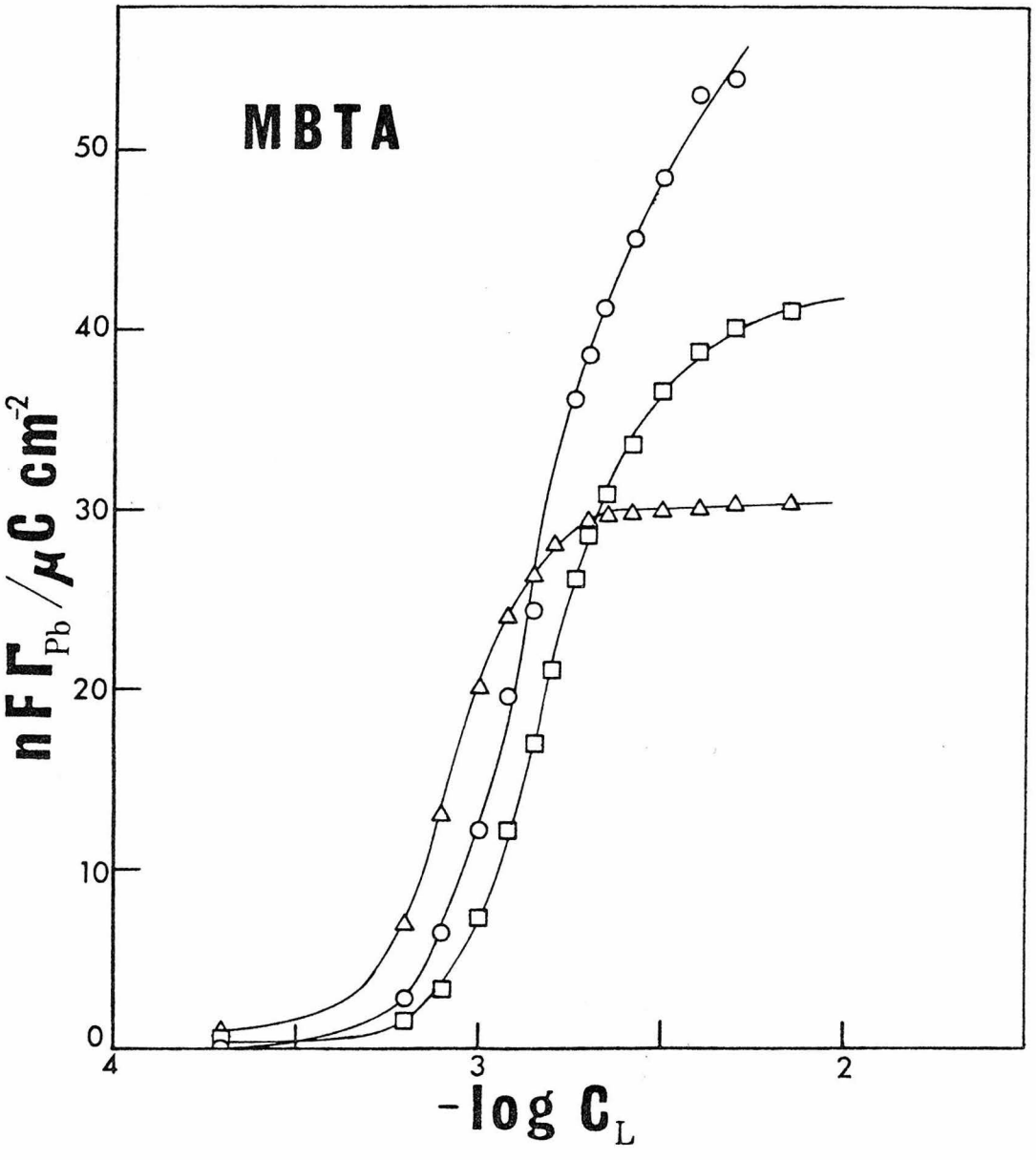
MBTA
50
40
30
20
10
0
4
3
2
nFΓPb /μC cm-2
-log CL

FIGURE II-9

Potential dependence of the amount of adsorbed lead as determined by chronocoulometry for solutions containing .5 mM Pb^{+2} in 1 M $NaClO_4$ with the following concentrations of trisodium thioacetato-succinate (TAS). A - .6 mM; B - .8 mM; C - 1.0 mM; D - 1.2 mM; E - 1.5 mM; F - 2.0 mM; G - 2.8 mM. Each point represents an average of three chrono-coulometric experiments.

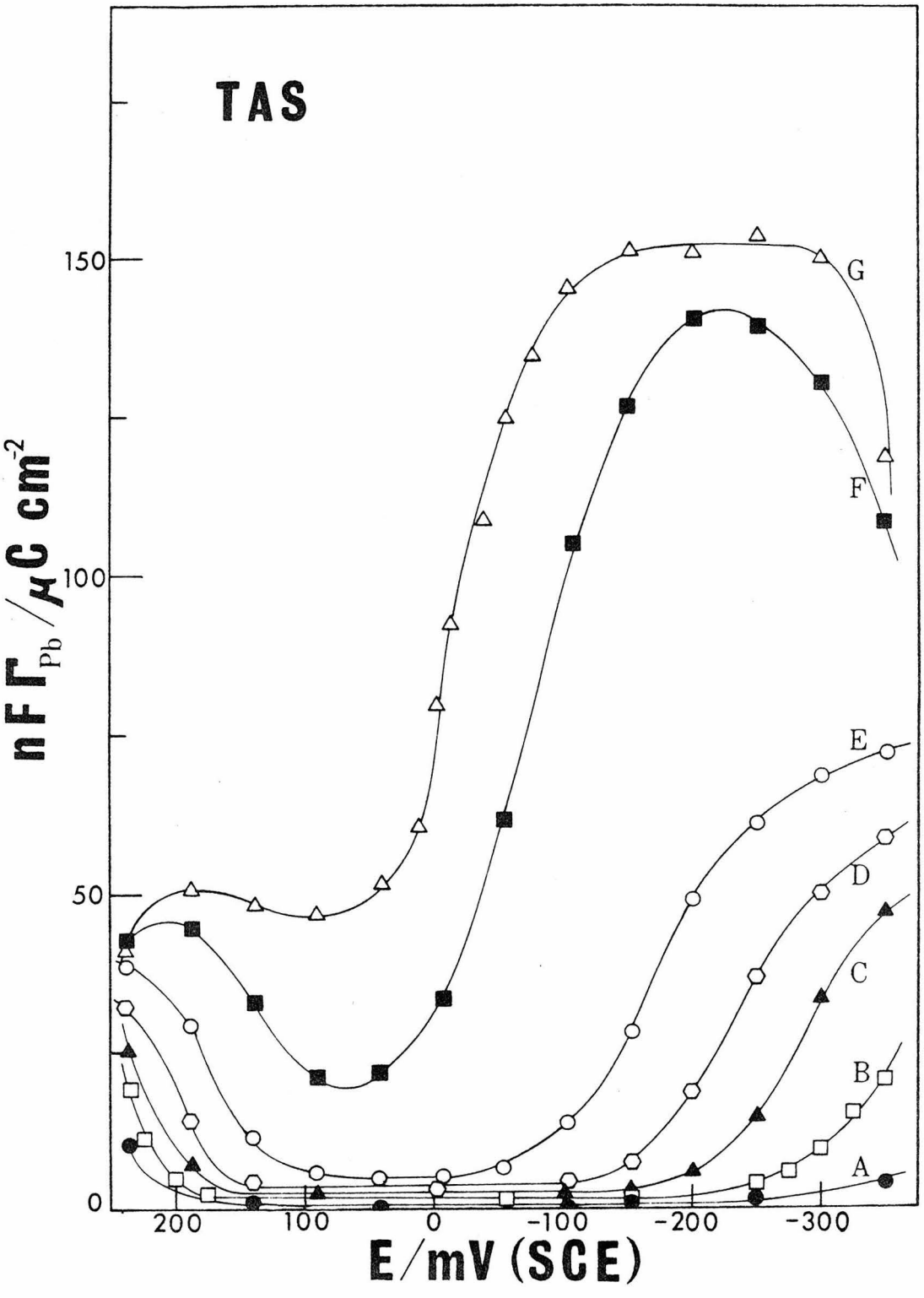
TAS
150
100
50
0
nFΓPb /μC cm-2
200
100
0
-100
-200
-300
E/mV (SCE)
A
B
C
D
E
F
G

FIGURE II-10

Amount of lead or cadmium adsorbed as a function of the logarithm of thioacetatosuccinate ion concentration for a solution of 1 M $NaClO_4$ with the following conditions: 1 mM Pb^{+2} - (■) +200 mV; (▲) 0.0 mV; (●) -300 mV; 0.5 mM Pb^{+2} - (□) +200 mV; (○) -300 mV; (⬢) 1 mM Cd - 300 mV.

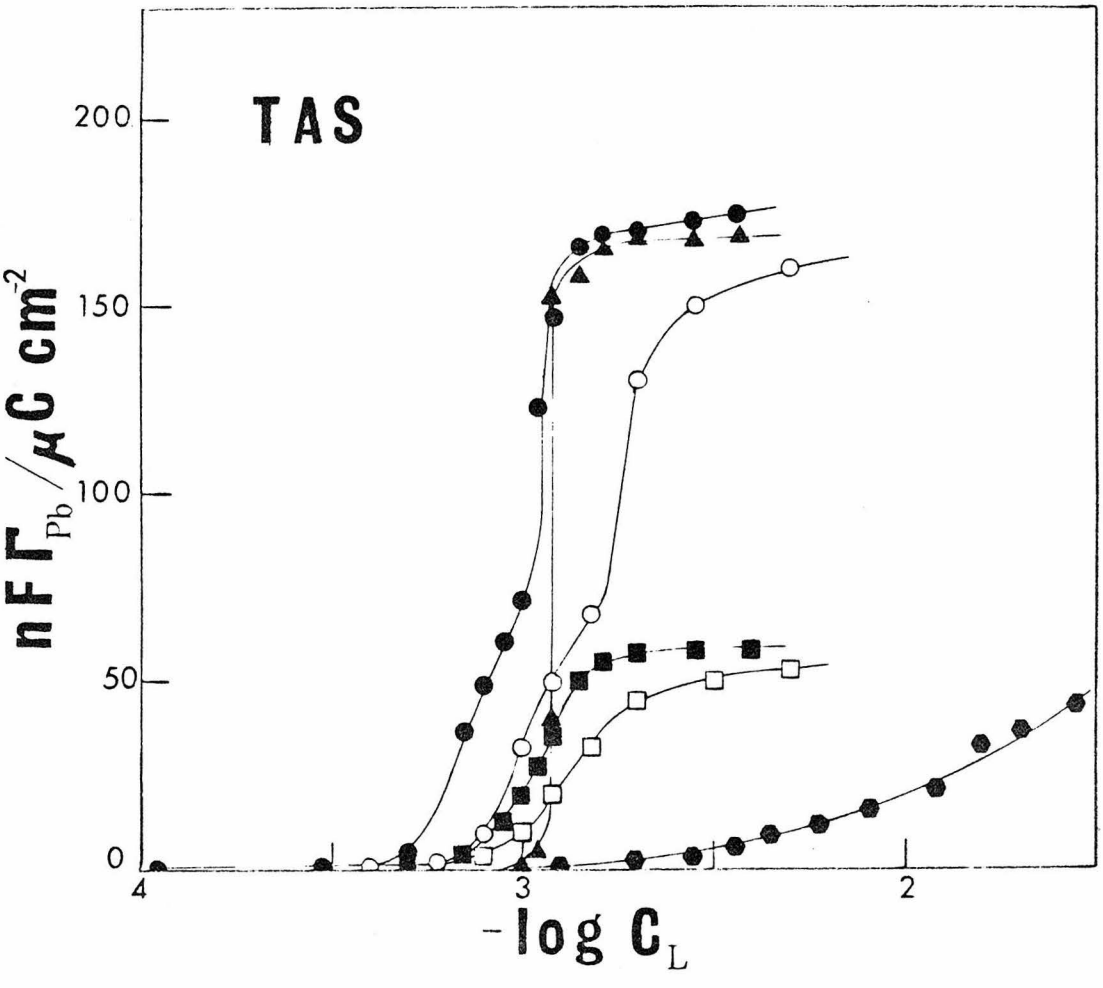
TAS
200
150
100
50
0
4
3
2
nF Γ Pb /μC cm-2
-log C L

FIGURE II-11

Potential dependence of the amount of adsorbed lead as determined by chronocoulometry for solutions containing .5 mM Pb^{+2} in 1 M $NaClO_4$ with the following concentrations of tetrasodium thiodisuccinate (TDS). A - .2 mM; B - .3 mM; C - 5 mM; D - .6 mM; E - 1.0 mM; F - 1.8 mM; G - 4 mM; H - 8 mM; I - 16 mM. Each point represents an average of three chronocoulometric experiments.

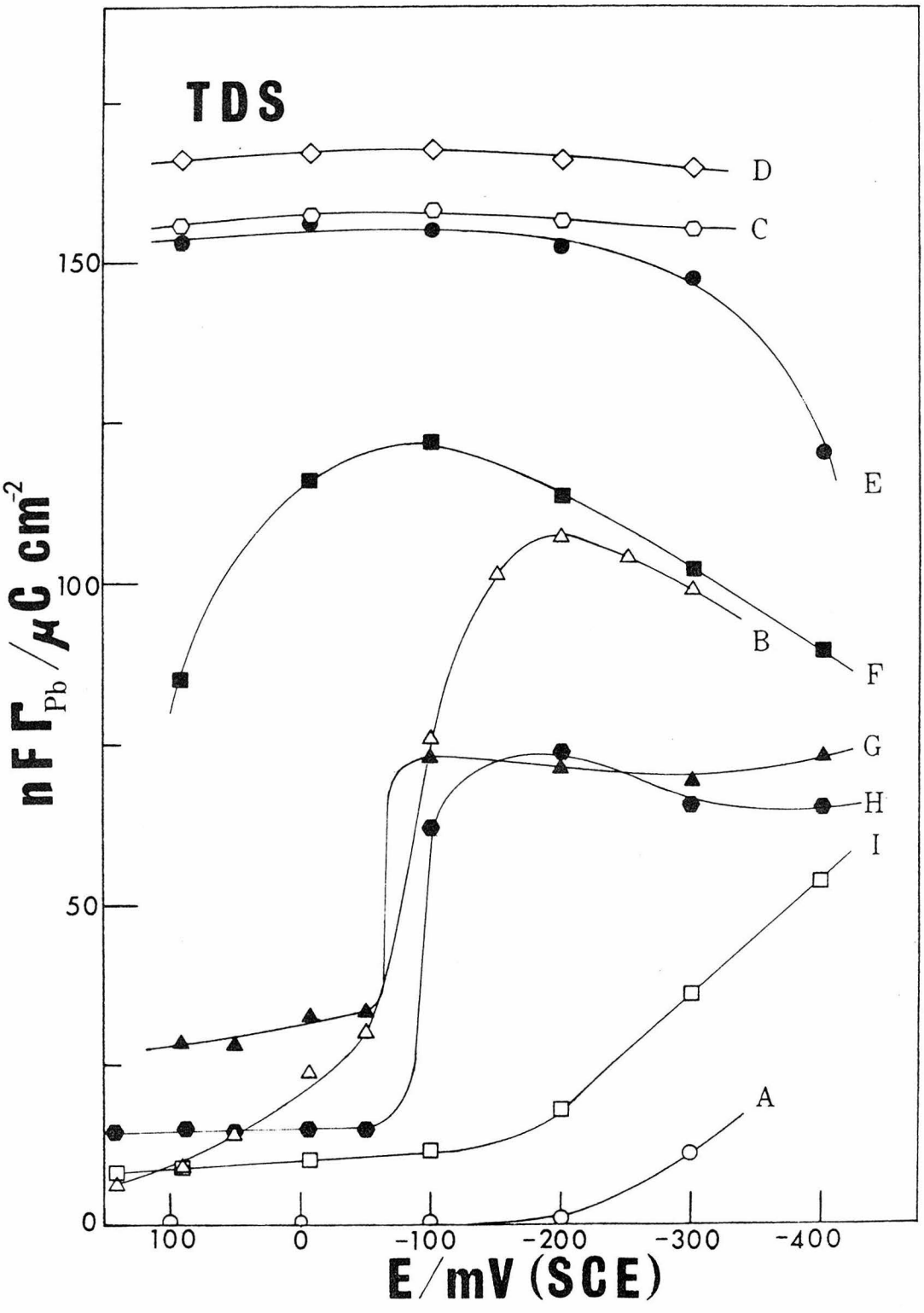
TDS
D
C
150
E
B
F
100
G
H
I
50
A
0
100
0
-100
-200
-300
-400
E/mV (SCE)
nF Γ Pb /μC cm-2

FIGURE - II-12

Amount of adsorbed lead as a function of the logarithm of thiodisuccinate concentration for the open symbols and lead concentration for the closed symbols in 1 M $NaClO_4$ with the following additional conditions: varying Pb^{+2} with 4 mM thiodisuccinate - (●) +100 mV; (■) -300 mV; varying TDS with .5 mM Pb^{+} - (○) +100 mV; (□) -300 mV.

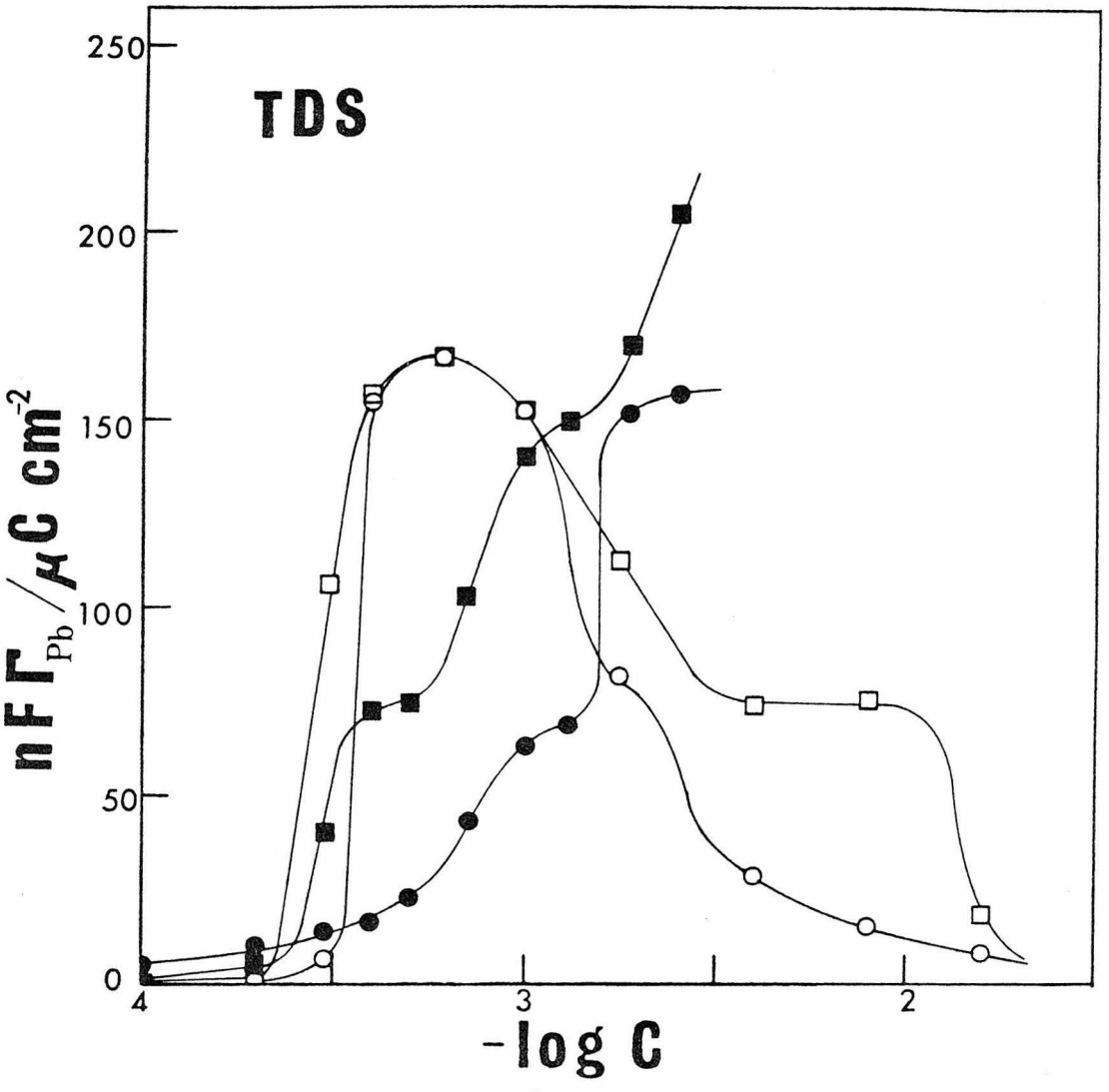
TDS
250
200
150
100
50
0
4
3
2
-log C
nF Γ Pb /μC cm-2

containing lead and thioethercarboxylate ligands. At least two stable phases are indicated by all the systems studied, one which is stable at positive potentials and the other at more negative potentials.

Many of the properties of the surface phase formation as described by Murray[2-4] for the surface precipitation of $PbBr_2$, PbI_2 and TlBr are similar to the properties of the systems studied here.

The measured maximum coverages of metal ions were large and were very close to a coverage calculated for a close packed layer of M-X units on the mercury surface (e.g., 8.2×10^{-10} moles $-cm^{-2}$ for PbI_2).

The lead bromide and lead iodide layers were formed more readily at positive potentials while thallium bromide showed the opposite potential dependence characterized by up to two distinct discontinuities each of which was followed by a region where the coverage was potential independent.

For both the lead halide systems and thallium bromide discontinuities were also observed in the halide ion concentrations dependence of the adsorption. The position of the discontinuities could be closely related to a surface solubility constant, K_{surp}.

$$K_{surp} = [M^{n+}][X^-]^n$$

The values determined for K_{surp} were a factor of 3 to 4 smaller than the solubility product constant (K_{sp}) determined for precipitation from the bulk of the solution. For TlBr two discontinuities were found and a second K'_{surp} was determined, which was associated with the formation of a second monolayer of thallium bromide on top of the first monolayer, and had a value between K_{surp} and K_{sp}.

The position of the steep increases in the ligand concentration dependence for the adsorption of lead from solutions containing thioethercarboxylates could not be corelated to any solubility constant law. The steep increases with these ligands occurred at ligand concentrations more than twenty times lower than the discontinuities observed by Murray,[2-4] however no bulk precipitation could be observed from .5 mM Pb^{+2} solutions with ligand concentrations as high as .1 M. The much more complex solution equilibria due to the polydentate character and protonation equilibria or a supersaturation effect could be responsible for this behavior.

When plotted on isotherm coordinates the surface coverage for both Murray's surface crystals and the surface phases studied here reach a saturation value much more easily than a Langmuirian or Henry's Law adsorption isotherm would predict.[15] Attractive interactions between

the adsorbing particles is the usual interpretation when isotherms reach saturation over a narrow concentration range. It is not at all surprising that attractive forces are involved in the formation of close-packed or nearly close-packed layers.

Several similarities also exist between the systems reported here and class II or anion assisted adsorption.[16-19] The main similarities are that white metal cations are involved and the ligands form complexes with the cations in the bulk. These similarities are outweighed by several other properties which are not in agreement with the anion assisted adsorption model. 1) The ligands are not adsorbed to any extent from solutions when no metal is present except at very positive potentials. 2) The adsorption observed in this study is much greater than any adsorption attributed to anion assistance. These factors strongly support the notion that anion assisted adsorption is probably not the mechanism involved in the adsorption of lead thioethercarboxylates except perhaps at very positive potentials.

THE STRUCTURE OF THE SURFACE PHASES

It is clear from the previous section that surface phases are being formed on the mercury surface. The actual structure of the phases is left primarily to speculation because the amount of lead in the layer under any given conditions is the only variable amenable to direct measurement. Some properties can be indirectly observed however.

The importance of the lead carboxylate bonding in the layer can be demonstrated by acidifying a solution from which adsorption occurs with $HClO_4$ to a pH where the carboxylate groups of the ligands are protonated. No adsorption is measured from solutions of pH 2 or below.

Despite the large adsorption the double layer charge extracted from the chronocoulometric data shows that only relatively small changes (0 to -7 $\mu C \text{-} cm^{-2}$ for adsorption of 160 $\mu C \text{-} cm^2$) in this parameter result when compared to the blank at initial potentials negative of -100 mV. Murray[4] argued from similar observations that the TlBr surface phase was neutral. Even though the comparison of charge changes is for two different interfaces (the mercury-solution and surface phase-solution) larger charge changes would be expected if even one excess charge per metal were present in the layer. This would correspond to charge in the layer of 80 $\mu C/cm^2$. The presence of less than stoichiometric

excess charge cannot be totally ruled out however. The fact that the adsorption of this phase increases towards the p.z.c. much like a neutral organic molecule is further evidence of electroneutrality.

Relative double layer charge changes of the opposite sign of 0 to 4 $\mu C/cm^2$ are observed for potential steps from potentials positive of 0.0 millivolts. This behavior is attributed to the formation of a different stable phase which exists only at positive potentials. Measurements of the electrode capacitance and resistance for a system where a phase change is suspected support this notion. Figure II-13 simultaneously shows capacity, resistance and adsorption measurements from the same solution which is .5 mM in Pb^{+2} and 2 mM in TAS. At positive potentials as the adsorption decreases the resistance is within a few ohms of a solution containing only 1 M $NaClO_4$ but huge increases in the capacity of the electrode are observed. When the adsorption begins to increase again as the potential is made more negative than 0 mV a sudden drop in the capacity to below the value of the blank is observed concurrent with a sudden increase in the resistance. At very negative potentials where the reduction of Pb^{+2} is diffusion controlled the resistance and capacity return to within 10% of the value of the blank. This behavior is consistent with a two phase model each of which contain lead and

FIGURE II-13

Plot showing simultaneously the variation with potential of the amount of adsorbed lead, electrode capacitance and resistance for a solution of 1 M $NaClO_4$: (■) resistance; (●) capacitance and .5 mM Pb^{+2} 2 mM thioacetatosuccinate and 1 M $NaClO_4$: (□) resistance; (○) capacitance; (Δ) amount of adsorbed lead.

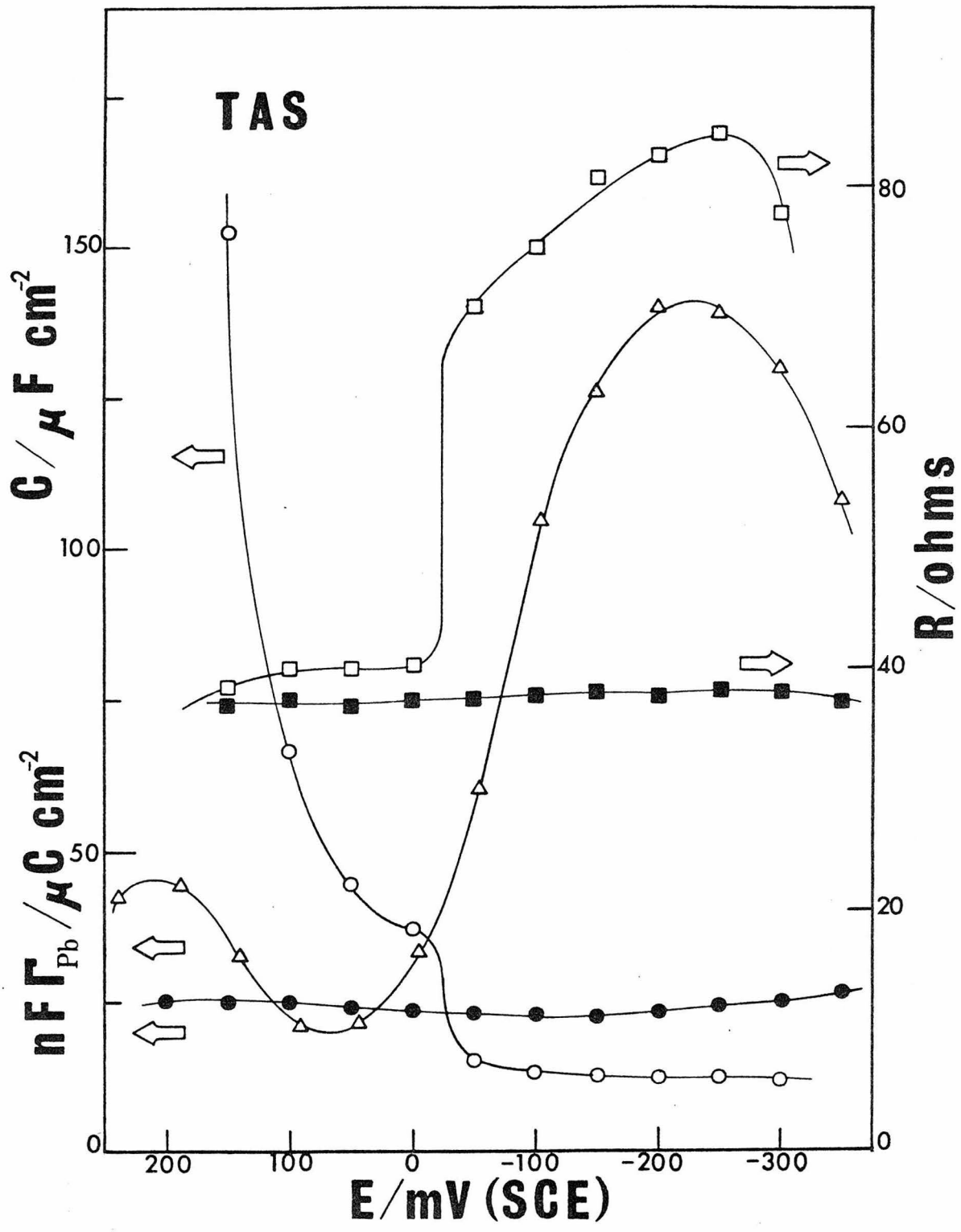
TAS
C/μF cm⁻²
nFΓPb/μC cm⁻²
R/ohms
E/mV (SCE)
150
100
50
0
80
60
40
20
0
200
100
0
-100
-200
-300

ligand but have different properties. Very similar capacity data with regions of greatly enhanced capacity and other regions of suppressed capacity have been reported when a surface layer is present on a mercury[20,21] or amalgam[22,23] electrode.

The value of the double layer capacitance (C_{dl}) in the presence of a phase monolayer is given by equation II-1.[20]

$$C_{dl} = \left(\frac{\partial q^m}{\partial E}\right)_{q^{mon}} + \left(\frac{\partial q^{mon}}{\partial E}\right)_{q^m} \qquad \text{(II-1)}$$

Where q^m is the electrode charge and q^{mon} is the charge needed to generate the monolayer. The first term will generally give rise to a "geometric" capacity of ~20 μF $-cm^{-2}$. For a value >> 20 μF $-cm^{-2}$ as observed at positive potentials there must be a contribution from the second term which would arise from a change with potential of the electronic or ionic charge associated with the phase. This could be brought about by incorporation of interstitial charge into the film or the adsorption of species at the solution film interface.

With all these facts in mind a model for the structure of the two phase types observed with lead thioether-carboxylates can be formulated.

The phases which are stable at positive potentials where the ligand sulfur-mercury interaction would be expected to

be strong will likely have a structure similar to that shown below for the ligand TDA.

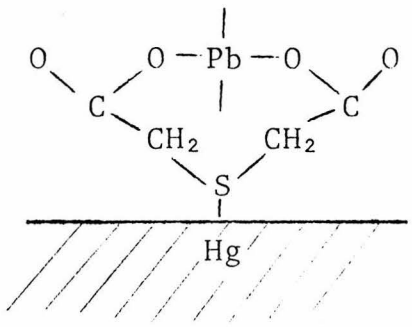

This type of structure is given support from a number of observations. 1) The charge and capacitance increases when excess ligand is added even though no increase in the amount of lead accumulated at the interface can be measured. This could be due to competitive ligand adsorption but more likely to the addition of an extra ligand to the now less coordinately saturated non-sulfur coordinated lead atom. The presence of ClO_4^- anions adsorbed on or contained within the film is also possible. 2) The potential dependence of layers which are postulated to have a ligand between the metal and the electrode such as $PbCl_2$, $PbBr_2$ and PbI_2 is the same as observed for this phase.[2]

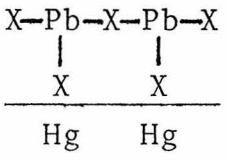

3) The adsorption of a compound which is identical but with an oxygen atom in place of the sulfur (DGA) has a much smaller adsorption at positive potentials than observed when a sulfur is present (Figure II-16). This is due to the much weaker interaction between mercury and an ether oxygen atom. 4) The alignment of the molecules perpendicular to the field at the surface and the charge separation induced could result in the large observed capacity increase.

The phases which are stable at potentials negative of ~ -100 mV to the potential at which lead is reduced to the amalgam (~ -400 mV) is characterized by capacity decreases and in most cases larger adsorption. A drop in capacity could be the result of the molecular dipoles being oriented parallel to the field in a two dimension structure.

The crystal structure of analogous cadmium thiodiacetate dihydrate[24] and other cadmium carboxylate hydrate compounds*[25-28] as well as TDA[29] by itself reveals that compounds of this type tend to crystallize in polymeric layered structures with hydrogen bonded water molecules holding the layers together.

---

* No crystal structures of lead compounds are available probably because of leads high scattering cross section which would result in the location of lighter atoms being very uncertain.

Opalescent plates are formed from a concentrated equimolar solution of lead and thiodiacetate which suggests that the lead compounds crystallize in layered structures also.

The layered structure of the analogous crystals and the similarity between the potential dependence of the adsorption of these phases, organic adsorbates and TlBr make it attractive to postulate the formation of a layer of polymeric phase on the electrode surface.

Thallium bromide[3,4] unlike the lead halide layers increases its coverage at more negative potentials perhaps because hydrophobic forces and TlBr lattice energy, not the Hg-Br interaction is controlling the phase stability. The smaller electrode water interaction as the potential is made closer to the p.z.c. enables the hydrophobic side of the phase to replace the water on the electrode surface.

In order to construct some model of the surface phase one might expect structures which resemble the bonding found in the various molecular crystals of the white metal carboxylate compounds a few examples of which will be described.

Cadmium formate dihydrate[25] forms a three dimensional polymer with two formates linking together cadmium atoms which are arranged in face centered positions in the cell. The polymer is further strengthened by hydrogen bonds between coordinated water molecules and formate oxygen atoms.

Cadmium diacetate dihydrate[26] contains cadmium atoms coordinated to seven oxygen atoms with both acetate groups bidentate. The oxygen atom of one of the acetates bridges to another cadmium atom and forms a continuous cadmium-oxygen spiral.

Cadmium malonate monohydrate[27] also has a seven coordinate cadmium with molecular units arranged in a polymeric structure of twelve membered star shaped rings.

Bis(S-methyl-L-cysteinato)cadmium(II)[28] [$Cd(SMC)_2$] has two SMC coordinate to the cadmium atom through N and O bonds with a curious lack of metal sulfur interaction. The distorted octahedral geometry about the cadmium is completed by two carboxylate oxygen atoms from neighboring ligands forming a planer polymer.

Cadmium thiodiacetate (TDA) hydrate[24] contains tridentate TDA bonded to the cadmium atom with two carboxylate oxygens and the sulfur atom coordinating. The distorted octahedral geometry is completed by bonds from two adjacent carboxylate oxygens which extend the polymer and a water molecule bonded trans to the sulfur atom. A pictoral summary of these structures is shown in Figure II-15A-E.

The construction of models suggests that many other possibilities for the formation of polymeric lattices exist. A planar coordination of TDA to the lead atom could perhaps be stabilized by a two-dimensional environment at the electrode surface. The more complex ligands have even more possibilities

FIGURE II-14

Summary of some polymeric structures in the crystals of carboxylate complexes.

A. Cadmium Formate Cihydrate, Ref. 25.

B. Cadmium Acetate Cihydrate, Ref. 26.

C. Cadmium Malonate Monohydrate, Ref. 27.

D. Cadmium $(SMC)_2$, Ref. 28.

E. Cadmium Thiodiacetatedihydrate, Ref. 24.

a

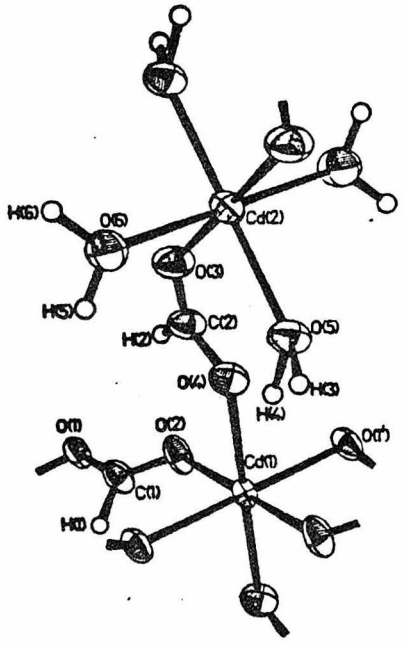

Perspective view of cadmium(II) formate dihydrate showing slightly more than the asymmetric unit.

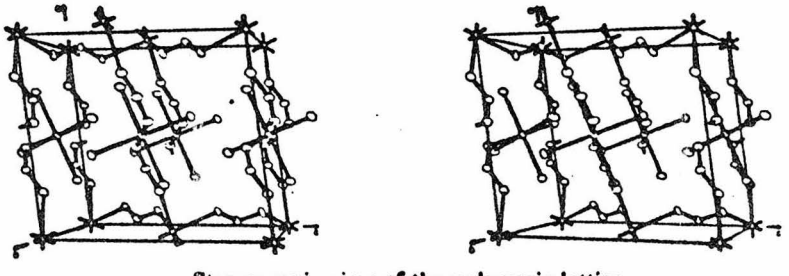

Stereoscopic view of the polymeric lattice.

b

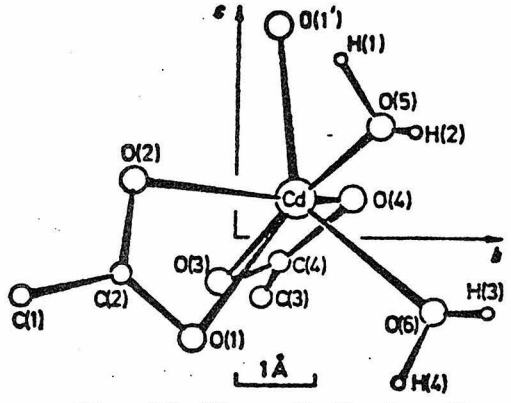

View of the Cd co-ordination down the *a* axis

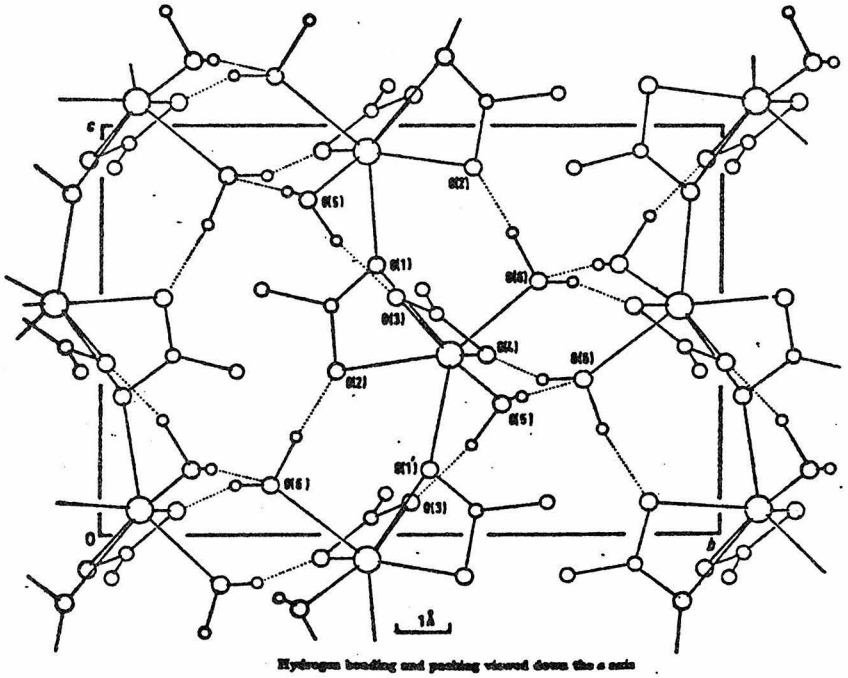

Hydrogen bonding and packing viewed down the *a* axis

C

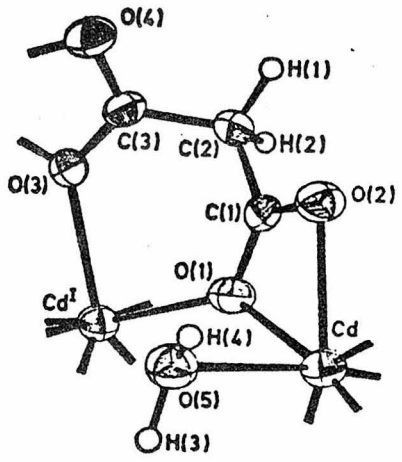

Perspective view with all non-hydrogen atoms represented by 50% probability thermal ellipsoids

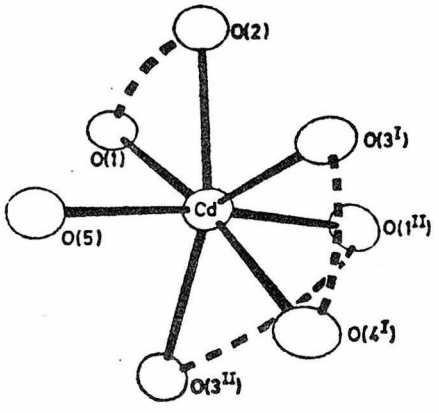

Perspective view of the co-ordination around Cd. Broken lines connect pairs of chelating atoms

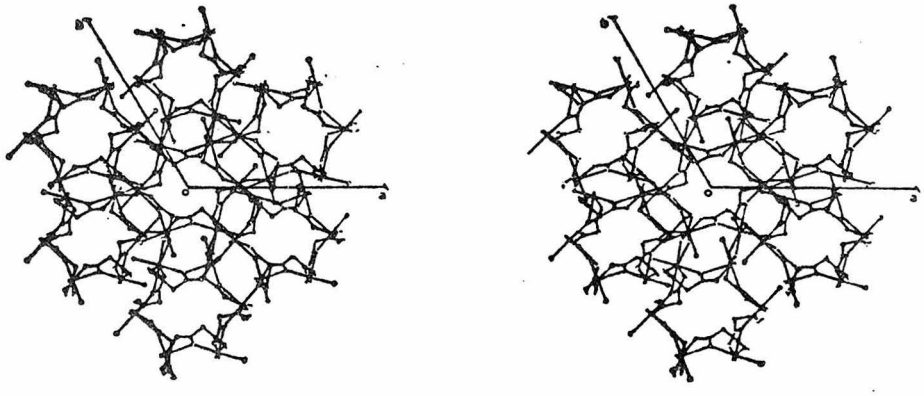

Stereoscopic view of the polymeric lattice looking down the *c* axis

d

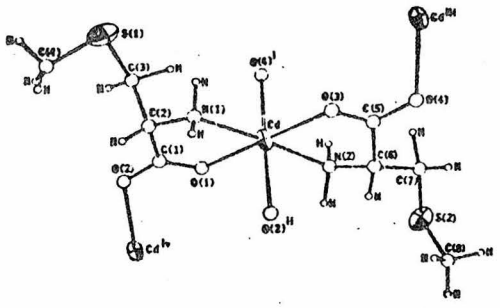

View of the coordination around the cadmium center in $Cd(SMC)_2$. The thermal ellipsoids for Cd and S atoms are scaled at the 40% probability level. Other atoms are represented as circles of arbitrary size.

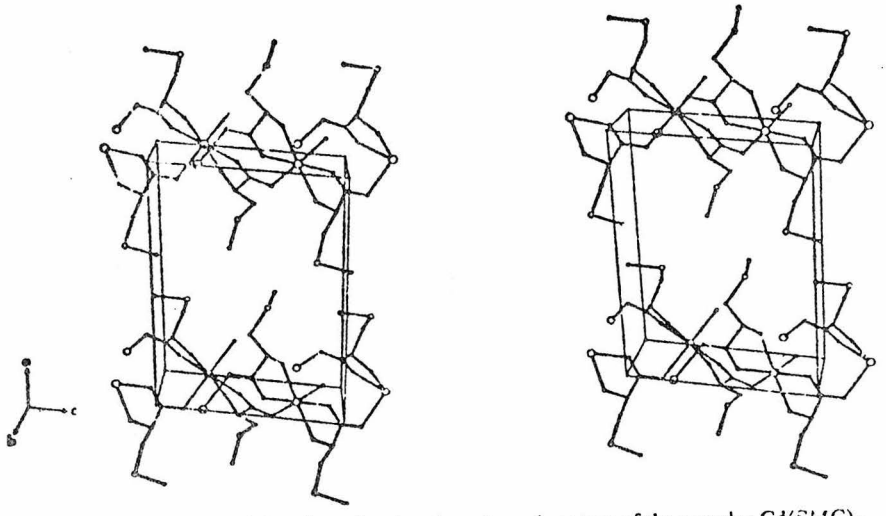

Stereoscopic pair of drawings showing the polymeric nature of the complex $Cd(SMC)_2$, which extends approximately in the crystallographic *b*–*c* plane.

e

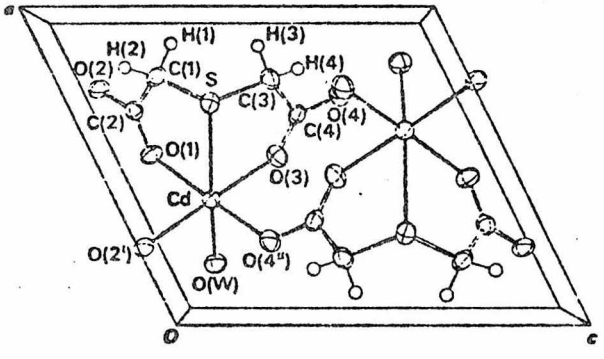

A perspective view of the structure along *b*

because they can complex more than one lead atom per ligand with a variety of possible coordination geometries. Not surprisingly the phases formed by TDS and TAS contain the most lead ions with as many as one lead for every two mercury atoms on the surface.

A simple calculation can also give insight into the structure of the layers. From the crystal structure of cadmium(II) thiodiacetate hydrate[24] with the assumption that the two longest crystallographic axis will lie parallel to the mercury surface a simple calculation shows that $nF\Gamma$ of the metal for such a structure would be about 90 $\mu C\text{-}cm^{-2}$* almost exactly twice the value observed for PbTDA from .1 M $NaClO_4$ at saturation at a potential where the film is completely formed. Under the same conditions from 1 M $NaClO_4$ only a third of this crystallographically packed value is measured. Systematic absences of metal ions with electroneutrality of the system maintained by protonation of carboxylates could be the explanation for this behavior. A more spread out lattice formed in a two dimensional environment could also be an explanation. Other systems (TDA, TDS) however show adsorption which is comparable to the 150 $\mu C\text{-}cm^{-2}$ calculated from the TDA model using the short crystallographic axes and probably reflects the multiple metal binding ability of these ligands or the formation of multilayers.

---

* If the two shortest axes are used, a value of ~ 150 $\mu C\text{-}cm^{-2}$ is calculated.

The exact structure and stoichiometry of these interesting surface phases cannot be totally elucidated until a reliable method for ascertaining the concentration and speciation of the various ligands which are in excess at the interface can be developed. Yet the question can still be asked as to why the layers are formed at all and only at the interface.

The property which distinguished the electrode-electrolyte interface from the bulk solution is that very high electrical field strength that is present in the interfacial region. The dipole structuring effects brought about by the electric field could induce the alignment necessary for the propagation of such structures at concentrations much below those needed for observation of the bulk thermodynamic formation of three dimensional structures.

In other words the field is influencing the entropy term in the thermodynamic expression for the free energy of formation of the phase.

In summary, it is believed that the stable phase at positive electrode potentials is probably an example of anion assisted adsorption with attractive forces as a result of bridging carboxylates cross-linking the structure. This structure may actually be an example of a functionalized mercury electrode. Extension of this concept to complexes containing metals with more catalytic activity may prove to be

fruitful since reasonably large metal surface excesses are obtained.*

The polymeric phase which exists primarily at more negative potentials may be formed because of a solubility or hydrophobic effect again with attractive interactions arising from cross linking the structure with carboxylates. The larger metal ion surface concentrations in these phases also make structures like this attractive candidates for the design of surface catalysts.

The reduction of oxygen to hydrogen peroxide proceeds at electrodes when either phase is present on the surface so it appears that electron transfer is not inhibited by the presence of the layers.**

THE ADSORPTION OF THIOETHERCARBOXYLATES WITH METALS OTHER THAN LEAD

Figure II-15 shows the potential dependence of the adsorption of a variety of the ligands used in this study when Cd^{+2} is the metal ion present in the solution. Like the lead systems studied there are strongly potential dependent

---

* A typical ruthenium concentration which has been achieved on a modified electrode is ~20 $\mu C\text{-}cm^{-2}$.

** Some surface phases ($PbBr_2$, $PbCl_2$)[2,21] are known to inhibit electron transfer reactions at the surface.

regions and regions where the adsorption is relatively potential independent. Unlike the lead systems the adsorption of cadmium is a strong function of the equilibration time before the potential step, and is in general much weaker. The amount of cadmium measured at the interface was strongly time dependent even after 60 seconds of exposure to the solution with the electrode potential being held at the initial value. In order to compare with the lead systems and for expediency of measurement, 5 seconds was maintained as the equilibration time.

The ligand concentration dependence of the adsorption for Cd^{+2} and TAS is shown in Figure II-10 along with the Pb^{+2} curves with the same ligand. A plateau indicating a saturation value is not evident in the figure. The shape of this curve is reminiscent of isotherms reported by Murray for TlBr adsorption under conditions where the TlBr surface crystal was incompletely formed.[4] When these "prediscontinuity isotherms" were fit to an isotherm of the Frumkin type an interaction parameter indicating attractive interactions between adsorbing units was obtained. It is possible that the adsorption of the cadmium would eventually lead to stable layers but only at much larger concentrations of the adsorbing components. However, because of the fact that adsorption equilibrium was not established in these systems the reason no layers are observed could

FIGURE II-15

Potential dependence of the amount of adsorbed cadmium as determined by chronocoulometry for solutions containing 1 mM Cd^{+2} in 1 M $NaClO_4$ with the following ligand composition and concentration. (○) 20 mM disodium thiodiacetate; (□) 1 mM dihydrogendisodium 2,2'thiobis[ethyl-iminodi(acetate)]; (⬭) 8 mM trisodium thioacetato-succinate; (◇) 20 mM disodium methylenebisthio-acetate; (△) 4 mM tetrasodium thiodisuccinate.

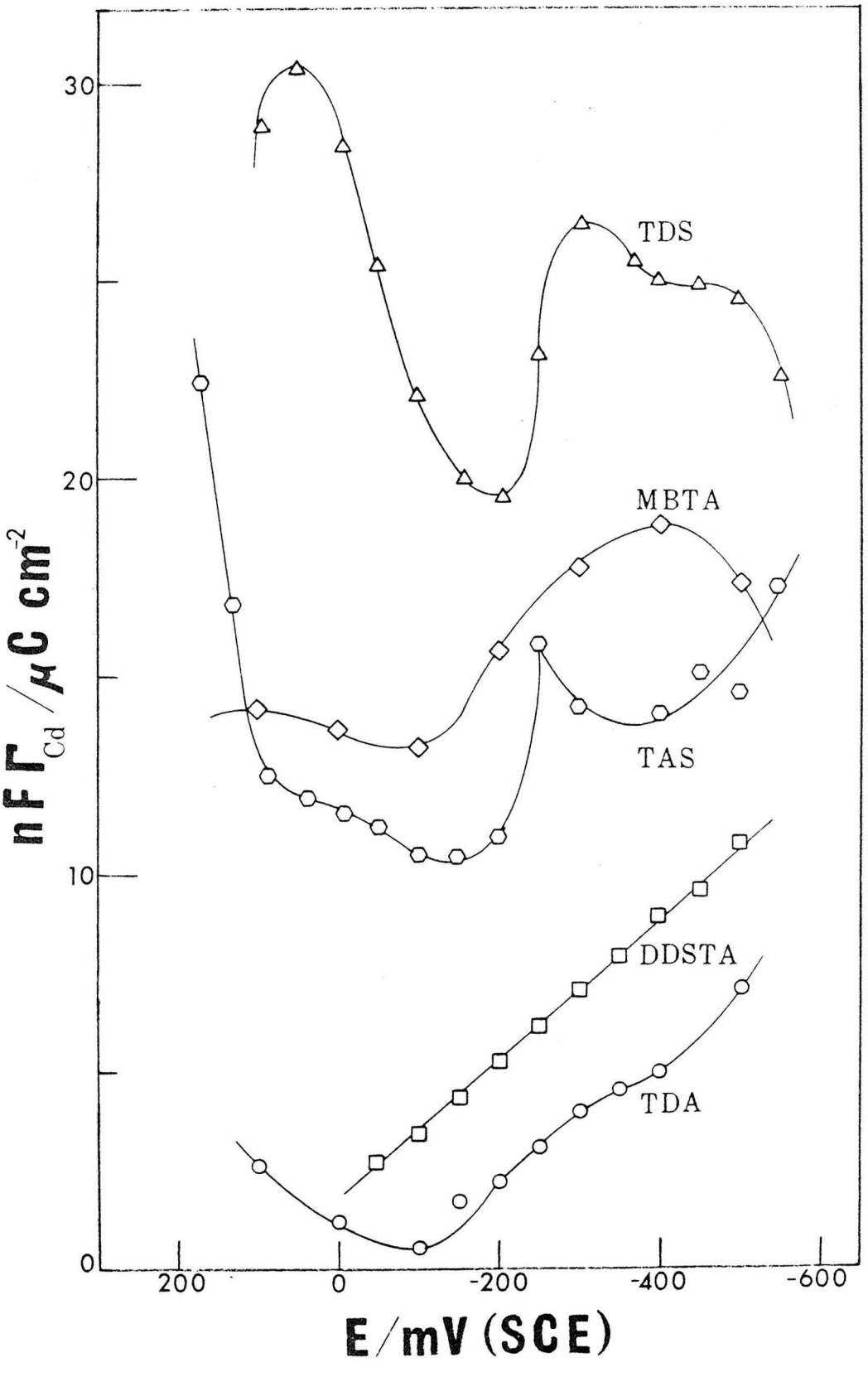
30
20
10
0
200
0
-200
-400
-600
TDS
MBTA
TAS
DDSTA
TDA
nF Γ Cd /μC cm-2
E/mV (SCE)

also be kinetic. The fact that cadmium forms weaker complexes than lead with these ligands[30] and also more soluble complexes (for Cd TDA at least) could be a factor in their weaker adsorption. The potential dependence of the adsorption of thallium(I) from a solution of TDS is shown in Figure II-16 . Although much weaker than the adsorption of the lead TDS complex the shape of the potential dependence is almost identical to that of PbTDA. One must suggest that similar phenomena are controlling the adsorption of both lead and thallium which is not unexpected considering the proximity of these elements in the periodic table.

Zinc(II) forms complexes with the ligands utilized in this study which are of comparable strength to the cadmium complexes.[30] No adsorption of Zn^{+2} could be detected from solutions containing any of the ligands previously discussed. Crystal structures of $Zn(SMC)_2$[28] and other zinc(II) carboxylate complexes[31] reveal that multi-dimensional polymers are not as readily formed in these crystals. One dimensional polymeric structures as found in $Zn(SMC)_2$ crystals[28] would probably not gain as much stability from a hydrophobic environment as a two dimensional structure. The solubility of ZnTDA is also much greater than either CdTDA of PbTDA.

A complex obtained by mixing 1 mM Eu^{+3} and 1 mM DDSTA was found to adsorb to the extent of ~9 $\mu C \cdot cm^{-2}$ at potentials

FIGURE II-16

Potential dependence of the metal adsorption from solution containing various complexes in 1 M $NaClO_4$ pH 4-5: (○) 1 mM Pb^{+2} 10 mM diglycolate ion; (□) 2 mM Tl^{+} 4 mM thiodisuccinate; (▲) ~1 mM Eu DDSTA; (■) 240 μM Cr DDSTA (violet isomer); (●) 27 μM Cr DDSTA (pink isomer).

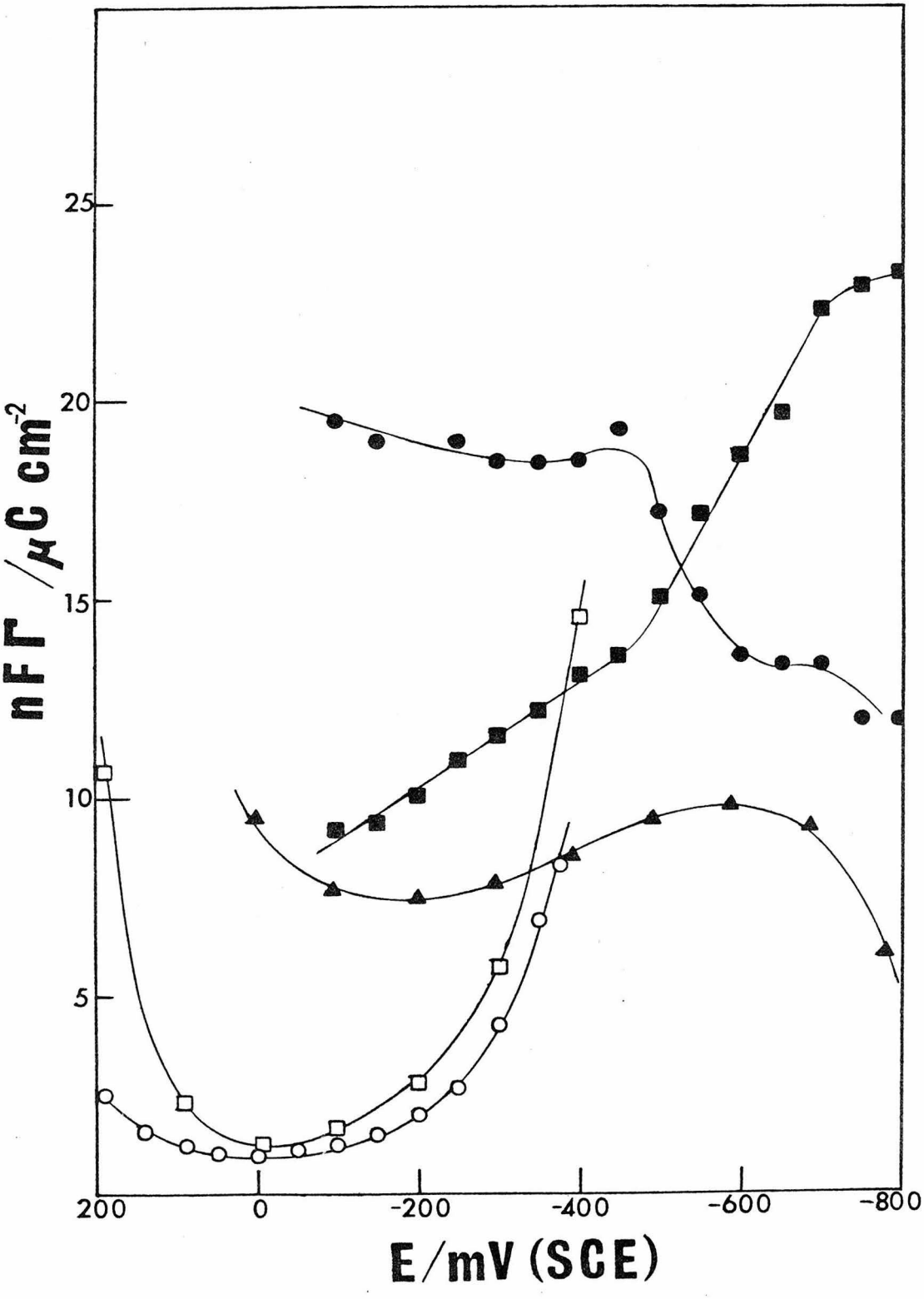
25
20
15
10
5
nFΓ /μC cm⁻²
200
0
-200
-400
-600
-800
E/mV (SCE)

from 0 to -700 mV (Figure II-16). Any explanation of this phenomenon by postulating a polymeric species suffers from the fact that Eu(III)(EDTA) does not adsorb.[32] A Eu-S interaction could be responsible for inducing adsorption but no strong rare-earth-sulfur interaction was found in a crystal of Nd(III)TDA tetrahydrate chloride.[33] However Nd(III)TDA coordination was a complex nine coordinate polydedron structure with polyhedra linked in a two dimensional polymer by bridging carboxylates.

Two different isomers of a complex with a formula Cr(III)DDSTA are very strongly adsorbed with saturation coverages of 30 $\mu C\text{-}cm^{-2}$ observable from concentrations as low as 100 μM for the pink isomer. The adsorption of these complexes and the ligand by itself will be discussed by Peerce.[34] The low concentrations at which saturation occurs suggests that the adsorption of these complexes is connected to an increase in the ligand field stabilization energy of the d^3-chromium(III) as in class IV adsorption.[14]

CONCLUSION

The model presented for the adsorption of a variety of metal ions from solutions of ligands containing both thioether and carboxylate functionality should not be construed as being definitive. The number of possibilities for other models to explain the data are large, however

I believe the basic model presented does the best job of encompassing the largest fraction of the experimental results.

Development of additional experiments would be required to completely define the structure of the surface phases. A technique for independently determining the surface concentration of ligands would be invaluable. Studying the kinetics of an electrode reaction on or through the layer could supply data about the excess charge associated with the layer. The kinetics of layer formation of both lead and cadmium containing phases would be an interesting sidelight worthy of further study. Temperature studies would be useful in the elucidation of the enthalpy and entropy contributions to the free energy of formation of the surface phase.

The ultimate goal of such studies would perhaps be the development of a surface phase with a metal-ligand system which demonstrates catalytic activity towards a bulk soluibilized substrate while still maintaining fast electron transfer kinetics with the electrode surface.

REFERENCES

(1) F. C. Anson, Accounts of Chem. Res., 8, 400 (1975).

(2) H. B. Herman, R. L. McNeely, P. Surance, C. M. Elliot and R. W. Murray, Anal. Chem., 46, 1258 (1974).

(3) C. M. Elliot and R. W. Murray, J. Am. Chem. Soc., 96, 3321 (1974).

(4) C. M. Elliot and R. W. Murray, Anal. Chem., 48, 259 (1976).

(5) Carl A. Koval and Fred C. Anson, Anal. Chem., submitted for publication.

(6) M. S. Wrighton, private communication.

(7) R. W. Murray and P. R. Moses, J. Am. Chem. Soc., 98, 7435 (1976).

(8) R. W. Murray and J. R. Lenhard, J. Electroanal. Chem., 78, 195 (1977).

(9) R. D. Armstrong, J. Electroanal. Chem., 26, 387 (1970).

(10) J. M. Kolthoff, W. Stricks and N. Tanaka, J. Am. Chem. Soc., 77, 4739 (1955).

(11) I. M. Kolthoff and C. Barnum, J. Am. Chem. Soc., 63, 520 (1941).

(12) K. M. Joshi, M. R. Bapat and S. W. Dhawale, Electrochimica Acta, 15, 1519 (1970).

(13) L. Pospíšil and J. Kůta, Col. Czech. Chem. Com., 34, 3047 (1969).

(14) S. N. Frank and F. C. Anson, J. Electroanal. Chem., 54, 55 (1974).

(15) P. Delahay, "Double Layer and Electrode Kinetics", Interscience, New York, N.Y. (1965).

(16) R. W. Murray and D. J. Gross, Anal. Chem., 38, 392 (1966).

(17) G. W. O'Dom and R. W. Murray, J. Electroanal. Chem., 16, 327 (1968).

(18) F. C. Anson and D. J. Barclay, Anal. Chem., 40, 1791 (1968).

(19) D. J. Barclay and F. C. Anson, J. Electroanal. Chem., 28, 71 (1970).

(20) R. D. Armstrong and E. Barr, J. Electroanal. Chem., 20, 173 (1969).

(21) M. Sluyters-Rehbach, J. Breukel, K. A. Gijsbersen, C. A. Wijnhorst and J. H. Sluyters, J. Electroanal. Chem., 38, 17 (1972).

(22) R. D. Armstrong, J. D. Milewski, W. P. Race and H. R. Thirks, J. Electroanal. Chem., 21, 517 (1969).

(23) R. D. Armstrong, W. P. Race and H. R. Thirsk, J. Electroanal. Chem., 23, 351 (1969).

(24) S. H. Whitlow, Acta. Cryst., B31, 2531 (1975).

(25) W. Harrison and J. Trotter, J. Chem. Soc. Dalton, 956 (1972).

(26) M. L. Post and J. Trotter, Acta. Cryst. B30, 1880 (1974).

(27) W. Harrison and J. Trotter, J. Chem. Soc. Dalton, 1923 (1974).

(28) P. DeMeester and D. J. Hodgson, J. Am. Chem. Soc., 99, 6884 (1977).

(29) S. Paul, Acta. Cryst., 23, 491 (1967).

(30) L. G. Sillen and A. E. Martell, "Stability Constants", Chem. Soc. London, 1964.

(31) R. B. Wilson, P. DeMeester and D. J. Hodgson, Inorg. Chem., 16, 1498 (1977).

(32) L. Kisova, M. Sluyters-Rehback and J. H. Sluyters, J. Electroanal. Chem., 40, 29 (1972).

(33) T. Malmborg and Å. Oskarsson, Acta, Chemica Scandinavica, 27, 2923 (1973).

(34) P. Peerce, Ph.D. Thesis, California Institute of Technology, 1978.

PART III

APPENDICES

APPENDIX I

A BRIEF INTRODUCTION TO DOUBLE LAYERS AND ELECTRODE KINETICS

THE ELECTRICAL DOUBLE LAYER

Whenever an electrode is placed in an electrolyte solution an interphase or interfacial region known as the electrical double layer is formed. This double layer consists of charges and dipoles (usually solvent molecules) which have responded to the anisotropic forces which exist at a phase boundry and not in the bulk of the electrolyte. Charge on the electrode is compensated by an equal and opposite charge on the solution side of the interface and vice versa.

Helmholz first described a model for the double layer in 1853. His model consisted of a sheet of charge adjacent to the electrode surface. Gouy and Chapman in 1913 independently came up with a diffuse model similar to a Debye-Hückel treatment of ionic clouds. Stern, in turn, combined the two treatments into a model which had a compact layer next to the electrode and a diffuse region extending into the bulk of solution. Stern's model and various modifications are the basis for most modern double layer studies.

The Stern model consists of three important regions. The inner Helmholz plane (iHp), the outer Helmholz plane

(oHp) and the diffuse portion of the double layer. The iHp is closest to the electrode and characterized by solvent molecules and ions which have lost their solvation sheaths. These ions, which have a specific interaction with the electrode, are said to be specifically adsorbed, contact adsorbed or super-equivalently adsorbed. Anions are more prone to interact with the electrode in this way and virtually all anions are specifically adsorbed, fluoride and hydroxide ions being the notable exceptions. The outer Helmholz plane consists of ions which are electrostatically attracted to the charged electrode but still retain their solvent sheaths. The diffuse portion of the double layer is the area extending from the outer Helmholz plane into the bulk of the solution. As its name implies this layer does not consist of a sheet or plane of charge but is the region where uncompensated electrode charge is gradually compensated into the bulk of the electrolyte. The layer is diffuse because thermal and electrostatic forces in this region are approximately of the same magnitude whereas in the Helmholtz layers, chemical and electrostatic forces predominate. Figure 1 shows a representation of the electrical double layer in the presence and absence of adsorption and the appropriate potential profiles.

The charge separation in the double layer makes the interface act much like a capacitor. This capacitor-like

FIGURE 1

Schematic representation of the double layer under the condition of (A) no adsorption and (B) superequivalent adsorption. Potential-distance profiles are shown to the right for each case.

A

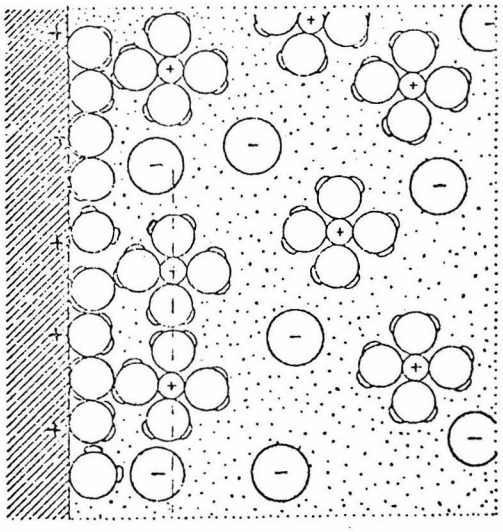

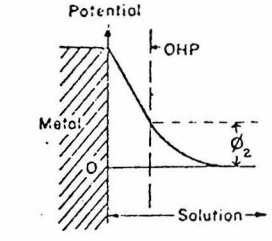

No contact – adsorption
($q_{CA} = 0$)

B

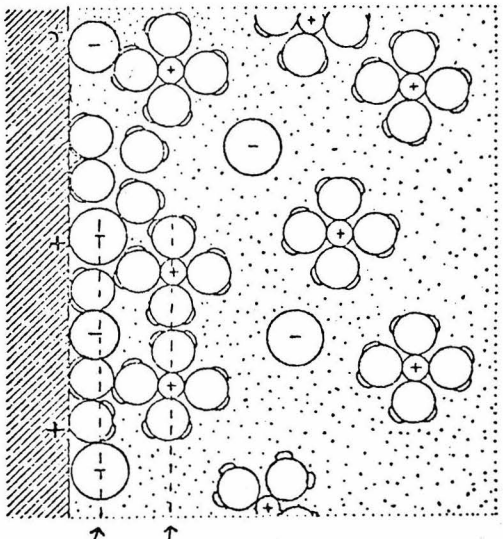

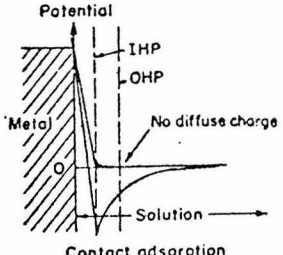

Contact adsorption
$|q_M| \leq |q_{CA}|$

IHP OHP DIFFUSE LAYER

property causes potential variations across the Helmholz and diffuse layers.

There is a linear potential drop across the Helmholz layers where the charges exist in sheets. The potential distance profile in the diffuse layer is given by the Gouy-Chapman equation.

It is these potential variations which make an understanding of the double layer important to the study of electrode kinetics. Since the rate is expressed in terms of potential it is important to have a knowledge of any potential losses which may come about at the electrode-electrolyte interface.

Mercury occupies a special position in the study of the electrochemical double layer for a number of reasons. First, it has a large hydrogen overvoltage which allows one to study processes in a wide potential range before the solvent molecules react. Secondly it is a liquid which is advantageous because it guarantees a renewable and smooth reproducible surface. A liquid has the added advantage of possessing a measurable thermodynamic quantity, the interfacial tension, which can supply valuable information about the electrode, such as electrode capacity and electrode charge.

ELECTRODE KINETICS

Electrode kinetics involves the study of the rate of a transfer of charge from one phase to another (usually from an electrode to solution or vice versa). The free energy change (ΔG) in the overall reaction is a linear function of the electrode potential (E)

$$d\Delta G = -nFdE \tag{1}$$

where n is the number of electrons transferred and F is the Faraday (96,500 coulombs). The similar expressions for the free energy of activation of the forward and reverse processes are as follows:

$$d\Delta G_f^{\ddagger} = \alpha nFdE \tag{2}$$

$$d\Delta G_r^{\ddagger} = -(1-\alpha)nFdE \tag{3}$$

where α is a number between zero and one, called the electrochemical transfer coefficient, which tells one something about the symmetry of the energy barrier. In most cases the transfer coefficient is assumed to be independent of E which allows one to write:

$$\Delta G_f^{\ddagger} = \Delta G_{of}^{\ddagger} + \alpha nFE \tag{4}$$

$$\Delta G_r^{\ddagger} = \Delta G_{or}^{\ddagger} - (1-\alpha)nFE \qquad (5)$$

Since an exponential relation exists between a rate constant and a free energy of activation one can vary an electrochemical rate constant by merely changing the applied potential. This allows one to study rates over many orders of magnitude.

If one considers the simple reaction

$$Ox^{+x} + ne^- \rightleftharpoons Red^{+(x-n)}$$

which is first order in either direction thus allows us to write the rates as:

$$v_f = k_f[Ox]_{x=o} \qquad (6a)$$

$$v_r = k_r[Red]_{x=o} \qquad (6b)$$

where $[Ox]_{x=o}$ and $[Red]_{x=o}$ are the concentrations of the two species at the electrode surface. In terms of current 6a and 6b become

$$i_f = nFv_f \qquad (7a)$$

$$i_r = nFv_r \qquad (7b)$$

so that the net current density measured is the difference between the forward and reverse currents:

$$i = i_f - i_r \tag{8}$$

$$i - nF(v_f - v_r) \tag{9}$$

At equilibrium the net current (rate) is zero, however charges are still being exchanged at the interface equally in both directions (i.e., $i_f = i_r$). This not directly measurable current is called the exchange current (i_o). The exchange current can be measured with an isotope experiment or by an electrochemical experiment described below.

From the exponential rate relationship and eqns (4) and (5) we obtain:

$$k_f = k_{of}\exp[-\alpha(\frac{nF}{RT})E] \tag{10}$$

$$k_r = k_{or}\exp[(1-\alpha)(\frac{nF}{RT})E] \tag{11}$$

where k_{of} and k_{or} are rate constants when E = 0. This however depends upon your choice of a reference potential so $E = E_e$ is chosen. At this potential i = 0 and $v_f = v_r$ so

$$[Ox]_{x=o} k_{of} \exp[-\alpha(\frac{nF}{RT})E_e] = [Red]_{x=o} k_{or} \exp[(1-\alpha)(\frac{nF}{RT})E_e] \quad (12)$$

One can now define the standard rate constant k_s as the rate constant under standard conditions ($E^o = E_e$, $i = 0$, $[Ox]_{x-o} = [Red]_{x=o}$).

$$k_s = k_{of} \exp[-\alpha(\frac{nF}{RT})E^o] = k_{or} \exp[(1-\alpha)(\frac{nF}{RT})E^o] \quad (13)$$

From eqns. (10) - (13) one can express the rate constant at a given potential in terms of the standard rate constant:

$$k_f = k_s \left\{\frac{[Red]_{x=o}}{[Ox]_{x=o}}\right\}^{\alpha} [\exp -\alpha(\frac{nF}{RT})\eta] \quad (14)$$

$$k_r = k_s \left\{\frac{[Ox]_{x=o}}{[Red]_{x=o}}\right\}^{1-\alpha} \exp[(1-\alpha)(\frac{nF}{RT})\eta] \quad (15)$$

where $\eta = (E-E_e)$ and is called the overpotential. The current in either direction is obtained by multiplying eqns. (14) and (15) by the concentration of the reacting species and nF:

$$i_f = nFk_s [Ox]_{x=o}^{1-\alpha} [Red]_{x=o} \exp[-\alpha(\frac{nF}{RT})\eta] \quad (16)$$

$$i_r = nFk_s [Ox]_{x=o}^{1-\alpha} [Red]_{x=o}^{\alpha} \exp[(1-\alpha)(\frac{nF}{RT})\eta] \quad (17)$$

and at $\eta = 0$

$$i_f - i_r = i_o = nFk_s[Ox]^{1-\alpha}_{x=o}[Red]^{\alpha}_{x=o} \qquad (18)$$

From eqns. (16), (17), (18) and (8) we can write an expression for the net current at any overpotential:

$$i = i_o\left\{\exp[-\alpha(\frac{nF}{RT})\eta] - \exp[(1-\alpha)(\frac{nF}{RT})\eta]\right\} \qquad (19)$$

If one measures the $i - \eta$ relationship for a reaction one can obtain the parameters i_o and α. If η is made large one of the exponentials is large and the other negligible and taking logs one obtains:

$$\eta = (\frac{RT}{\alpha nF})\ln(i_o) - (\frac{RT}{\alpha nF})\ln(i) \qquad (20)$$

where a plot of η against $\ln(i)$ yields α from the slope and i_o from the intercept. Eqn. (20) is known as the Tafel equation. If large η values are not obtainable (i.e., the reaction is very fast) the condition $\eta << \frac{RT}{\alpha nF}$ is used to linearize eqn. (19):

$$i = -i_o(\frac{RT}{nF})\eta \qquad (21)$$

Under these conditions i_o is obtainable from the i - η plots and α from eqn. (18).

The derivation presented lacks any consideration for double layer effects. As would be expected the double layer may have a considerable influence on the electrode reaction. There are two considerations. First the reaction occurs not at the electrode surface (x = 0) as the derivation implies. Electrochemical reactions are assumed to occur at the outer Helmholz plane (oHp). Because of this the concentration is expressed at the oHp rather than the electrode surface by equation:

$$[Ox]_{oHp} = [Ox]_{bulk} \exp\left(\frac{-zF\phi_2}{RT}\right) \tag{22}$$

where ϕ_2 is the outer Helmholz potential.

The second consideration is that the effective potential at the oHp is not η but $\eta - \phi_2$. Incorporating this into our rate equation one obtains

$$i_f = [Ox]_{bulk} \exp\left(\frac{-zF\phi_2}{RT}\right) \exp\left[-\alpha\left(\frac{nF}{RT}\right)(\eta-\phi_2)\right] \tag{23}$$

and the Tafel equation becomes:

$$\eta - \phi_2 = \left(\frac{RT}{\alpha nF}\right) \ln i_o - \left(\frac{RT}{\alpha nF}\right) \ln i + \frac{zF\phi_2}{RT} \tag{24}$$

From a plot of $\eta - \phi_2$ versus $\ln i + \frac{zF\phi_2}{RT}$ we can obtain α from the slope and the exchange current is related to the intercept. These modifications were first introduced by A. N. Frumkin and are many times referred to as the Frumkin corrections. One drawback of the Frumkin treatment is that ϕ_2 potentials must be known independently for the concentration and electrolyte in which the rate measurements are taken.

APPENDIX II

A PROGRAM FOR THE DETERMINATION OF CHARGE-POTENTIAL CURVES AT A DROPPING MERCURY ELECTRODE

THEORY

The current passed during the growth of an ideal, spherical mercury drop potentiostatted at a constant potential is given by

$$i(t) = q^m\frac{dA}{dt} + 7.082 \times 10^4 nD^{1/2}C^o m^{2/3}t^{1/6} \qquad (1)$$

where i(t) is the net current, q^m is the double layer charge per unit area, D is the diffusion coefficient of any species which is reacting, C^o is its concentration, n is the number of electrons involved per mole of reactants, m is the flow rate of the capillary used and t is the drop time. Assuming an ideal spherical drop, the area of the drop is given by:

$$A(t) = .8515m^{2/3}t^{2/3} \qquad (2)$$

Substituting this into eqn. (1) and integrating:

$$Q(t) = .8515m^{2/3}t^{2/3}q^m + 6.07nm^{2/3}t^{7/6}D^{1/2}C^o \qquad (3)$$

Dividing eqn. (3) by $0.815m^{2/3}t^{2/3}$ we obtain:

$$\frac{Q(t)}{.8515m^{2/3}t^{2/3}} = q^m + 7.14nD^{1/2}C^o t^{1/2} \qquad (4)$$

which reduces to:

$$Q(t)/A = q^m + st^{1/2} \qquad (5)$$

Therefore a plot of Q/A versus $t^{1/2}$ will have an intercept q^m, the charge on the electrode, and a slope s which is proportional to the concentration of reversibly reacting Faradaic impurities which undergo electrochemical reaction.

DESCRIPTION AND OPERATION OF PROGRAM

A computer program was written to collect charge-time data at various potentials. It utilizes the PDP 11/40 mini-computer system with a computer controlled potentiostat and integrator. A schematic representation of the computer system is shown in Figure 1. The operator calls the program into core, initializes the various parameters and can run the program in either s manual or automatic mode.

The program begins with the computer asking for the various constants it requires. When the initialization

FIGURE 1

Block diagram of PDP 11/40 minicomputer system on which the charge potential program was implemented.

PDP 11/40 MINICOMPUTER SYSTEM

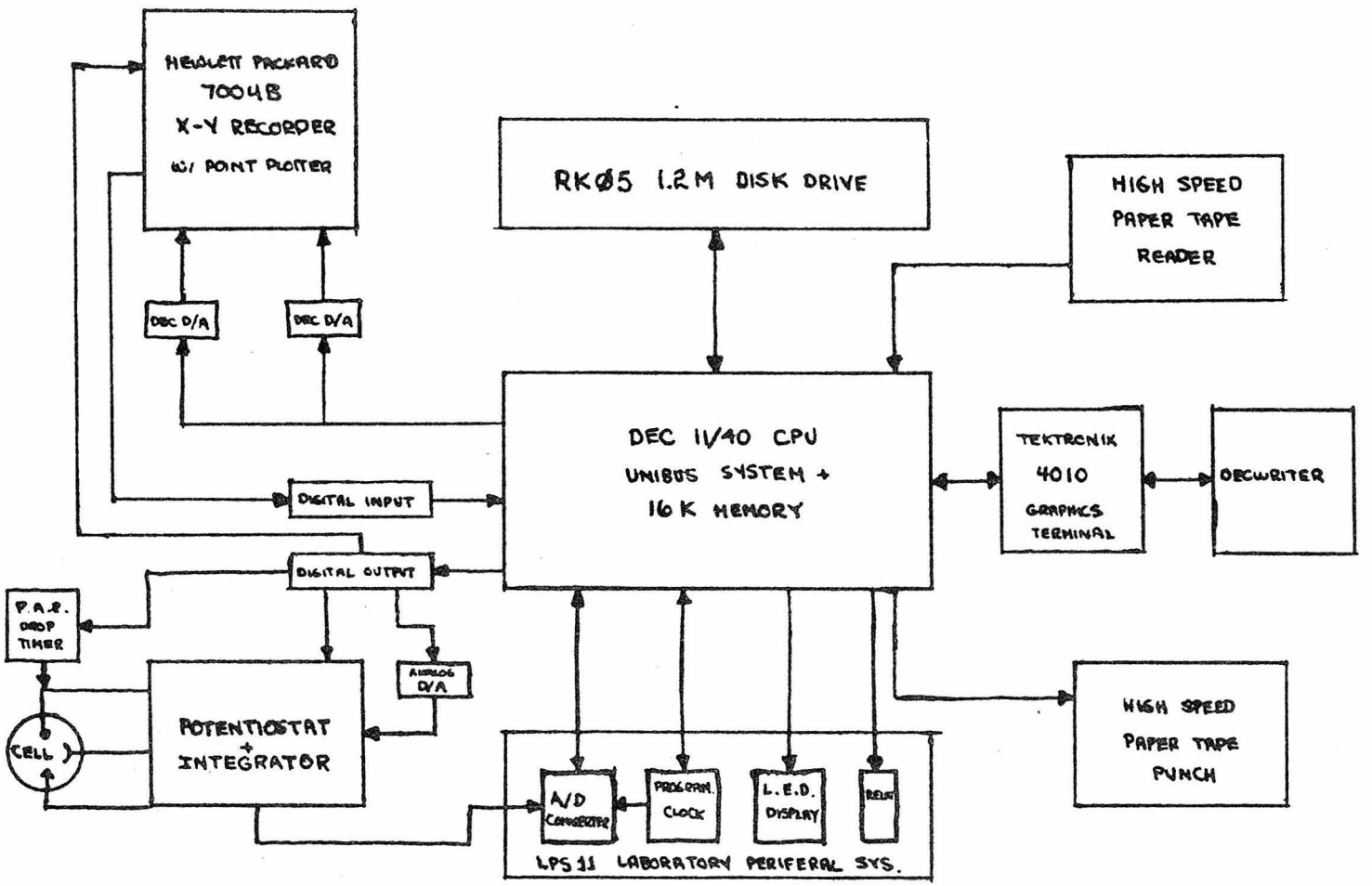

parameters are inputted, the computer displays the potential it will use to acquire data, sends a pulse to the drop knocker, waits for the drop to fall and acquires data from zero time to the specified droptime. In the automatic mode the computer would then least square the data against the square root of time and output the intercept (q^m), slope, deviations and the ratio of double layer to Faradaic charge. This completed, it displays the potential again, knocks another drop and repeats the same potential the desired number of times before incrementing the potential. A sample output for the automatic mode is shown in Table 1.

The manual mode allows the operator the option to look at raw data and manipulate it in a number of ways. It also allows the operator to choose the potential for each experiment and to vary the least-square limits on the same data set.

Figure 2 shows a flow chart for the program which illustrates the options and operation of the program.

Table 1. Typical Output from the Program

TABLE OF INITIALIZATION PARAMETERS

THE DROP TIME IS 4.000 SECONDS

THE FLOW RATE IS 1.209 MILLIGRAMS/SECOND

THE CURRENT MEASURING RESISTOR IS 5.000 KOHMS

THE RC TIME CONSTANT IS 0.001 SECONDS

THE STARTING POTENTIAL IS 148.926 MILLIVOLTS

THE FINAL POTENTIAL IS -1198.739 MILLIVOLTS

THE POTENTIAL INCREMENT IS -48.828 MILLIVOLTS

4.0 POINTS TAKEN AT EACH INCREMENT

LEAST SQUARE LIMITS 0.750 AND 2.000 SECONDS

A DATA POINT WILL BE TAKEN EVERY 5.000 MILLISECONDS

PROGRAM WILL CYCLE AUTOMATICALLY

111 IS THE TOTAL # OF TRIALS TO BE DONE

A005 000000
$CO

THE LEAST SQUARE LIMITS ARE 0.750 AND 2.000 SECONDS

RUN	VOLTAGE	CHARGE	QDEV	SLOPE	SDEV	RATIO
1	148.926	18.267	0.031	-2.792	0.027	-4.627
2	148.926	17.894	0.033	-2.961	0.028	-4.273
3	148.926	17.669	0.029	-2.994	0.025	-4.173
4	148.926	17.639	0.024	-2.999	0.021	-4.159
5	100.098	15.924	0.021	0.889	0.018	12.659
6	100.098	16.000	0.018	0.949	0.016	11.926
7	100.098	16.035	0.026	0.971	0.022	11.673
8	100.098	15.912	0.020	0.880	0.017	12.788
9	51.270	14.436	0.028	1.546	0.024	6.604
10	51.270	14.368	0.021	1.495	0.018	6.795
11	51.270	14.419	0.023	1.522	0.020	6.701
12	51.270	14.345	0.022	1.452	0.019	6.985
13	2.441	13.285	0.028	2.944	0.024	3.191
14	2.441	13.340	0.027	2.947	0.023	3.201

FIGURE 2
(next three pages)

Brief flow chart showing overall structure of the charge-potential program.

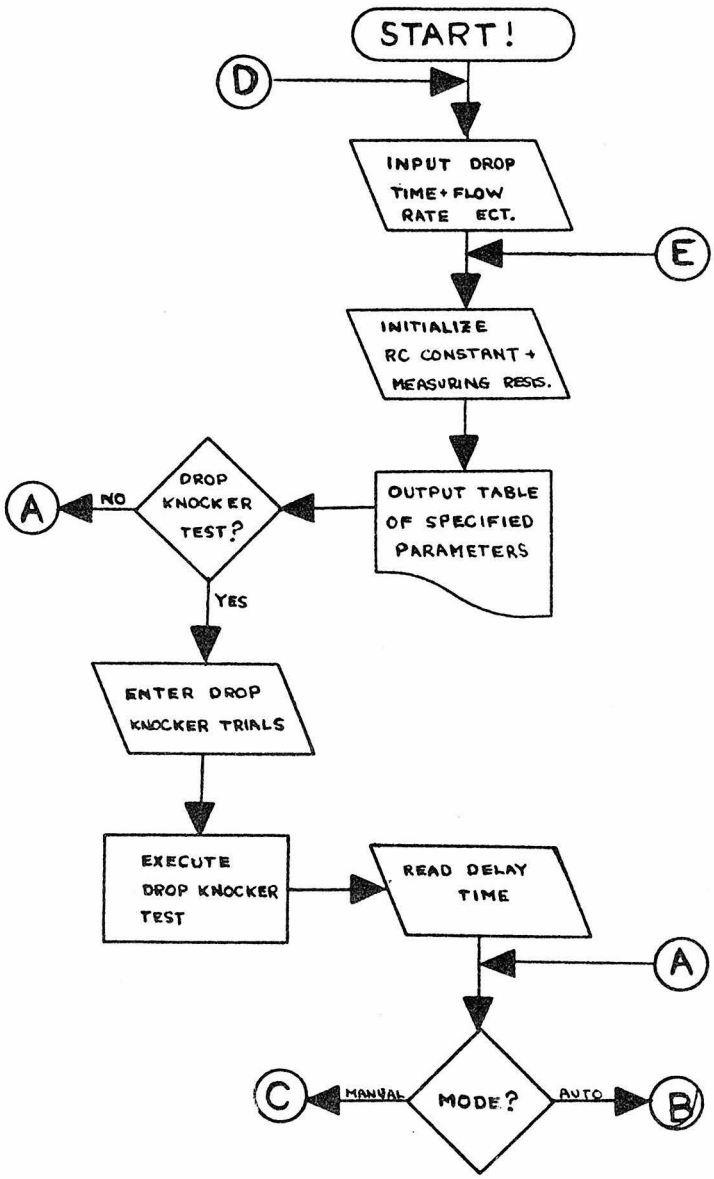
START!
D
INPUT DROP TIME + FLOW RATE ECT.
E
INITIALIZE RC CONSTANT + MEASURING RESIS.
OUTPUT TABLE OF SPECIFIED PARAMETERS
DROP KNOCKER TEST?
NO
A
YES
ENTER DROP KNOCKER TRIALS
EXECUTE DROP KNOCKER TEST
READ DELAY TIME
A
MODE?
MANUAL
C
AUTO
B

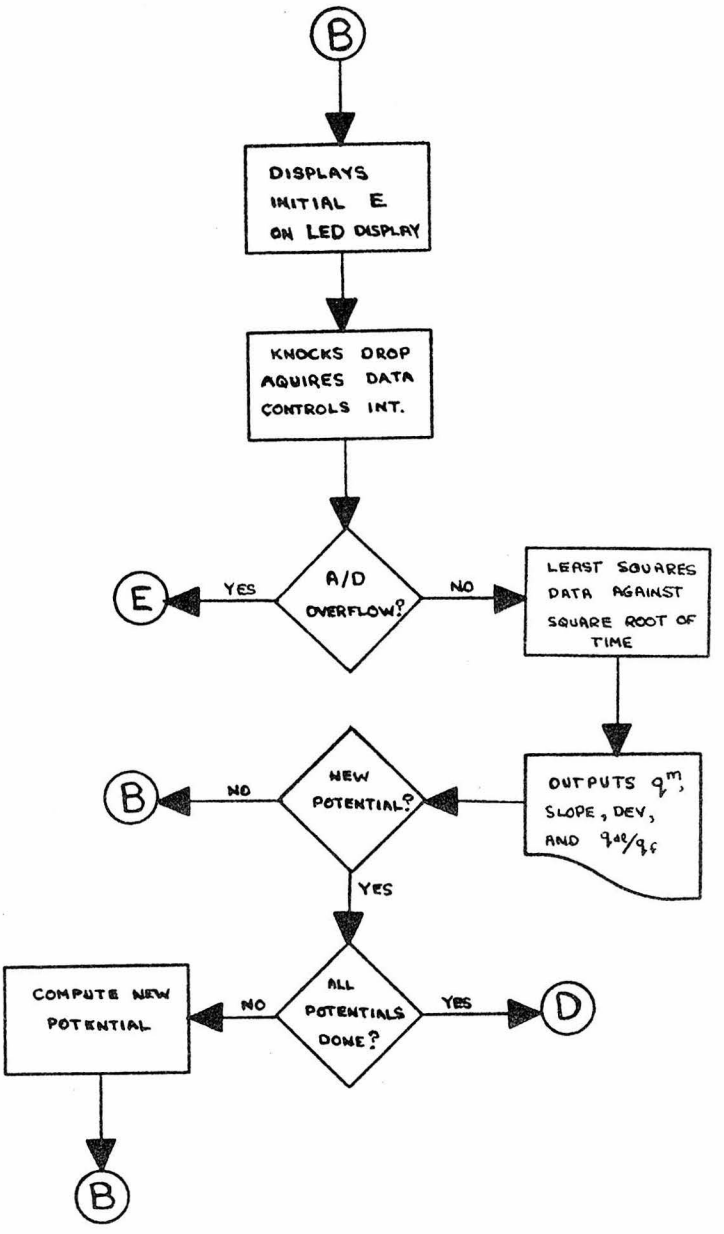
B
DISPLAYS INITIAL E ON LED DISPLAY
KNOCKS DROP AQUIRES DATA CONTROLS INT.
A/D OVERFLOW?
YES
E
NO
LEAST SQUARES DATA AGAINST SQUARE ROOT OF TIME
OUTPUTS q^m, SLOPE, DEV, AND q_{ae}/q_f
NEW POTENTIAL?
NO
B
YES
ALL POTENTIALS DONE?
NO
COMPUTE NEW POTENTIAL
B
YES
D

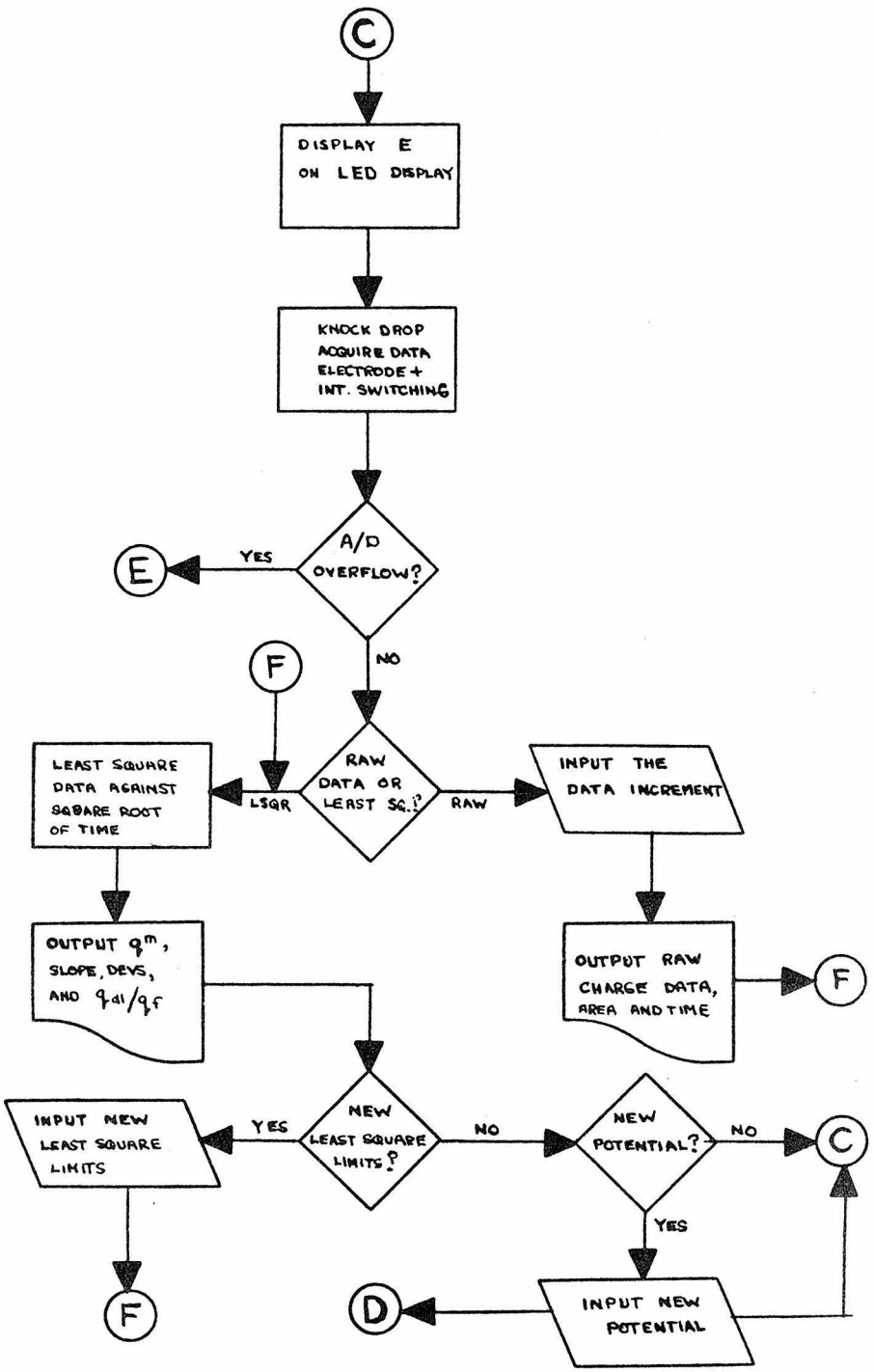
C
DISPLAY E ON LED DISPLAY
KNOCK DROP ACQUIRE DATA ELECTRODE + INT. SWITCHING
A/D OVERFLOW?
YES
E
NO
F
RAW DATA OR LEAST SQ.?
LSQR
LEAST SQUARE DATA AGAINST SQUARE ROOT OF TIME
RAW
INPUT THE DATA INCREMENT
OUTPUT q^m, SLOPE, DEVS, AND q_{dl}/q_f
OUTPUT RAW CHARGE DATA, AREA AND TIME
F
NEW LEAST SQUARE LIMITS?
YES
INPUT NEW LEAST SQUARE LIMITS
NO
NEW POTENTIAL?
NO
C
YES
F
D
INPUT NEW POTENTIAL

APPENDIX III

Table of Symbols Used

q^i	Specifically adsorbed charge
q^m	Charge on the electrode
ϕ_2	Potential drop across the diffuse layer
α	Intrinsic electrochemical transfer coefficient
E	Electrode Potential vs SCE
μ	Ionic strength
R	Gas constant
T	Temperature in °K
F	The Faraday
z	Charge of ion
k_{app}	Apparent rate constant
ϕ_r	Potential at the reaction site
γ	Interfacial tension
$\Gamma_{\pm}$	Superficial excess of anions (cations)
α_{app}	Apparent electrochemical transfer coefficient
X^-	Halide ion
A	Electrode area
K_{surp}	Surface solubility product
C	Concentration of species
K_{sp}	bulk solubility product
D	Diffusion coefficient

C_{dl}	Double layer capacitance
q^{mon}	Charge of a monolayer
n	number of electrons in an electrochemical reaction
ΔG	Free energy charge
ΔG^{F}	Free energy of activation
i	Current
i_o	Exchange current
η	Overpotential $E - E_e$
k_s	Standard rate constant
m	Flow rate
t	drop time

PART IV

PROPOSITIONS

PROPOSITION I

MEASUREMENT OF THE REDOX PROPERTIES OF EXCITED STATE MOLECULES

The conversion of solar energy at a semiconductor electrode can occur by at least two mechanisms. The first mechanism proceeds by a photon interacting directly with the electrode and exciting an electron into the conduction band where it can be used to do electrical work or directly photoelectrolyze water to a useful fuel, hydrogen.[1,2] A second mechanism utilizes a highly absorptive molecule near or adsorbed on the electrode surface to mediate the solar to electrochemical energy conversion.[3] This mechanism would exploit the higher redox reactivity of a photo-excited state molecule. Unfortunately very little is known about the electrochemical properties of excited state species. Several techniques are proposed which could provide a fundamental understanding of the redox properties of excited state molecules.

Most of the experimental investigations of excited state electrochemistry have been plagued with background effects which occur when light impinges directly on the electrode surface. These effects which include local heating, reactions of adsorbed solvent or electrolyte and reactions of excited[4-6] electrode materials (as with semiconductor electrodes) can

effectively mask any photo-assisted electron transfer reactions of solution species that one may wish to study.

One approach which may circumvent many of these problems is to generate the photochemical products in the absence of any electrode and then quickly transport them to an electrode surface.

A rotating photoelectrode is one possibility for accomplishing the mass transport of excited state molecules. A modification of previous photoelectrodes is diagramed below.

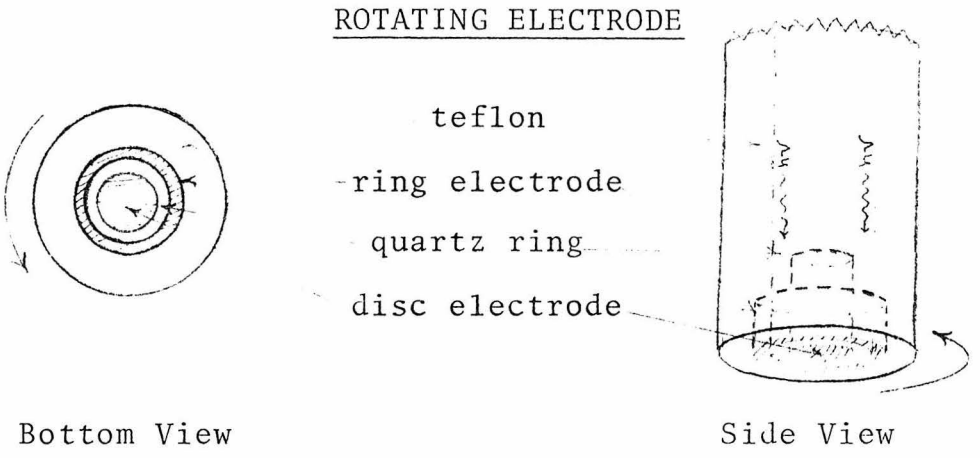

Rapid rotation of this electrode transports the solution across the center disk to a transparent quartz region through which the solution may be irradiated by means of a monochromatic light source or tunable laser, the beam of which is optically shaped into a ring of light to avoid intensity losses.

TECHNIQUE FOR PRODUCING A RING OF LIGHT

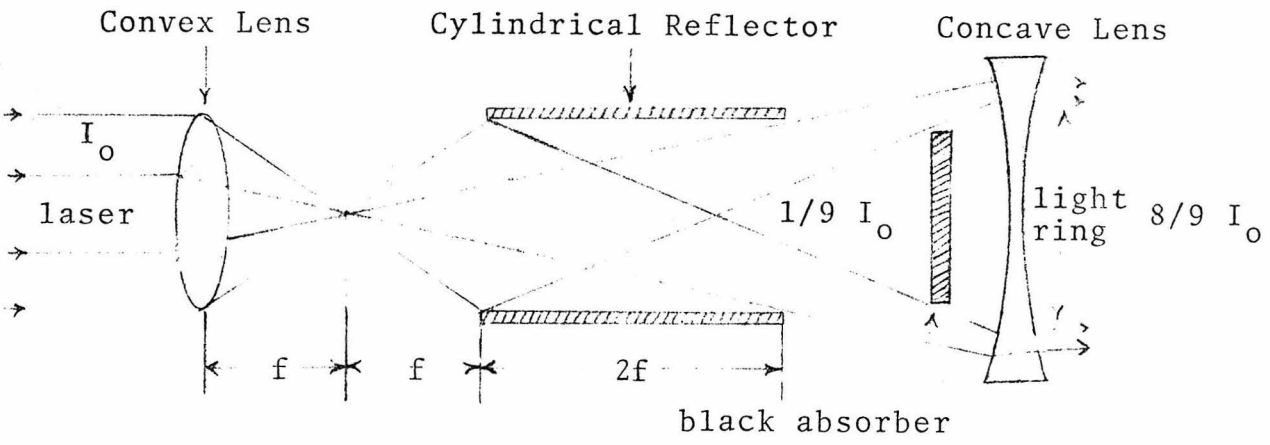

Photoassisted electron transfer effects may still be masked if there is any scattering of light back to the electrode surface.

A technique termed hydrodynamic modulation has been employed to effectively eliminate background effects at rotating electrodes.[10] The idea is to superimpose a small sinusoidal variation of the rotation speed about a fixed value. By using a phase locked detection system only the currents resulting from the modulation are detected. Mass transfer of photogenerated species to the electrode surface is a rotation speed dependent process and will respond to the modulation, whereas non-mass transfer processes such as background photoelectric effects,

charging currents and solid electrode surface reactions will be discriminated against.[11]

The electrode described coupled with hydrodynamic modulation offers additional advantages for the study of photoassisted electron transfer. The current from the disk electrode can be nulled against the current from the ring electrode using a bridge or operational amplifier circuit. If the current balance is brought about at a potential just before the oxidation or reduction of the ground state reactant in the absence of the reactant and/or light, small shifts from the zero due to enhanced reactivity of the photoexcited molecules should be measurable when the reactant is added or the light source is activated.

Mass transfer equations have been solved for laminar flow conditions at rotating electrodes.[12] Maintaining laminar flow limits the speed of electrode rotation and thus the transit time for any short lived excited state species to reach the electrode surface. In rotating ring disk studies the insulating gap between the ring and disk electrodes is made as small as possible to shorten the transit time. No insulating gap is needed between the quartz ring and ring electrode which would be expected to improve the transit time. However, under laminar flow conditions it is unlikely that the transit time could be lowered to much below one millisecond.[13]

Turbulant flow at extremely fast rotation speeds would increase the mass transfer to the electrode but the mass transfer equations for turbulant flow at rotating electrodes are inadequate.[14] It

is possible however that the nulling technique coupled with light chopping (it is doubtful that hydrodynamic modulation is possible at extremely high rotation rates or under turbulant flow conditions) and phase detecting slightly out of phase of the light chopping frequency would not be affected by the turbulant flow.

Another electrode configuration which would have some advantages over the rotating electrode would be a double tube electrode in a flow system with the two tubes being separated by a quartz gap as diagrammed below. Laminar flow in a double tube

DOUBLE TUBE ELECTRODE

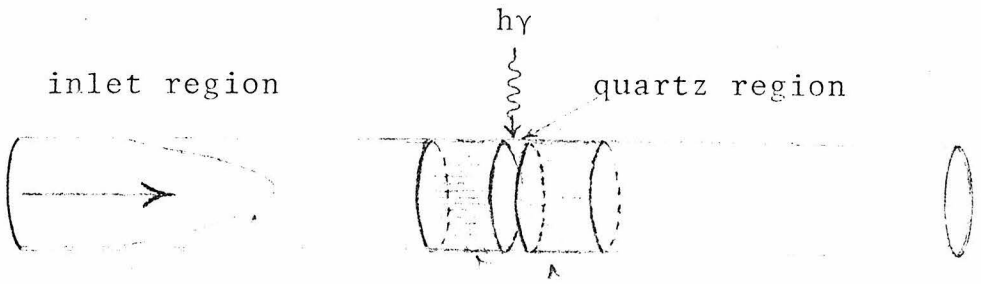

laminar flow profile tube electrodes

electrode with a long inlet region were the subject of study by digital simulation and yielded results comparable to the rotating ring-disk electrode.[15] A flow system of similar geometry was used for measuring fast kinetics by Gerischer et al.[16] The tube electrode configuration has the advantage of a more symmetrical electrode arrangement about the incident light. The symmetry would make nulling of background phenomena, as described for the rotating electrode, much more reliable. Higher mass transfer rates under laminar flow conditions can be achieved in a tube electrode when compared to a

rotating electrode.[14] A recent publication suggests the possibility of hydrodynamic voltammetry in flow through tubular electrodes[17] although phase detection with light chopping is still a possibility for increasing the signal to noise ratio. A simple calculation which was done using the Levich expression for the current due to laminar flow in tubular electrodes[14] and a typical electrode geometry, flow rate and excited state population indicated currents as high as 200 nanoamperes could be measured for an excited state lifetime of ten microseconds. Excited state triplet lifetimes in solution at room temperature of up to four hundred microseconds have been observed for some lactone and dione molecules.[18] The rather high quantum yields (>0.4) also measured for these systems[18] make them attractive candidates for observing excited state electron transfer reactions. Tris-bipyridine ruthenium(III) would be an inorganic molecule of interest for these studies even though the triplet lifetime in solution is probably less than ten microseconds. Aromatic hydrocarbons and dye molecules would be interesting also because of their long-lived triplet states.

The effect of flow rate (or rotation rate), quantum yield and excited state lifetime on the observed current would be an interesting problem for digital simulation.[19]

Comparison of the behavior when metallic electrodes are interchanged with semiconducting materials of various band gaps could provide valuable data about the energetics involved in the electron transfer reactions. Back reactions and through-space energy transfer would reduce any observable effect at a metal electrode, however, a system with a fast chemical step to electro-inert products after electron transfer could minimize the back reaction. Semiconductor materials with the correct band gap would be capable of distinguishing any anodic and cathodic components of the current observed at a metal electrode. The direction of the current is important because of the prediction that an excited molecule is both a better oxidant and reductant than the same molecule in the ground state.[3]

The irradiation wavelength dependence of the observed current would yield information about the electronic states associated with the excited state electron transfer. Other information could also be obtained using either of the electrode configurations described. The electrochemistry of photo-generated transient species can be studied. This is analogous to the rotating photoelectrode described by Johnson.[7,20]

first electrode: no rxn

quartz region: $A \xrightarrow{h\nu} A^* + S \longrightarrow B$

second electrode: $B \pm ne^- \longrightarrow C$

A photochemical reaction which could prove interesting is the ferrioxalate photoreaction where an intermediate has been detected but not characterized.[21.22]

$$Fe(ox)_3^{3-} \xrightarrow{h\nu} Fe(ox_3)^{3-*}$$

$$Fe(ox)_3^{3-*} \longrightarrow [\text{metastable state}]$$

$$[\text{metastable state}] \longrightarrow Fe(ox)_2^{2-} + ox^-$$

$$ox^- + Fe(ox)_3^{3-} \rightleftharpoons ox^{2-} + \left[(ox)_2Fe\begin{matrix}O\text{-}CO\\ |\\ O\text{-}CO\end{matrix}\right]^{2-}$$

$$\left[(ox)_2Fe\begin{matrix}O\text{-}CO\\ |\\ O\text{-}CO\end{matrix}\right]^{2-} \longrightarrow Fe(ox)_2^{2-} + 2CO_2$$

The photochemical behavior of short lived electrogenerated reactants has not received much attention. A reaction scheme may be illustrated as follows:

first electrode:	$A \pm ne^- \longrightarrow B$
quartz region:	$B + h\nu \longrightarrow B^* + S_1 \longrightarrow D$
	$B + S_2 \longrightarrow C(\text{inert})$
second electrode:	$D \pm ne^- \longrightarrow E$

Electrogenerated radical species would be interesting candidates for these studies since many highly stable anion and cation radicals that are highly colored in

solution are known and the photoelectrochemistry of such species could prove interesting.

It is hoped that these techniques may yield fundamental information about the electron transfer characteristics of excited state molecules. Perhaps this information could be used to increase the efficiency of photovoltaic devices by increasing their quantum efficiency or allowing them to utilize a greater portion of the solar spectrum.

REFERENCES

(1) A. Fujishima and K. Honda, Nature, 238, 37 (1972).

(2) A. Fujishima and K. Honda, Bull. Chem. Soc. Japan, 44, 1148 (1971).

(3) H. Gerischer, Physical Chemistry, H. Eyring, B. Henderson, N. Jost eds., Academic Press, New York, 1970, Vol. 9A, p. 463.

(4) G. C. Barker and D. McKeown, J. Electroanal. Chem., 62, 341 (1975).

(5) S. S. Fratoni and S. P. Perone, Anal. Chem., Vol 48, 287 (1976).

(6) G. C. Barker, A. W. Gardner and D. C. Sammon, J. Electrochem. Soc., 113, 1182 (1966).

(7) D. C. Johnson and E. W. Resnick, Anal. Chem., 44, 637 (1972).

(8) A. Fujishima et. al., J. Am. Chem. Soc., 97, 4134 (1975).

(9) R. Kompfner, private communication

(10) B. Miller, M. I. Bellavance and S. Bruckenstein, Anal. Chem., 44, 1983 (1972).

(11) B. Miller and S. Bruckenstein, J. Electrochem. Soc., 121, 1558 (1972).

(12) V. G. Levich, Acta. Phys. Chim. URSS, 17, 257 (1942).

(13) W. J. Albery and M. L. Hitchman, Ring Disk Electrodes, Clarendon Press, Oxford, 1971.

(14) V. G. Levich, Physiocochemical Hydrodynamics, Prentice Hall Inc., Englewood Cliffs, N.J., 1962.

(15) J. Flanagan, Master's Thesis, Texas Tech University, 1973.

(16) H. Gerischer, I. Mattes and R. Braun, J. Electroanal. Chem., 10, 553 (1965).

(17) W. J. Blaedel and D. G. Iverson, Anal. Chem., 49, 1563 (1977).

(18) E. F. Ullman and N. Baumann, J. Am. Chem. Soc., 90, 4158 (1968).

(19) D. C. Johnson, et. al., Anal. Chem., 46, 865 (1974).

(20) P. R. Gaines, V. E. Peacock and D. C. Johnson, Anal. Chem., 47, 1373 (1975).

(21) C. A. Parker and G. G. Hatchard, J. Phys. Chem., 63, 22 (1959).

(22) W. J. Albery, M. D. Archer and R. G. Egdell, J. Electroanal. Chem., 82, 199 (1977).

PROPOSITION II

DOUBLE LAYER STRUCTURE AND ELECTRODE KINETICS IN LIQUID AMMONIA

Anhydrous liquid ammonia is an amphiprotic, very weakly acidic, slightly ionized solvent which makes it appealing as an electrochemical media but has seen relatively little use in this role. It is proposed that a systematic investigation of double layer properties and electrode kinetics in liquid ammonia be undertaken which would provide data for interesting comparisons with available data in aqueous electrolytes.

The small dielectric constant (16.9 at 25° as compared to 78.5 for water at 25°)[1] leads to high solution resistances which makes the use of iR compensation necessary for any non-steady-state electrochemical measurements even though many commonly employed supporting electrolyte salts dissolve to concentrations in excess of 0.1 molar (e.g. NH_4NO_3, NH_4Cl, KNO_3, KI, $NaClO_4$).[2] The liquid range for ammonia (-77.7° to -33.4° at one atmosphere) makes it ideal for low temperature studies of chemical species which are unstable at room temperature or in the presence of strong proton donors, an end to which Bard and co-workers have addressed themselves in a series of recent papers.[3-5] Vacuum line techniques for handling and purifying liquid ammonia have been reported to virtually eliminate impurities (especially water) from the solvent.[3]

Reference electrodes which have been used successfully in liquid ammonia include the electron electrode, the

lead-lead(II) couple and a mercury pool. Pilot ions such as thallium(I) give reproducible behavior in the solvent.[2]

Laitinen and co-workers[6-9] have demonstrated the utility of stationary and dropping mercury electrodes in liquid ammonia. A large potential range is available limited by the anodic dissolution of mercury to mercuric ions in the positive direction and (in the absence of easily reduced supporting electrolyte ions) by the formation of solvated electrons in the cathodic direction (-2.3 volts versus a mercury pool). A high pressure polarographic cell as described by Schaap et.al.,[10] allows the use of liquid ammonia as a solvent from 25°, where ammonia has a vapor pressure very close to ten atmospheres,[1] to -38° where mercury freezes.

Murtazaev[11-13] has measured electrocapillary curves at 0° in liquid ammonia for solutions of chloride, bromide iodide and nitrate ions and observed a decrease in the interfacial tension and shift of the electrocapillary maximum (ECM) to more negative potentials due to the adsorption of the halide ions. The shift in the ECM and the decreases in interfacial tension are generally greater than for the same electrolytes in aqueous solution, an effect which has been attributed to weaker solvation of anions in the non-aqueous media. Na^+, K^+ and NH_4^+ have indicated some specific adsorption at more negative

potentials in this media. Capacity measurements by Payne[14] at -36.5° confirmed Murtazaev's observation that the amount of adsorption of anions was in the usual order $I^- > Br^- > Cl^- > NO_3^-$.

A systematic study of interfacial tension, capacitance or electrode charge at varying ion concentrations has not been undertaken but would yield thermodynamic information about the superficial excesses of ions at the mercury-ammonia interface. A comparison of the superficial excesses in water and liquid ammonia at the same temperature would yield insights into the importance of solvation, work terms and dielectric properties to the adsorption process. The Gouy-Chapman equation for a z-z electrolyte

$$\phi_2 = \frac{2RT}{zF} \operatorname{arcsinh}\left[\frac{q^2\pi}{2RT\varepsilon C_s}\right]^{\frac{1}{2}}$$

would predict a ϕ_2 potential for a given electrode charge and electrolyte composition that would be considerably larger in liquid ammonia than in water at the same temperature due to liquid ammonia's lower dielectric constant. The ϕ_2 potential which appears in the "work term" of many isotherm expressions for ionic adsorption[15] could be another factor in the apparent increased adsorption of ions observed in liquid ammonia.

No studies of electrode kinetics have been carried out in liquid ammonia although such a study would be of interest for a variety of reasons, a few of which will be discussed below.

The ϕ_2 potential also appears in kinetic equations to correct an electrode reaction rate for the double layers influence.[16] The validity or unapplicability of the Frumkin approach (which involves the use of thermodynamic data and Gouy-Chapman theory to arrive at rate corrections) in liquid ammonia would be supplemental to the present scrutiny this procedure is receiving when applied to aqueous solutions.[17-19]

A comparison of standard rate constants for simple one electron electrode reactions in solvents with different dielectric properties would yield information about the importance of the dielectric environment in an electron transfer reaction. Even though some workers have found this parameter to be unimportant over a limited range of dielectric constants (68 to 88) for the homogeneous neptunium(V) - neptunium(VII) electron exchange reaction.[20]

Grossman and Garner[21] have measured the self exchange rate for the hexaammines of cobalt(II) and cobalt(III) in liquid ammonia and found the rate to be 30 to 10^4 times faster than rates measured in concentrated aqueous ammonia. The activation energy for the exchange reaction

in liquid ammonia was unusually high for an electron transfer reaction (23 kcal) and an alternate mechanism involving ligand dissociation before electron transfer was proposed. It would be interesting to measure the electrode reaction rate of $Co(NH_3)_6^{3+}$ in liquid ammonia to discover if a similar increase in the heterogeneous rate also occurs.

The electrode kinetic behavior in water of aquo complexes of chromium(III)[22] and ammine complexes of cobalt(III)[23] and chromium(III)[24,25] has been the subject of several recent publications and Chapter Two of Part One of this thesis. Differences in solvated radii which result in different reaction sites and pathways have been invoked with various degrees of success to explain the kinetic trends observed. Examination of the electrode kinetics of these transition metal complexes in liquid ammonia would provide data for some interesting comparisons with the behavior in water.

The plus two oxidation state of cobalt and chromium exchange ligands rapidly with the solvent whereas the plus three oxidation state of both metals is inert. Upon reduction in aqueous solution the ammine complexes of the plus three oxidation state undergo rapid ligand exchange to aquo species[26] while no change in ligand character occurs in the aquo complexes. In liquid ammonia

this behavior would be reversed which would allow the electrode kinetics of the oxidation of the labile ammine complexes of the plus two oxidation state of chromium and cobalt to be studied. The aquo complexes of chromium(III) and cobalt(III) would undergo ligand substitution after reduction in liquid ammonia and provide an interesting contrast to their behavior in water.

REFERENCES

(1) "Handbook of Chemistry and Physics", The Chemical Rubber Co., 45th ed., Cleveland, Ohio, 1964.

(2) C. K. Mann in "Electroanalytical Chemistry", Vol. 5 A. Bard, ed., Marcel Dekker, New York, NY (1969).

(3) A. Demortier and A. J. Bard, J. Am. Chem. Soc., 95, 3495 (1973).

(4) W. Smith and A. J. Bard, J. Am. Chem. Soc., 97, 5203 (1975).

(5) W. Smith and A. J. Bard, J. Am. Chem. Soc., 97, 6491 (1975).

(6) H. A. Laitinen and C. J. Nyman, J. Am. Chem. Soc., 70, 2241 (1948).

(7) H. A. Laitinen and C. J. Nyman, J. Am. Chem. Soc., 70, 3002 (1948).

(8) H. A. Laitinen and C. E. Shoemaker, J. Am. Chem. Soc., 72, 663 (1950).

(9) H. A. Laitinen and C. E. Shoemaker, J. Am. Chem. Soc., 72, 4975 (1950).

(10) W. B. Schaap, R. F. Conley and F. C. Schmidt, Anal. Chem., 33, 498 (1961).

(11) A. M. Murtazeav, Acta Physicochim URSS, 12, 225 (1940).

(12) A. M. Murtazeav and M. Abramov, Zh. Fiz. Khim., 13, 350 (1939).

(13) A. M. Murtazeav and I. Igamberdyev, Zh. Fiz. Khim, 14, 217 (1940).

(14) R. Payne, Ph.D. Thesis, University of London, 1962.

(15) P. Delahay, "Double Layer and Electrode Kinetics", Interscience, New York, N.Y. (1965).

(16) A. Frumkin, Z. Phys. Chem., 164A, 121 (1933).

(17) M. J. Weaver and F. C. Anson, J. Electroanal. Chem., 65, 711 (1975).

(18) M. J. Weaver and F. C. Anson, J. Electroanal. Chem., 65, 737 (1975).

(19) B. Parkinson and F. C. Anson, J. Electroanal. Chem., in press.

(20) D. Cohen, J. C. Sullivan, E. S. Amis and J. C. Hindman. J. Am. Chem. Soc., 78, 1543 (1956).

(21) J. J. Grossman and C. S. Garner, J. Chem. Phys., 28, (1953).

(22) M. J. Weaver and F. C. Anson, Inorg. Chem., 15, 1871 (1976).

(23) M. J. Weaver, private communication.

(24) M. J. Weaver and T. L. Satterburg, J. Phys. Chem., 81, 1773 (1977).

(25) F. C. Anson, A. Yamada and M. G. Finn, Inorg. Chem., 16, 2124 (1977).

(26) H. A. Laitinen and P. Kivalo, J. Am. Chem. Soc., 75, 2198 (1953).

PROPOSITION III

USE OF A CATALYTIC ELECTROCHEMICAL DETECTOR FOR THE DETERMINATION OF In^{+3} BY HIGH PRESSURE LIQUID CHROMATOGRAPHY

Indium reduction is catalyzed by adsorbed ligand bridging anions such as thiocyanate and iodide. Pospísil and DeLevie,[1] Aikens[2] et al. and others[3] have studied this phenomenon. For thiocyanate the following mechanism has been established.

$$In(H_2O)_6^{+3} + 2SCN^-_{ads} \xrightarrow{\text{slow}} In(SCN)^+_{2\,ads} + 3e^- \xrightarrow{\text{fast}} In^o_{(Hg)} + 2SCN^-_{ads}$$

As one can see there is no net consumption of the adsorbed ligand. The presence of these adsorbed anions causes the reduction of In^{+3} to occur at a potential considerably less cathodic than the uncatalyzed reduction. Figure 1 shows typical polarograms for the iodide-catalyzed reduction.[2]

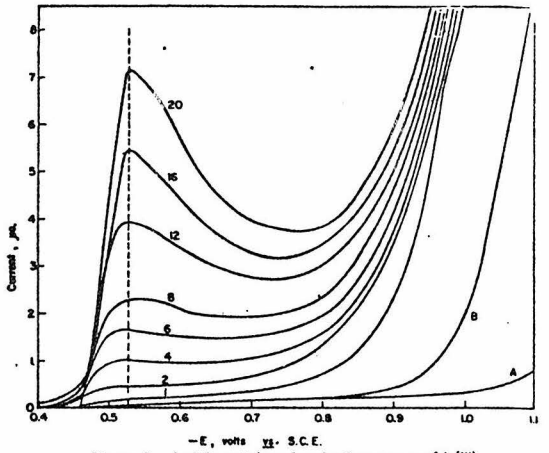

Figure 1. Iodide-catalyzed reduction waves of In(III)
1M $HClO_4$, In(III) = 10^{-3}M
Numbers on curves represent [I] × 10^5, M
A. $HClO_4$ only
B. $HClO_4$ plus In(III)

Thiocyanate and iodide are both very strongly adsorbed on mercury electrodes at potentials where indium reduction occurs. Indium is not easily analyzed by electrochemical techniques particularly at trace levels. It is proposed that this system be exploited to construct a forced flow liquid chromatographic detector for analysis of indium in solution.

Johnson and Larochelle[4] have demonstrated the sensitivity and practicality of coulometric electrochemical liquid chromatograph detector systems. Johnson and Taylor[5] extended this method to catalytic systems, specifically the catalysis of the electrooxidation of Sb(III) by iodide adsorbed on platinum. The tubular plastinum electrode that was used is diagrammed in Figure 2.[4]

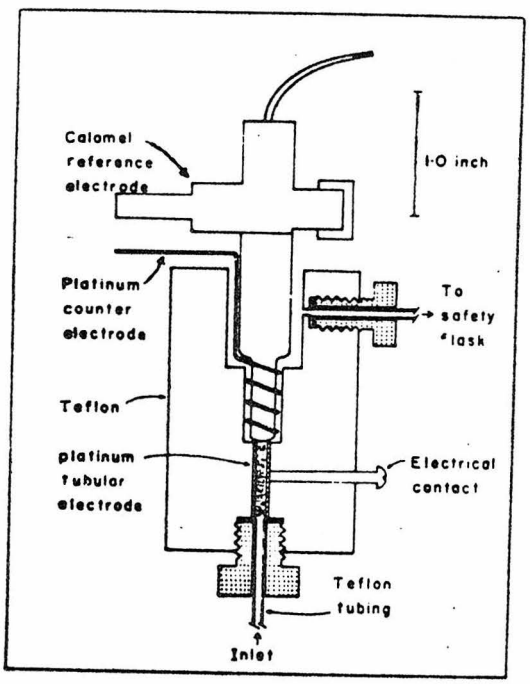

Fig. 2. Cross-section of detector for forced-flow liquid chromatography.

The electrode is made 100% efficient by packing it with very small pieces of platinum wire.

A modified liquid chromatograph similar to that described in references 4 and 6 is shown in Figure 3.

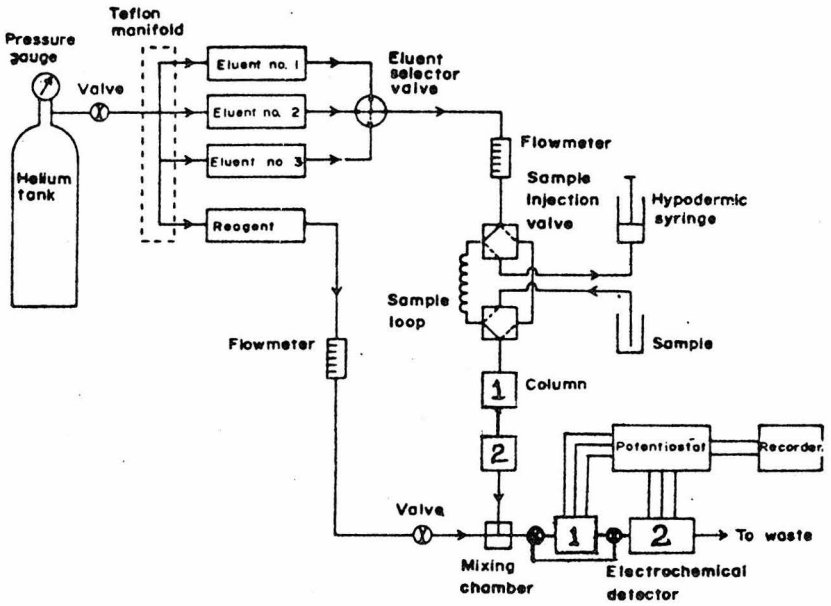

Fig. 3 Schematic diagram of liquid chromatograph.

The analysis procedure proposed is described as follows. First the platinum in both detectors is plated with mercury by passing a mercury solution through both detectors while the potential of the detector is held where mercury will be deposited from the solution. This is done to increase the hydrogen over-potential of the detector. Secondly a thiocyanate or iodide solution is

passed through detector number 2 and not through the first detector. Then the system is purged of all excess ligand.

The pH of the system should be kept around 3 which is the optimum pH for indium reduction and keeps the indium present as $In(H_2O)_6^{+3}$.[2] The supporting electrolyte should be a sodium perchlorate perchloric acid mixture or any other non-complexing anion system. After the system is clear of excess iodide or thiocyanate the sample is introduced from the sample loop and is passed through one or two ion exchange columns. The first column is an anion exchange column which would exchange all anions for perchlorate or nitrate to prevent any catalysis from occurring in detector number 1. The second ion exchange column would be an optional cation exchange column to separate any extra components or interferences. The second cation exchange column could also be used to concentrate In^{+3} if ultra-trace levels from large samples were of interest. A change in eluant concentration would be required to elute the indium in a narrow band.

When the indium has passed through the columns it then passes through the first detector. This detector is held at a potential of about -500 millivolts versus SCE where no indium can react without the ligand bridging catalysts which have been carefully excluded. However, most other electroactive species which are not dependent upon

electrocatalysis will be reduced at this potential. The indium is then transported to the final detector which had been allowed to collect the adsorbed ligand and is held at a potential of -500 mV versus SCE where the adsorption of the ligands is still strong and the reduction rate of the indium is fast[2] (see Figure 1). The amount of indium in the sample is then obtained from simple integration of the current of the chromatographic peak and the equation

$$X = \frac{Q}{nF} \qquad (1)$$

where X is the number of moles in the sample, n is the number of electrons permole electrolyzed and F is Faraday's constant and Q is the integrated charge. The method is advantageous because the Faraday is the only calibration constant needed and for indium the three electron reduction contributes to large signals. Johnson and Taylor[5] have concluded that detectors like this could be used at the subpart per billion level. This method is also very amenable to computer automation with a computer interfaced to control the eluant, sample introduction, flow rate, electrode pretreatment and current integration.

REFERENCES

(1) R. DeLevie and L. Pospisil, J. Electroanal. Chem., 25, 245 (1970).

(2) D. A. Aikens and A. J. Engel, Anal. Chem., 37, 203 (1965).

(3) M. A. Loshkarev and A. A. Karazov, Electrochimya, 3, 39 (1967).

(4) D. C. Johnson and J. Larochelle, Talanta, 20, 959 (1973).

(5) D. C. Johnson and C. R. Taylor, Anal. Chem., 46, 2 (1974).

(6) M. D. Seymour, J. P. Sickafoose and J. S. Fritz, Anal. Chem., 43, 1734 (1971).

PROPOSITION IV

THE SYNTHESIS AND ELECTROCHEMISTRY OF SOME TRIPLE DECKER SANDWICH COMPOUNDS

Bis(η^5-cyclopentadienyl) transition metal complexes, MCp_2, have been known for about 25 years. There is a large and varied chemistry of these metallocenes or sandwich compounds. More recently Werner and Salzer[1] prepared for the first time a triple decker sandwich compound, the tris(η^5-cyclopentadienyl) dinickel cation, $Ni_2Cp_3^+$, by reaction with carboniums ions, e.g. $[C(C_6H_5)_3]^+$ and $C_7H_7^+$.

$$2Ni(C_5H_5)_2 + [CPh_3]BF_4 \xrightarrow{CH_3NO_2} [Ni_2(C_5H_5)_3]BF_4 + C_5H_5CPH_3$$

The structure of this compound was determined[2] and shows the two metal atoms between three parallel Cp rings with the two nickels making a dimer. The existance of such a species was first suggested by Schumacher and Taubenest[3] who studied the mass spectrum of nickelocene. They found that the $Ni_2Cp_3^+$ cation was formed by an ion-molecule reaction and correctly predicted the structure (Figure 1,1a).

$$M(C_5H_5)^+ + M(C_5H_5)_2 \longrightarrow [M_2(C_5H_5)_3]^+ \quad M = Fe, Ni$$

Triple decker complexes of cobalt and iron are also known. These compounds have a middle ring and sometimes all rings which are not Cp ligands but a carborane or thioborane ring. A summary of the structures of the compounds reported to this date are shown in Figure 1.

It is proposed that the electrochemical behavior of these compounds and the synthesis and electrochemistry of several proposed compounds including mixed metal compounds be investigated. Spectral, magnetic measurements and x-ray diffraction would be applied to any new molecules prepared.

Hoffmann, et al.,[7] have analyzed the molecular orbital diagram for $Ni_2(Cp)_3^+$. Their analysis indicated that a degenerate pair of e_1'' orbitals occupied by four electrons of the 34 electron system, are not essential for bonding.

The prediction is that the oxidation by up to four electrons is possible. The dimer of nickel(IV)'s would be extremely unstable as is the two electron oxidation product of nickelocene[8] which is only seen at low temperature (-40° C).[9] However a one electron oxidation product of nickelocene, the nickelecinium cation, is quite stable.[8,9] According to Hoffmann et al.,[7] there is a significant Ni-Ni interaction in $Ni_2Cp_3^+$ despite the large distance (3.576 Å). It would be very interesting to find out if the oxidation occurs by one or two electron steps.

Werner and Salzer have also reported synthesis of triple decker nickel sandwiches with methyl and t-butyl

FIGURE 1

Structures of triple decker sandwich compounds which have been synthesized.

1. a. $[(\eta^5\text{-}C_5H_5)_3Ni_2]^+$

   b. $[(\eta^5\text{-}CH_3\text{-}C_5H_4)_3Ni_2]^+$

   c. $[(\eta^5\text{-}t\text{-}C_4H_9\text{-}C_5H_4)_3Ni_2]^+$

2. $(\eta^5\text{-}C_5H_5)_2[3,4\text{-}(C_2H_5)_2\text{-}2,5(CH_3)_2\text{-}1,2,5(SB_2C_2)]Fe_2$

3. a. $(\eta^5\text{-}C_5H_5)_2(2,3\text{-}C_2B_3H_5)Co_2$

   b. $(\eta^5\text{-}3\text{-}CH_3\text{-}2,3\text{-}C_2B_3H_5)(\eta^5\text{-}C_5H_5)_2Co_2$

4. $(\eta^5\text{-}C_5H_5)_2(\eta^5\text{-}2,4\text{-}C_2B_3H_5)Co_2$

5. $[3,4,\text{-}(C_2H_5)_2\text{-}2,5(CH_3)_2\text{-}1,2,5\text{-}SB_2C_2]_3Co_2$

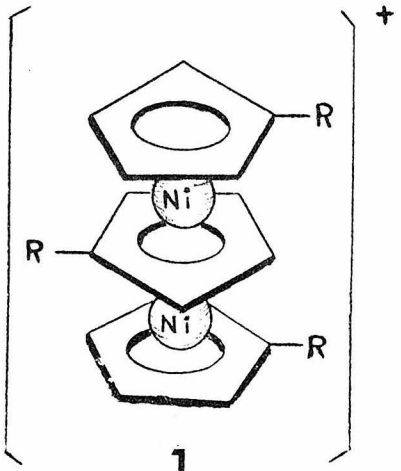

1

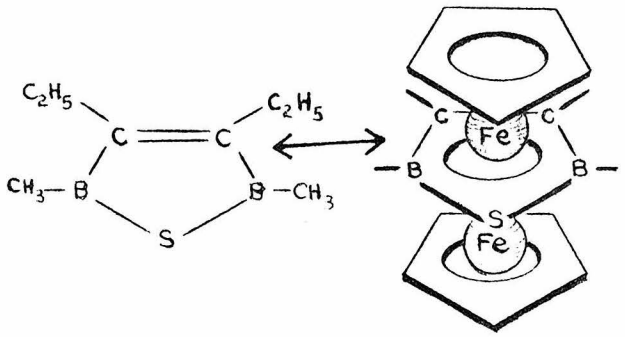

2

a R = H ref 1
Ni-Ni = 3.576 Å

b,c R = CH_3, t-C_4H_9 ref 10

34 electrons

ref 6
Fe-Fe = 3.236 Å

30 electrons

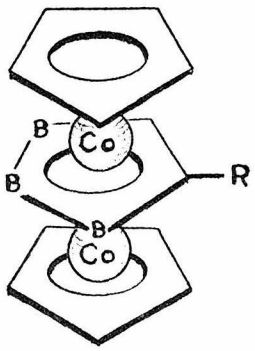

3

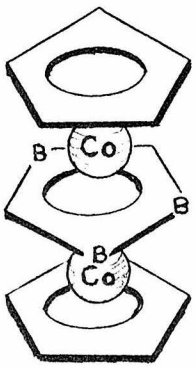

4

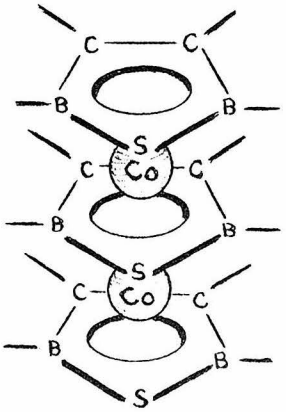

5

a R = H

b R = CH_3
Co-Co = 3.14 Å

ref 4

30 electrons

ref 4

30 electrons

ref 5

30 electrons

SUMMARY OF TRIPLE DECKER COMPOUNDS REPORTED

substituents on the Cp rings.[10] Large shifts in the oxidation potential of ferrocene derivatives can be observed by substituting on the rings.[11-15] Stability of air and water sensitive compounds, 1a,b,c, and oxidation products might be achieved by tayloring the electron donating and withdrawing ability of the ring substituents.

The electrochemistry of the triple decker, air and water stable cobalt compounds, 3a,b, 4 and 5, would be interesting. Again the question of Co-Co(3.14 Å) interactions could be addressed. ESR and magnetism studies of any odd electron electrochemical products would also provide insight into metal-metal interactions.

The cobalt triple deckers are 30 electron complexes and contain no electrons in the e_1' orbitals which were filled in 1a. Stable reduction products may be observed for compounds 3a,b, 4 and 5. The iron triple decker[2] is also a 30 electron system and similar predictions could be made for its electrochemical behavior.

This 30 electron island of stability could be used to predict the existence and structure of a mixed metal triple decker sandwich compounds. Figure 2[6,7,8] shows the structure of these compounds. Possible synthetic routes are suggested from the observation that the fragment $CpFe^+$ is found in the mass spectra of ferrocene.[3] A similar fragment has also been postulated in the photo-

FIGURE 2

Structures of some proposed triple decker sandwich compounds.

6. $(\eta^5\text{-}C_5H_5)Fe(\eta^5\text{-}2\text{-}3\text{-}C_2B_3H_5)Co(\eta^5\text{-}C_5H_5)$

7. $(\eta^5\text{-}C_5H_5)Fe(\eta^5\text{-}2\text{-}3\text{-}C_2B_3H_5)_2Co$

8. $(\eta^5\text{-}C_5H_5)[\eta^5\text{-}(1,2,3,4,5,)\text{-}CH_3)_5\text{-}C_5]_2Fe_2$

9. $(\eta^5\text{-}C_5H_5)Ni[\eta^5\text{-}(1,2,3,4,5CH_3\text{-}O)_5C_5]_2Fe$

10. $(\eta^5\text{-}C_5H_5)Ni(\eta^5\text{-}2,3\text{-}C_2B_3H_5)Co(\eta^5\text{-}C_5H_5)$

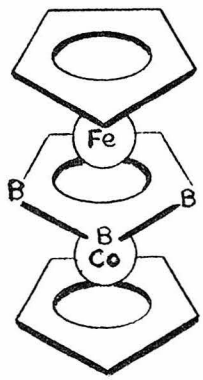

6

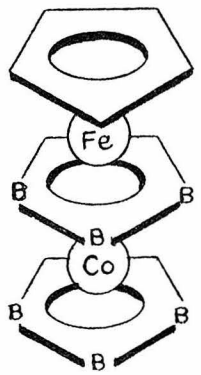

7

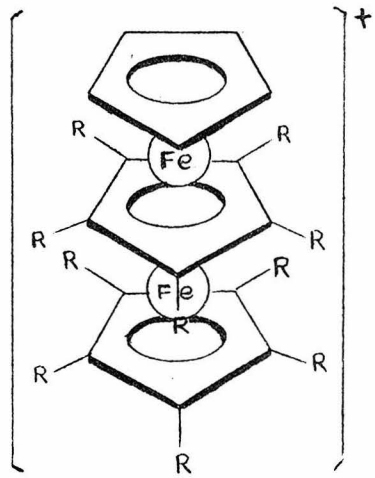

8

30 ELECTRON SYSTEMS

R = O-CH_3, CO_2^-, $COOCH_3$

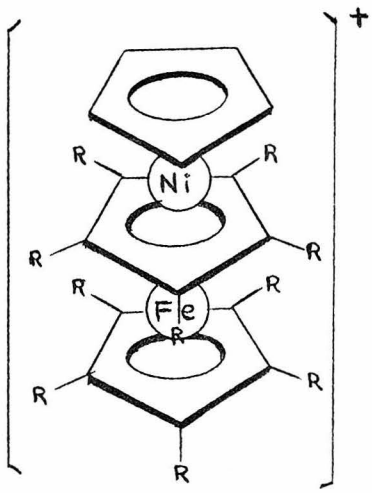

9

34 ELECTRON SYSTEMS

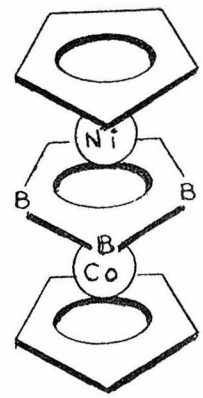

10

R = O-CH_3, CO_2^-, $COOCH_3$

STRUCTURE OF PROPOSED COMPOUNDS

decomposition of η^5-cyclopentadienyl η^6-benzyl iron(II) in acetonitrile.[16]

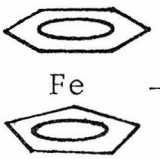

$$2 \quad \text{Fe} \quad \xrightarrow[CH_3CN]{h\nu} \quad [Fe(CH_3CN)_6]^{2+} + Fe(Cp)_2 + C_6H_6$$

A small, steady state concentration of $(C_5H_5)Fe(C_6H_6)$ could be photolized in the presence of an excess of $(\pi\text{-}C_2B_3H_7)Co(\pi\text{-}C_5H_5)$[4,17] to yield compound 6.

$$FeCp^+ + (\pi\text{-}C_2B_3H_6)CoCp \longrightarrow CpFe(\pi\text{-}C_2B_3H_6)CoCp$$

The same reaction in the presence of the precursor of compound 5 would hopefully yield compound 7. The 30 electron species[8] prepared from the same route could perhaps be stabilized by substitution on the ferrocene rings of the ferrocene reactant.

Electrochemical synthesis is another possible route to these and similar complexes. When the electrochemically generated nickelocene dication decomposes[8,9] a likely

intermediate is a $NiCp^+$ ion which has also been observed in mass spectral studies.[3] Reaction of this fragment with the properly substituted ferrocene would yield compound 9 which is a 34 electron species as are the triple decker nickel compounds (1a,b,c). The ferrocene derivative would have to be stable to oxidation at a potential where the unstable nickelocene dication can be generated >770 mV. Multiple methoxy, carboxylate or methylformate substitution of the ferrocene rings has been shown to shift the oxidation potential beyond 850 mV.[15]

Compound 10 is another 34 electron species which might be synthesized electrochemically in the same manner as compound 9.

The predictions of new triple decker sandwich structures could continue ad nausem. I have limited the discussion to electronic configurations which have empirically proved to be stable (30 and 34 electrons). The electrochemical behavior of the already prepared and proposed triple deckers may lead to the understanding of this empirical rule as well as to the discovery of intermediate electronic configurations. It seems reasonable to suggest that a half filled e_1'' shell (32 electrons) might also be stable.

REFERENCES

(1) H. Werner and A. Salzer, Synth. Inorg. Metal-org. Chem., 2, 239 (1972).

(2) H. Werner and A. Salzer, Angew. Chem., 84, 949 (1972).

(3) E. Schumacher and R. Taubenest, Helv. Chim. Acta., 47, 1525 (1964).

(4) P. C. Beer, V. R. Miller, L. G. Sneddon, R. N. Grimes, M. Mathew and G. J. Palenik, J. Am. Chem. Soc., 95, 3046 (1973).

(5) W. Siebert and W. Rothermel, Angew. Chem. Int. Ed., 16 (1977) 333.

(6) W. Wiebert, T. Renk, K. Kinberger, M. Bochmann and C. Krüger, Angew. Chem. Int. Ed., 15, 779 (1976).

(7) J. W. Lauher, M. Elian, R. H. Summerville and R. Hoffmann, J. Am. Chem. Soc., 98, 3219 (1976).

(8) G. Wilkinson, P. L. Pauson and F. A. Cotton, J. Am. Chem. Soc., 76, 1970 (1954).

(9) R. J. Wilson, L. F. Warren and M. F. Hawthorn, J. Am. Chem. Soc., 91, 758 (1969).

(10) H. Werner and A. Salzev, Angew. Chem., 84 949 (1972).

(11) J. A. Page and G. Wilkinson, J. Am. Chem. Soc., 74, 6149 (1952).

(12) G. Hoh, W. E. McEwen and J. Kleinberg, J. Am. Chem. Soc., 83, 3949 (1961).

(13) W. F. Little, C. N. Reilley, J. D. Jonson, K. N. Lynn and A. P. Saunders, J. Am. Chem. Soc., 86, 1376 (1964).

(14) T. Kuwana, D. F. Bublitz and G. L. K. Hoh, J. Am. Chem. Soc., 82, 5811 (1960).

(15) M. Sabbatini and E. Cesarotti, Inoroganica Chimica Acta, 24, L9 (1977).

(16) K. Mann, private communication

(17) L. G. Sneddon and R. N. Grimes, submitted for publication.

PROPOSITION V

A PHOTOGRAPHIC SHUTTER AND APERTURE SYSTEM WITH NO MOVING PARTS

In the last ten years photography has made significant advances towards becoming a populist art form. The availability of sophisticated yet versatule and easy to operate single lens reflex 35 mm cameras has played a very significant part in this advancement. With all the improvements which have been made in optics, miniaturization of electronics and exposure systems, there has been relatively little change in the design of shutter and aperture mechanims. The complicated system of leaves, bearing springs, releases, etc., is one of the main problem areas in camera operation and maintenance. The moving parts are subject to wear, fatigue and variability of performance with temperature. A design of a shutter and aperture system for use in a 35 mm single lens reflex camera which contains no moving parts is proposed.

The drawings which make up the physical picture of this device comprise Figure 1. The device consists of a flat glass disk which is actually a sandwich of two glass plates containing an interstitial layer of liquid crystal. The liquid crystal material will be discussed later. Alternate layers of vapor deposited gold, tin oxide and

FIGURE 1

Approx. 3X scale drawing of proposed design of liquid crystal shutter and automatic exposure system. Note that the width of the side view is greatly expanded.

Front View

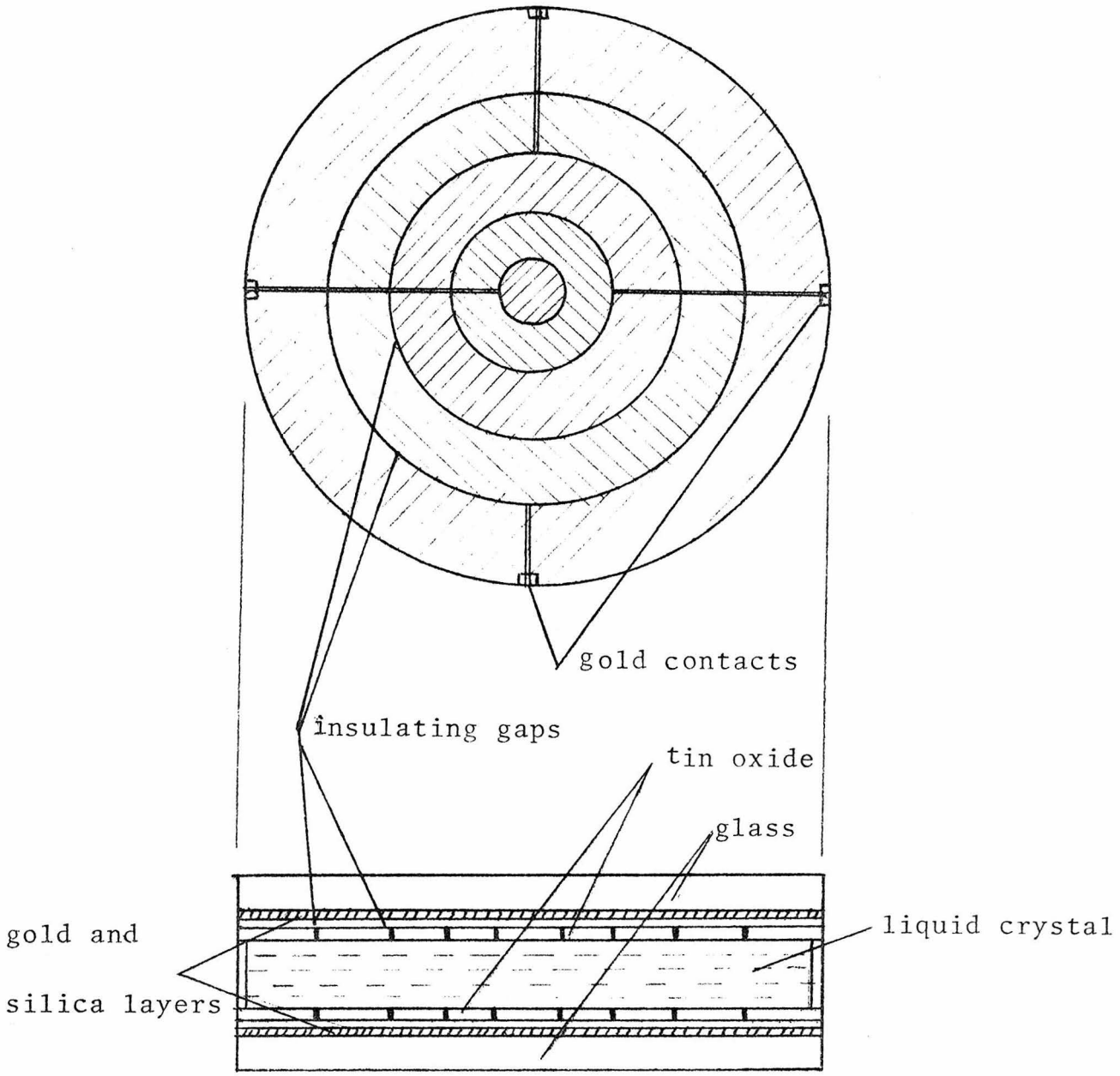

Side View (width greatly enlarged)

silica will be layed down on the inside of the glass plates in such a way as to define concentric rings of electrodes each of which has its own gold contact lead to the outside of the disk. Vapor depositions and etching procedures many times more complex than this are commonplace in integrated circuit manufacture. The radius of the concentric rings is such that they will define a full or fractional f-stop. The device would be placed between the front and rear element of each interchangeable lens in the same location the diaphram and leaf shutter is located in a conventional lens for a camera without a focal plane shutter.

A thin film of a nematic mesophase liquid crystal sandwiched between glass surfaces usually exhibits marked birefringence when viewed between crossed polarizers. A nematic mesophase is a liquid crystal in which the long range order is confined to a statistically parallel orientation of the long molecular axis. If the long molecular axis of the nematogen are oriented more or less uniformally normal to the glass surface, the film appears clear to the eye and between crossed polarizers is optically extinct. If this film is mounted between glass plates which have a conducting surface (e.g., a transparent coating of tin oxide) and a voltage is applied, the alignment of the molecules is disturbed and the film scatters light

and becomes opaque.[1] The effect is purely reflective (not light emitting) and so the contrast between the clear (off) and opaque (on) states is maintained even in bright light when this effect is applied to display devices.[1] The dynamic scattering effect of nematic liquid crystals has been known for many years - a patent of Barnett and Levin[2] relates to its use in light valves.

New developments in the synthesis of liquid crystal molecules and electrode coating technology have reduced the response time from the opaque to transparent state to below 1 millisecond.[3] Some orientational changes in these new liquid crystal systems induce the film to become totally internally reflective or completely transparent. One millisecond is usually the fastest shutter speed needed on even the most advanced camera so the response is well within the specifications needed for a shutter system. The temperature stability of newly developed liquid crystal mesophases contribute to their attractiveness for such an application.[3]

The shutter system would operate by becoming transparent in a concentric region which defines the correct f-stop needed for a period of time equal to the required shutter speed.

Digital electronics is already employed for control of the two types of automatic exposure systems employed

on modern 35 mm cameras, shutter speed preferred and aperture preferred. Camera manufacturers elaborate very extensively about the virtues of the type of automatic exposure system which they chose to build into their camera. Certainly there are advantages inherent to both systems. Part of the beauty of the proposed system would be the ease by which either system could be implemented. A switch would be all that would be required to go from either automatic exposure system or to a manual exposure option. The digital electronics required would be simpler and consume less power than the systems currently being manufactured.

The problem of the thin liquid crystal layer being 100% opaque when no picture is being exposed is already solved in the design of a modern 35 mm camera. The single lens reflex camera contains a 45° mirror directly behind the lens which directs the image up through the micro-prism and into the viewfinder of the camera before an exposure is taken. When composing the picture the liquid crystal display could be completely transparent or stopped down to give the photographer a depth of field preview. When the shutter is triggered a field would be applied and the liquid crystal would become opaque after which the mirror is flipped up where upon the correct f-stop and shutter speed would automatically be sequenced by removal of the field in the correct areas for the exposure time. Any exposure of the film through opaque liquid crystal areas would only be for

the relatively short time in which the mirror is up. If the liquid crystal was as much as 3% transmitting the exposure through the dark portion would be 5 f-stops less than through the transparent region even at the smallest aperture.

With the application of the technology which has been applied to integrated circuits and liquid crystal displays it is probable that shutter-aperture mechanisms of this type could be manufactured at a fraction of the cost of the conventional devices now employed by the camera industry. The mass production cost would probably be low enough to allow incorporation into the popular instamatic and instant cameras. Movie cameras are another possible application of such a shutter system. Elimination of wear, fatigue and maintenance of a mechanical system would be achieved.

One additional aspect of the proposed device should be mentioned. The absence of moving parts in this design would remove the obtrusive "click" from the act of picture taking. Besides the effect on the conventional psychology of the photographic event (perhaps an optional mechanical "click" could be added) a shutter of this type would benefit the candid photographer or a photographer working a normally quiet event such as a wedding where the noise of the shutter is very distracting.

REFERENCES

(1) T. Kallard (Ed.),"Liquid Crystals and Their Applications", Optosomic Press, New York, N.Y. (1970).

(2) L. Barnett and N. Levin, British Patent, 441, 274 (1936).

(3) H. S. Lim, Private communication.